

## Table of Contents

<b>Table of Contents</b>	<b>3</b>
<b>Acknowledgments</b>	<b>6</b>
<b>Summary</b>	<b>7</b>
<b>Deutsche Zusammenfassung</b>	<b>11</b>
<b>Chapter 1: Introduction</b>	<b>17</b>
<b>Chapter 2: Filling the voids in the SRTM elevation model — A TIN-based delta surface approach</b>	<b>23</b>
2.1 Introduction	24
2.1.1. Methods to fill the voids	25
2.2 Materials	27
2.2.1. Study area	27
2.2.2. SRTM data	27
2.2.3. Russian topographic maps	27
2.2.4. Hole-filled SRTM data from CIAT	28
2.2.5. GPS control points	28
2.3 Methods	29
2.3.1. The TIN delta surface fill method	29
2.3.2. Detailed method description	30
2.3.3. Validation and analysis of the DEMs	32
2.4 Results	32
2.5 Discussion	35
2.6 Conclusions	38
<b>Chapter 3: Typology of oases in northern Oman based on Landsat and SRTM imagery and geological survey data</b>	<b>41</b>
3.1 Introduction	42
3.1.1. Geology of the Oman Mountains	42
3.2 Area of interest and dataset description	45
3.2.1. Study area	45
3.2.2. Vegetation dataset	45
3.2.3. Topographic dataset	47
3.2.4. Hydrologic dataset	47
3.2.5. Geologic dataset	47
3.2.6. Topographic dataset	49
3.2.7. Exclusion of natural vegetation	49
3.2.8. Classification validation	51
3.2.9. Topographic analysis	52
3.2.10. Hydrologic analysis	53
3.2.11. Geologic analysis	53
3.2.12. Cluster analysis	55

3.3	Results	55
3.3.1.	Oasis locations	56
3.3.2.	Verification of oasis locations	56
3.3.3.	Distribution of input parameters	56
3.3.4.	Cluster description	58
3.4	Discussion	60
3.4.1.	Cluster characterization	60
3.4.2.	Factors determining oasis locations	63
3.5	Conclusions	63
<b>Chapter 4: Hydrological sustainability of mountain oases in northern Oman</b>		<b>67</b>
4.1	Introduction	68
4.2	Materials and Methods	69
4.2.1.	Study sites	69
4.2.2.	Spring flow	71
4.2.3.	Water age	72
4.3	Results	75
4.3.1.	Spring flow	75
4.3.2.	Water ages	77
4.4	Discussion	81
4.4.1.	Spring flow	81
4.4.2.	Water age	83
4.4.3.	Hydrological sustainability of the oases	85
4.5	Conclusions	86
<b>Chapter 5: Climate change affects traditional high-altitude fruit production systems in Oman</b>		<b>91</b>
5.1	Introduction	92
5.2	Materials and Methods	94
5.2.1.	Study sites	94
5.2.2.	Tree counts	94
5.2.3.	Temperature measurements	95
5.2.4.	Long-term temperature data	97
5.3	Results	98
5.4	Discussion	100
5.5	Conclusions	105
<b>Chapter 6: Effects of land use changes on the hydrological sustainability of mountain oases in northern Oman</b>		<b>109</b>
6.1	Introduction	109
6.2	Materials and Methods	113
6.2.1.	Study sites	113
6.2.2.	Assessment of current and historic land use	113
6.2.3.	Evapotranspiration modeling	115
6.2.4.	Measurement of climatic parameters	116
6.2.5.	Wind speed modeling	119
6.2.6.	Modeling of solar radiation	120
6.2.7.	Water availability	120

6.2.8.	Implementation of the models	122
6.2.9.	Historic water use	123
6.3	Results	124
6.3.1.	Current and historic land use	124
6.3.2.	Climatic parameters	125
6.3.3.	Water availability	128
6.3.4.	Evapotranspiration modeling	128
6.3.5.	Current and historic water demand	128
6.4	Discussion	131
6.5	Conclusions	134
<b>Chapter 7: Conclusions</b>		<b>137</b>
<b>Curriculum vitae</b>		<b>139</b>
<b>List of publications</b>		<b>141</b>

## Acknowledgments

First of all I want to thank Prof. Dr. Andreas Buerkert for getting me back to Witzenhausen, for teaching me science and for advising me throughout the process that led to this dissertation. Thanks also to Prof. Dr. Eva Schlecht for being part of and a driving force behind some of the scientific challenges to be met during the last 2½ years of this work. I also acknowledge Profs. Buerkert and Schlecht, as well as Prof. Dr. Bernard Ludwig and Prof. Dr. Rainer Georg Jörgensen, for evaluating this dissertation.

Throughout my research in Witzenhausen, Oman, Niger and Sudan I enjoyed the excellent working environment and scientific stimulations provided by my colleagues Dr. Jens Gebauer, Dr. Stefan Siebert, Dr. Katja Brinkmann, Dr. Maher Nagieb and Dr. Sulaiman Alkhanjari. During my field trips to Oman, I particularly enjoyed the company of and collaboration with Uta Dickhoefer, Thuwaini bin Said bin Hamoud Al Zakwani, Muhammed bin Ameir bin Omeir Al Riyami, Henning Jahn, Matthias Klaiss, Hamed bin Saif bin Majid Al Fhdy and Salim bin Rashed bin Marhon Al Toubi. I am also grateful for the kindness and hospitality of the farmers of Balad Seet, Maqta and the oases of Al Jabal al Akhdar.

For scientific contributions to some of the chapters of this dissertation I would like to thank Dr. Herbert Dietz, Prof. Dr. Werner Aeschbach-Hertig, Prof. Dr. Fred Scholz, Dr. Hany El-Gamal, Dr. Rolf Kipfer, Dr. Joachim Benz and Dr. Andreas Bachmann. I would also like to express my gratitude to the secretary of the Institute of Crop Science, Ms. Sigrid Haber, for contributing to the inner peace of this institution.

For infrastructural and financial support, I wish to thank the University of Kassel, Sultan Qaboos University, Muscat, Oman, the Agricultural Extension Service of Al Jabal al Akhdar, the Diwan of Royal Court of Oman and the German Research Foundation (Deutsche Forschungsgemeinschaft – DFG).

I also want to thank my family, Dr. Rolf, Almut, Volker and Dörte Lüdeling and my long-term Witzenhausen companions Florian Wichern, Beate Formowitz and Bastian Hoffmann, as well as the other members of my lunch group, for keeping me connected to normal life in times of intense research.

Last but by no means least I would like to thank Jessica Fischer Hunter for patiently waiting for me through the years of my PhD and for providing the necessary motivation for finishing in a timely manner.

## Summary

### *Sustainability of mountain oases in Oman*

#### *Effects of agro-environmental changes on traditional cropping systems*

To assess the natural resources of mountain oases in northern Oman using methods of landscape analysis, it was necessary to first improve an existing digital elevation model (DEM) of the Oman Mountains. The so-far best DEM of this region, which was derived from NASA's Shuttle Radar Topography Mission (SRTM) contains many data voids of often substantial size. In order to close these gaps, Russian topographic maps of northern Oman (1:200,000) were digitized and their altitude lines interpolated to form an elevation model, which could be used as a fill surface for the data gaps. For merging the resulting DEM with the SRTM data, buffers were constructed around all data voids in the area and the elevations of all pixels within these buffers extracted from both the SRTM and the fill surface. From these points, Triangular Irregular Networks (TINs) were created for each of the surfaces and converted to grids for use as a base surface for the void areas. For the fill surface, the resulting base surface was subtracted from the DEM and the result added onto the base of the SRTM DEM. The resulting surface could then seamlessly be merged with the original SRTM elevation model. The resulting DEM was evaluated using GPS points measured in various locations of the Oman Mountains.

Visual quality control by hillshading indicated that the surface had no major flaws, such as sills or unrealistic highs or lows. Comparison of the new surface, as well as a DEM created by the International Center for Tropical Agriculture (CIAT), with the control points indicated that the new surface corresponded much better with measured GPS positions than CIAT's attempt. The combination of digital and hardcopy maps yielded a better DEM than could be created using only existing digital datasets. The newly developed method was useful for eliminating the absolute bias inherent in historic topographic survey data, while preserving most of its relative accuracy.

For assessing and classifying the natural settings of oases in northern Oman, this dataset was combined with information derived from hydrologic modeling, Landsat satellite images and geologic survey data. Oasis locations were derived by calculating the Normalized Difference Vegetation Index (NDVI) from the red

and near infrared bands of the Landsat images, subtracting a regional average of 101 by 101 pixels, averaging the result over 3 by 3 pixels, and classifying the dataset into five classes using a natural breaks algorithm. The highest resulting class was interpreted as oasis core area. After evaluating the NDVI within buffers of increasing distances around these cores, all area within six pixels around the cores was interpreted as oasis area.

As topographic information, the mean elevation of each oasis and the relative height of the surrounding terrain were derived directly from the elevation model. Using the hydrologic modeling tools supplied by the HydroTools Extension to the ArcGIS Spatial Analyst, the distance to large and small streams (catchment areas of 100 km<sup>2</sup> and 10 km<sup>2</sup>) and the size of the contributing upslope area for each oasis were also calculated. As geologic variables, four influential geologic settings were identified and assigned categorical variables describing their proximity to each oasis. All oases were then grouped using cluster analysis.

The 2663 oases detected by this algorithm were categorized into six distinct oasis types. 'Plain Oases' (48.5%) are most frequent, being scattered around the plains on either side of the mountains and mostly fed by irrigation from wells. 'Foothill Oases' (46.2%) lie in the Samail and Hawasina foothills and mostly derive their water from wadi groundwaters that are channeled by the rocks of the foothills. 'Mountain Oases' (2.8%) lie at higher elevations than all other types and are characterized by proximity to Hajar limestones. Their irrigation water originates from springs emerging from the unconform boundary of limestones and underlying impermeable rocks. 'Urban Oases' (1.7%) are mostly parks or sporting facilities, which do not lie in hydrologically conclusive settings. 'Kawr Oases' (0.5%) are fed by springs emerging from limestones of the Kawr Group. Finally, 'Drainage Oases' (0.3%) are the largest traditional oases in northern Oman. They lie along a large wadi that drains almost the entire area west of the Oman Mountains. They therefore have a very stable water supply, leading to their large sizes of up to 436 ha.

In addition to large catchment areas, the sites of all traditional oases require some sort of water storage, from which water is dispensed gradually to allow crops to survive periods of drought. The functioning of this mechanism is one of the primary determinants of the hydrologic sustainability of Omani oases. To quantify their hydrologic sustainability, the flow dynamics of four irrigation channels at Balad Seet, 22 at Maqta and two at Al 'Ayn were analyzed over periods of between 19 and 34 months. Measurements were taken between 2000 and 2003 at Balad Seet and Maqta and in 2006 and 2007 at Al 'Ayn. This information was supplemented by determining water ages, the time between infiltration of rainfall and re-emergence as spring water, of water samples taken from two springs at Balad Seet, six springs at Maqta, and one spring each at Al 'Ayn, As Sumayiyah and Nakhl. The two methods used for dating were the <sup>3</sup>H-<sup>3</sup>He method, which measures the ratio of radioactive tritium to its decay product <sup>3</sup>He, and the SF<sub>6</sub> method, which derives ages from the concentration of

sulfurhexafluoride, whose exponentially increasing atmospheric concentration is reflected in meteoric water.

Water flows varied between 22 and 58 m<sup>3</sup> h<sup>-1</sup> at Balad Seet, between 4 and 9 m<sup>3</sup> h<sup>-1</sup> at Maqta and between 25 and 61 m<sup>3</sup> h<sup>-1</sup> at Al ‘Ayn. During dry spells, spring flow decreased by 12% a<sup>-1</sup> at Balad Seet and 30% a<sup>-1</sup> at Maqta. Water ages ranged between 2 and 10 years for Balad Seet, between 2 and 8 years for Maqta and around 8 years for all other springs. For Nakhl, no reliable water age could be determined due to high amounts of radiogenic helium in the sample. As for one sample from Maqta, the age of this sample was assumed to be >15 years.

Determining water ages was difficult in many cases, because of unsaturated flow conditions in the limestone aquifers and probably natural sources of SF<sub>6</sub>. These complications underscore the importance of using more than one tracer for water dating. All studied oases seem capable of enduring droughts of about five years relatively unharmed, but longer droughts should have severe effects on agricultural production at Balad Seet, Al ‘Ayn and especially at Maqta.

The high-altitude oases in Al Jabal al Akhdar are unique within Oman in that they meet the climatic preconditions for growing temperate and cold-loving subtropical tree and shrub crops. A common proxy for the climatic requirements of such crops is the number of chilling hours per winter, which are hours with temperatures below 7.2°C. To analyze how well the cultivated vegetation of oases in this region is adapted to the altitude-specific climatic conditions, all cultivated plant species were inventoried at the oases of Al ‘Ayn (including Al ‘Aqr and Ash Sharayjah) Qasha’, Salut and Masayrat ar Ruwajah, which lie along an elevation gradient stretching from 1030 to 1950 m a.s.l. To estimate chilling hours, temperatures were measured at half-hourly intervals at Al ‘Ayn, Qasha’ and Masayrat ar Ruwajah and interpolated for Salut. After verifying good correlations of all measured temperatures with records from an official weather station nearby, a regression was computed between the daily minimum temperature at the station and the number of chilling hours. From this regression, the numbers of chilling hours were estimated for 20 out of 24 winters between 1983 and 2007.

The cropping system of the lowest oasis, Masayrat ar Ruwajah was dominated by date palm (*Phoenix dactylifera* L.), while at all higher settlements (above 1400 m a.s.l.), pomegranates (*Punica granatum* L.) and other cold-loving subtropical fruit trees were most frequent. With increasing altitude, the proportion of temperate perennials, mostly rose bushes (*Rosa damascena* Mill.), increased up to 30% at Al ‘Ayn, the highest settlement.

The number of chilling hours declined rapidly by 17.4 per year at Al ‘Ayn, from 1047 in 1983/84 to less than 350 in all winters since 2003. Similarly, the mean annual decrease amounted to 12.1 at Qasha’, 6.4 at Salut and 0.8 at Masayrat ar Ruwajah. Due to the decline in chilling hours, climatic conditions at Qasha’ and Salut are no longer optimal for the oases’ main fruit crops, pomegranates and peaches. At the higher oasis of Al ‘Ayn, conditions are still cool enough during most winters for fructification of these trees. If the current

rate of chilling hour decline continues, however, farmers at Al ‘Ayn might also have to adapt their cropping patterns to the changed conditions.

One important adaptive measure to the variability of the oases’ water supply is keeping a certain proportion of the agricultural area under annual vegetation, which can be left uncultivated in times of water scarcity. Historic photographs of several oases in Al Jabal al Akhdar indicate that land use has changed over the past 30 years. To quantify the extent of these changes, the area under cultivated vegetation at the oases of Al ‘Ayn, Al ‘Aqr, Ash Sharayjah, Qasha’ and Masayrat ar Ruwajah was estimated from aerial photographs from 1978 and 2005 and roughly categorized. A detailed vegetation survey of all oases was also conducted in 2006.

Based on temperature, wind and radiation measurements and modeling tools to estimate the spatial distribution of wind and solar radiation, agricultural water demand of the oases was calculated by modeling evapotranspiration using the Penman-Monteith equation. Available water was also estimated by measuring the flow of the four main springs of this region.

The land use inventory indicated several land use changes, most markedly an expansion of the orchard areas at Qasha’ and Ash Sharayjah at the expense of annual fields, and a replacement of lime (*Citrus aurantiifolia* (L.) Swingle) orchards by field crops at Masayrat ar Ruwajah. Overall modeled water demand at all oases combined rose from 218,800 m<sup>3</sup> in 1978 to 256,377 m<sup>3</sup> in 2005. Monthly water demand showed a strong variation, with peak water requirements in June and low water needs in winter. This pattern was more pronounced in the higher oases than at Masayrat ar Ruwajah. At Qasha’, Al ‘Aqr and Ash Sharayjah, modeled water needs temporarily exceeded mean available water. In all oases, peak water requirements were above the minimum amount of water that was supplied by the springs. Due to recent land use changes, only Masayrat ar Ruwajah and Al ‘Ayn had large enough field crop areas in 2005 to be able to compensate for years of water supplies corresponding to the minimum encountered during our observation period.

Overall sustainability of all oases except Masayrat ar Ruwajah had decreased since 1978. This situation is aggravated by demographic changes, such as emigration and an ageing farming population, and competition for water by a new town nearby, which in 2005 already consumed about as much water as all oases combined.



## Deutsche Zusammenfassung

### *Nachhaltigkeit omanischer Bergoasen*

#### *Auswirkungen von Landnutzungs- und Umweltveränderungen auf traditionelle Anbausysteme*

Um die natürlichen Ressourcen nordomanischer Bergoasen mit Hilfe landschaftsanalytischer Methoden untersuchen zu können, war es zunächst nötig, ein existierendes Digitales Höhenmodell (Digital Elevation Model – DEM) zu verbessern. Das bisher beste DEM dieser Region, welches aus Daten der Shuttle Radar Topography Mission (SRTM) der NASA erzeugt wurde, enthält viele Fehlstellen teilweise beträchtlicher Größe. Um diese Löcher zu schließen, wurden russische topographische Karten des Nordoman digitalisiert und deren Höhenlinien zu einem DEM interpoliert, das als Fülloberfläche für die Datenlücken verwendet werden konnte. Um das so erzeugte Modell mit dem SRTM-Modell zu verschmelzen, wurden Puffer um alle Fehlstellen errechnet und die darin liegenden Höhen der Füll- und SRTM-Oberfläche als Punkte extrahiert. Zwischen allen Gruppen von jeweils drei benachbarten Punkten wurden dann für beide Punktsätze Flächen aufgespannt (Triangular Irregular Network – TIN) und die daraus entstehenden Oberflächen in DEMs umgewandelt. Diese Oberflächen eigneten sich als Sockeloberflächen für die von Fehlstellen betroffenen Gebiete. Für die Fülloberfläche wurde dann die entsprechende Sockeloberfläche vom Füll-DEM abgezogen. Nachdem das Ergebnis dieser Berechnung auf die Sockeloberfläche des SRTM-Modells aufgesetzt worden war, ließ sich das entstehende Modell nahtlos mit dem löchrigen SRTM-DEM verschmelzen. Die Genauigkeit des Ergebnisses wurde mit Hilfe von GPS-Messungen in verschiedenen Gebieten des Omanischen Gebirges überprüft.

Eine erste visuelle Überprüfung des Modells mit Hilfe eines simulierten Schattenwurfes zeigte keine größeren Schwächen auf, wie Schwellen oder unrealistische Hoch- oder Tiefpunkte. Ein Vergleich des Modells mit den GPS-Positionen, sowie einer vom International Center for Tropical Agriculture (CIAT) publizierten Oberfläche, ergab, dass die Höhenwerte des neuen DEMs sehr viel besser mit den GPS-Positionen übereinstimmten als die des CIAT-Modells. Die Kombination digitaler Höheninformationen mit aus Karten entnommenen Meereshöhen ergab eine sehr viel bessere Oberfläche als mit rein

digitalen Daten hätte erzielt werden können. Die entwickelte Methode war effektiv darin, den absoluten Fehler der topographischen Karten zu entfernen, während der größte Teil ihrer relativen Genauigkeit erhalten blieb.

Um die natürlichen Standorteigenschaften von nordomanischen Oasen zu charakterisieren und die Oasen zu klassifizieren, wurde das zuvor beschriebene Höhenmodell mit Ergebnissen hydrologischer Modellierung, Landsat-Satellitenbildern und einer geologischen Bestandsaufnahme kombiniert. Um Oasen aufzuspüren wurde der Normalized Difference Vegetation Index (NDVI) aus den Landsatbändern im roten und nah-infraroten Bereich berechnet, vom Ergebnis ein regionaler Durchschnitts-NDVI der 101 x 101 benachbarten Zellen abgezogen, von diesem Ergebnis ein 3 x 3 Zellen-Durchschnitt berechnet und das resultierende Raster mit Hilfe eines Natural-Breaks-Algorithmus klassifiziert. Die hellste Klasse dieser Klassifizierung wurde als Oasen-Kernfläche interpretiert. Nach Betrachtung des NDVI innerhalb von Pufferzonen in zunehmender Entfernung um diese Oasenkerne, wurden alle Flächen im Umkreis von 6 Pixeln um die Kerne als Oasenfläche interpretiert.

Zur Charakterisierung der topographischen Standorteigenschaften wurden die durchschnittliche Höhe der Oasenfläche und die Höhe des angrenzenden Terrains innerhalb von 2 km um die Oase direkt aus dem Höhenmodell ermittelt. Mittels der hydrologischen Modellierungserweiterung (HydroTools) zum ArcGIS Spatial Analyst wurden die Entfernungen zu großen und kleinen Wasserläufen (Einzugsgebiete von 100 km<sup>2</sup> und 10 km<sup>2</sup>) und die Größe des hangaufwärts gelegenen Einzugsgebietes abgeschätzt. Um die Geologie der Oasen zu beschreiben, wurden vier einflussreiche geologische Konstellationen identifiziert und jeder Oase kategorische Variablen zugewiesen, um die Nähe zu diesen Konstellationen zu beschreiben. Alle Oasen wurden dann mittels Clusteranalyse klassifiziert.

Aus den Daten kristallisierten sich 6 unterschiedliche Gruppen für die 2663 gefundenen Oasen heraus. ‚Ebenen-Oasen‘ (48,5%) traten am häufigsten auf. Sie liegen verstreut auf beiden Seiten des Gebirges und werden größtenteils durch Brunnen bewässert. ‚Vorgebirgs-Oasen‘ (46,2%) liegen in den Hawasina- und Samail-Vorgebirgen und erhalten ihr Wasser aus Wadi-Grundwasser, das durch die Vorgebirgs-Gesteine kanalisiert wird. ‚Bergoasen‘ (2,8%) liegen in größerer Höhe als alle anderen Oasentypen und werden durch die Nähe zu Hajar-Kalksteinen charakterisiert. Ihr Bewässerungswasser beziehen sie aus Quellen, die an der unkonformen Grenze zwischen Kalksteinen und wasserundurchlässigem Grundgebirge entspringen. ‚Stadt-Oasen‘ (1,7%) sind größtenteils Parks und Sportanlagen, die nicht an hydrologisch schlüssigen Standorten liegen. ‚Kawr-Oasen‘ (0,5%) bekommen ihr Wasser von Quellen, die aus Kalksteinen der Kawr-Gruppe entspringen. ‚Entwässerungs-Oasen‘ (0,3%) schließlich sind die größten traditionellen Oasen Nordomans. Sie liegen entlang eines bedeutenden Wadis, das nahezu die gesamte Fläche westlich des Oman-

Gebirges entwässert. Daher haben sie eine sehr stabile Wasserversorgung, die ihre große Fläche von bis zu 436 ha ermöglicht.

Neben großen Einzugsgebieten benötigen alle traditionellen Oasen eine Art Wasserspeicher, aus dem das zurückgehaltene Wasser allmählich freigegeben wird, um es den angebauten Kulturen zu ermöglichen, längere Dürrephasen zu überstehen. Das Funktionieren dieses Mechanismus ist eines der wichtigsten Bestimmungsmerkmale der hydrologischen Nachhaltigkeit omanischer Oasen. Um diese Nachhaltigkeit zu quantifizieren, wurde die Flussentwicklung von vier Bewässerungskanälen in Balad Seet, 22 in Maqta und zwei in Al 'Ayn über Zeiträume von zwischen 19 und 34 Monaten untersucht. Die Untersuchung umfasste die Jahre 2000 bis 2003 für Balad Seet und Maqta und 2006/2007 für Al 'Ayn. Für zwei Wasserproben aus Balad Seet, sechs Proben aus Maqta und jeweils eine Probe aus Al 'Ayn, As Sumayiyah und Nakhl wurden zusätzlich die Wasseralter bestimmt. Hierunter versteht man die Zeitspanne zwischen einem Regenereignis und dem Zutagetreten des gefallenen Niederschlages an einer Quelle. Zur Datierung wurden zwei verschiedene Methoden verwendet. Bei der  $^3\text{H}$ - $^3\text{He}$ -Methode erfolgt die Altersbestimmung über das Verhältnis des radioaktiven Tritiums im Wasser zu seinem Zerfallsprodukt  $^3\text{He}$ . Die  $\text{SF}_6$ -Methode ermittelt das Wasseralter aus der Konzentration des atmosphärischen Spurengases Schwefelhexafluorid im Quellwasser, welche die seit einigen Jahrzehnten exponentiell ansteigende Konzentration in der Atmosphäre widerspiegelt.

Die gemessenen Quellflüsse lagen zwischen 22 und 58  $\text{m}^3 \text{h}^{-1}$  in Balad Seet, zwischen 4 und 9  $\text{m}^3 \text{h}^{-1}$  in Maqta und zwischen 25 und 61  $\text{m}^3 \text{h}^{-1}$  in Al 'Ayn. Während einer Dürreperiode ging die Quellschüttung in Balad Seet um 12%  $\text{a}^{-1}$  und in Maqta um 30%  $\text{a}^{-1}$  zurück. Die Wasseralter lagen zwischen 2 und 10 Jahren in Balad Seet, zwischen 2 und 8 Jahren in Maqta und bei ungefähr 8 Jahren in allen anderen Oasen. Für Nakhl konnte wegen hoher Mengen radiogenen Tritiums kein zuverlässiges Wasseralter ermittelt werden. Ebenso wie für eine Probe aus Maqta liegt für diese Quelle das Wasseralter vermutlich bei mehr als 15 Jahren.

In vielen Fällen wurde die Wasseraltersbestimmung durch ungesättigte Flussbedingungen in den Kalkstein-Wasserleitern und vermutlich auch durch natürliche  $\text{SF}_6$ -Quellen verkompliziert. Dies untermauert die Wichtigkeit der Verwendung von mehr als einer einzigen Datierungsmethode. Alle untersuchten Oasen scheinen in der Lage, Dürren von etwa fünf Jahren relativ unbeschadet zu überstehen. Längere Trockenperioden dagegen haben wahrscheinlich ernstzunehmende Konsequenzen für die landwirtschaftliche Produktion in Balad Seet, Al 'Ayn und insbesondere in Maqta.

Die Hochgebirgsoasen in Al Jabal al Akhdar sind dadurch einzigartig in Oman, dass sie die klimatischen Bedürfnisse gemäßigter und kältebedürftiger subtropischer Baum- und Strauchkulturen erfüllen. Eine oft verwendete Maßzahl zur Beschreibung dieser Klimabedürfnisse ist die Anzahl der

Kältestunden im Winter, üblicherweise berechnet als Stunden mit Temperaturen unter 7.2°C. Um herauszufinden, wie gut die Kulturvegetation der Oasen dieser Region an die spezifischen Klimabedingungen der Höhenlagen angepasst ist, wurde eine Bestandsaufnahme aller Kulturpflanzen der Oasen von Al 'Ayn (inklusive Al 'Aqr und Ash Sharayjah), Qasha', Salut und Masayrat ar Ruwajah durchgeführt, die entlang eines Höhengradienten zwischen 1030 und 1950 m üNN liegen. Um die Kältestunden abzuschätzen, wurden in halbstündlichen Abständen die Temperaturen in den Gärten von Al 'Ayn, Qasha' und Masayrat ar Ruwajah gemessen und daraus die Temperaturen in Salut interpoliert. Nachdem sichergestellt wurde, dass zwischen den in den Oasen gemessenen Temperaturen und den von einer offiziellen Wetterstation in unmittelbarer Nähe aufgezeichneten Temperaturen eine enge Korrelation bestand, wurden Regressionen zwischen der Anzahl der Kältestunden in den Oasen und den an der Station gemessenen Minimaltemperaturen berechnet. Aus den Regressionsgleichungen wurden dann die Kältestunden für 20 von 24 Wintern zwischen 1983 und 2007 abgeleitet.

In Masayrat ar Ruwajah, der am niedrigsten gelegenen Siedlung, wurde das Oasensystem von Dattelpalmen (*Phoenix dactylifera* L.) dominiert, während in allen höheren Siedlungen (über 1400 m üNN) Granatapfelbäume (*Punica granatum* L.) und andere kältebedürftige Kulturen am häufigsten auftraten. Mit zunehmender Höhe nahm der Anteil von Kulturen aus den gemäßigten Breiten, insbesondere Rosen (*Rosa damascena* Mill.), bis auf 30% in Al 'Ayn zu.

Die Zahl der Kältestunden in Al 'Ayn nahm rapide um 17,4 Stunden pro Jahr ab, von 1047 im Winter 1983/84 auf weniger als 350 in allen Wintern seit 2003. Entsprechend ging die Kältestundenzahl in Qasha' um 12,1, in Salut um 6,4 und in Masayrat ar Ruwajah um 0,8 Stunden pro Jahr zurück. Wegen dieses Rückgangs sind die klimatischen Bedingungen in Qasha' und Salut nicht mehr geeignet für den Anbau von Granatäpfeln und Pfirsichen (*Prunus persica* L.), der Hauptkulturen dieser Oasen. Im höher gelegenen Al 'Ayn sind die Bedingungen in der Mehrzahl der Winter noch kühl genug, um für ausreichenden Fruchtansatz bei diesen Bäumen zu sorgen. Sollten die aktuellen Rückgangsraten bei den Kältestunden jedoch anhalten, könnten auch die Bauern in Al 'Ayn bald gezwungen sein, ihre Anbauverfahren auf die veränderten Bedingungen einzustellen.

Eine wichtige Anpassungsmassnahme an Schwankungen der in den Oasen für die Bewässerung zur Verfügung stehenden Wassermenge ist der Anbau von annualen Kulturen auf einem Teil der Fläche, der bei Wassermangel nicht bestellt wird. Historische Photographien einiger Oasen in Al Jabal al Akhdar legen nahe, dass sich die Landnutzung dort innerhalb der letzten 30 Jahre gewandelt hat. Um das Ausmaß dieser Veränderungen zu quantifizieren, wurden Luftaufnahmen von 1978 und 2005 analysiert und die darauf erkennbare Kulturvegetation von Al 'Ayn, Al 'Aqr, Ash Sharayjah, Qasha' und Masayrat ar Ruwajah grob nach Landnutzungstypen klassifiziert. Darüber hinaus wurde im

Jahr 2006 eine detaillierte Landnutzungskartierung durchgeführt, in der alle Bäume auf allen Terrassen erfasst wurden.

Aufbauend auf Messungen von Temperatur, Wind und Sonneneinstrahlung und durch Verwendung von Modellierungswerkzeugen zur Abschätzung der räumlichen Verteilung von Wind und Strahlungsintensität, wurde der landwirtschaftliche Wasserbedarf der Oasen mit Hilfe der durch die Penman-Monteith-Gleichung errechneten Evapotranspiration abgeschätzt. Die zur Verfügung stehende Wassermenge wurde durch Quellschüttungsmessungen ermittelt.

Die Kartierung zeigte einige Landnutzungsveränderungen auf, insbesondere eine Ausdehnung der Obstgartenfläche in Qasha' und Ash Sharayjah auf Kosten von Feldkulturen, und eine Verdrängung von Limonenhainen (*Citrus aurantiifolia* (L.) Swingle) in Masayrat ar Ruwajah durch Feldkulturen. Insgesamt stieg der jährliche Wasserverbrauch aller Oasen zwischen 1978 und 2005 von 218.800 m<sup>3</sup> auf 256.777 m<sup>3</sup> an. Beim monatlichen Wasserbedürfnis zeigte sich im Jahresverlauf eine starke Variabilität, wobei der höchste Verbrauch im Juni und sehr viel niedrige Verbräuche im Winter auftraten. Dieses Muster war in den höher gelegenen Oasen stärker ausgeprägt als in Masayrat ar Ruwajah. In Qasha', Al 'Aqr und Ash Sharayjah, überstieg der modellierte Wasserbedarf zeitweise die durchschnittlich verfügbare Wassermenge. In allen Oasen lagen die Wasserbedarfsspitzen oberhalb der bei minimaler Quellschüttung verfügbaren Wassermenge. Durch die Landnutzungsänderungen der letzten Zeit hatten nur noch Masayrat ar Ruwajah und Al 'Ayn im Jahr 2005 ausreichend große Ackerflächen, um Jahre in denen der Quellfluss nur dem von uns gemessenen Minimum entspricht, durch Variation der Anbauverhältnisse ausgleichen zu können.

Insgesamt ist die Nachhaltigkeit aller Oasen mit Ausnahme von Masayrat ar Ruwajah seit 1978 zurückgegangen. Diese Situation wird noch verschärft durch demographische Umwälzungsprozesse wie Abwanderung und eine Überalterung der landwirtschaftlichen Bevölkerung, und durch die Konkurrenz einer neuen Stadt in der Nähe um knappe Wasserressourcen. Der Wasserverbrauch dieser Stadt war 2005 schon in etwa genauso hoch wie der Bedarf an Bewässerungswasser in allen Oasen zusammen.



## Chapter 1

### Introduction

The Sultanate of Oman is located in the south-eastern corner of the Arabian Peninsula, bordering the United Arab Emirates, Yemen and Saudi Arabia. Most of the country's area of roughly 309,500 km<sup>2</sup> is covered by the Arabian Desert, one of the driest and most inhospitable regions in the world. Mean annual temperatures of up to 29°C (Fisher 1994), with extremes during the summer of well over 45°C are adverse to human settlement, and mean annual rainfalls of between 40 and 300 mm make rainfed agriculture impossible.

The defining topographic feature of northern Oman is the range of the Oman Mountains, which stretches in a long arc from the Musandam Peninsula in the north to the Ra's al Hadd, the easternmost tip of the country (Fig. 1.1). A large array of geologic processes contributed to the current composition and shape of this mountain range, and evidence of plate obduction, glaciation, submergence, corral reef formation, sediment deposition and erosion by ice, wind and water is visible all over the range (Glennie 2005, Glennie et al. 1974). Because of the different susceptibility of the various rock formations to erosive processes, the topography of the mountains is complex, with large sediment fans on either side of the range, extensive limestone plateaus on its flanks, an eroded basin in the center, and deeply incised valleys in the transitional zones between high and low terrain. The topography is so rugged that it has defied attempts of automatic mapping by remote sensing techniques until today. It is one of only a few regions in the world, where even the best near-global elevation model that is available today, the model derived from the Shuttle Radar Topography Mission (SRTM), is barely usable, because the steep slopes and deep valleys led to the failure of SRTM's stereo-imagery approach (Hall et al. 2005). The resulting elevation surface is thus littered with holes that are dispersed all over the mountain range. Since a consistent digital elevation model (DEM) is a necessity for hydrological studies at the landscape level, the second chapter of this dissertation strives to accomplish the rather technical task of closing these gaps.

After this preliminary step, it becomes possible to focus on the actual subject of this work, the oases of northern Oman, without running the risk of disappearing in topographic voids. Agricultural oases are scattered all over the Oman Mountains, and also in the lowlands to the east and west of the range. Overall, only 0.3% of the country's area has been classified as agricultural land (FAO 2007). This area is not homogeneously dispersed over the country, but its distribution appears to be correlated to landscape structure. According to FAO

statistics, 62% of this area is irrigated by groundwater using electric or diesel-powered pumps (FAO 2007). These areas lie in topographic settings of relatively shallow groundwater aquifers that can easily be reached by wells. The characteristics that define the positions of all other oases, and even the exact locations of these modern oases, are mostly unknown, and systematic studies of these locations are unavailable. The third chapter of this dissertation thus aims at determining the deciding factors for oasis locations by developing an algorithm to identify oasis positions, and analyzing topographic, hydrologic and geologic landscape features to develop a typology of oases in northern Oman. Such an oasis classification will lend a structure to research on oasis systems, which will be useful for focusing research on representative case studies and generalizing the results from such case studies to larger arrays of oases.

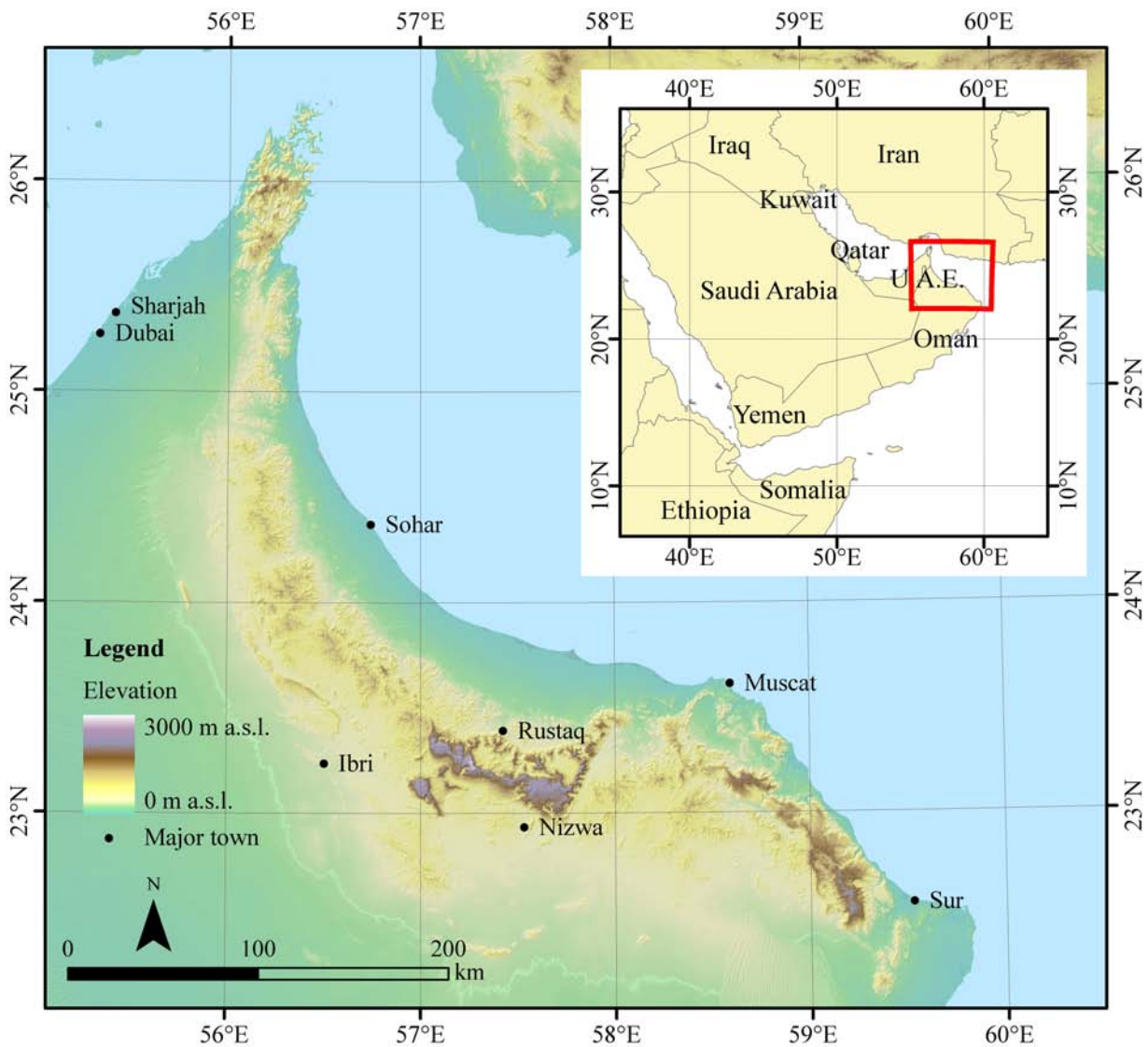


Figure 1.1. Topographic map of the Oman Mountains. The inset shows the location of Oman on the Arabian Peninsula.



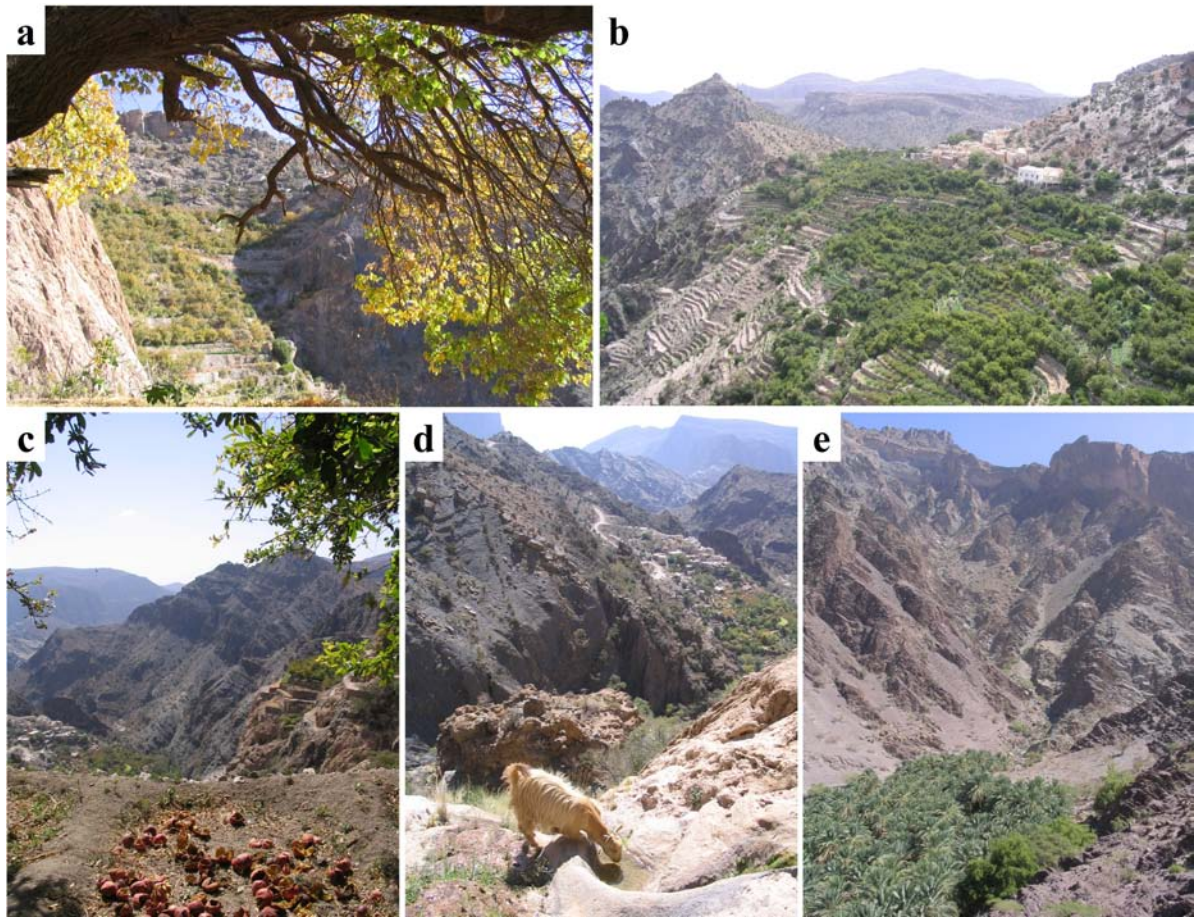


Figure 1.2. Panoramic view of Al Jabal al Akhdar: a) apricot tree of Ash Sharayjah with the terraces of Al ‘Aqr in the background, b) the terraces of Ash Sharayjah, c) pomegranate shells in Al ‘Aqr, d) a goat drinks from the falaj to Qasha’ (background), e) palm grove and setting of Masayrat ar Ruwajah.

The defining characteristics of traditional oases are expected to provide insights into the mechanisms that have ensured sustainable agricultural production over hundreds and, in some cases, thousands of years. Due to the climatic conditions in this region, the most critical resource for agricultural production is water. Rainfall events are much too scarce and erratic to allow reliance on them for supplying all water for the crops. Any oasis that maintains a permanent agricultural area thus requires some way of accessing larger amounts of water than would be supplied by rainfall over longer periods of time. Since the most important crop of most oases is the perennial date palm (*Phoenix dactylifera* L.), water is needed throughout the year in quantities large enough to ensure survival of date orchards during the hot summers. Hydrologic requirements of oases are thus a large catchment area, which collects rainfalls of a larger region and concentrates it near the site of the oasis, and a storage mechanism that retains rainfalls and dispenses the collected water gradually over time spans of several years. In the Oman Mountains, these hydrologic requirements are often met by the large limestone plateaus of the inner mountains, which act as catchment areas and store water inside large aquifers in the cavernous structure of the limestone. At topographic depressions, this water then surfaces where the limestones overlay impermeable formations underneath.

Similarly, water is often stored in wadi sediments, from which it can be channeled and put to use on agricultural fields. In such hydrologic settings, two main parameters determine the hydrological sustainability of a settlement: the amount of water that is available and the time the water is retained in the storage formations. The fourth chapter investigates these two parameters for a set of six oases in different hydrologic settings in the mountains, and draws conclusions about the sustainability of agricultural production at these oases.

Chapters 5 and 6 then focus on the small area of Al Jabal al Akhdar, a secluded mountain region, which harbors the highest agricultural settlements of Oman (Scholz 1984). Other than in the date palm-dominated oases of the lowlands, the farmers of Al Jabal al Akhdar cultivate pomegranates, peaches, walnuts, roses and other tree and shrub crops typically found in temperate and cool subtropical climates (Gebauer et al. 2007a; Fig. 1.2). Because of the uniqueness of this cropping system and its isolated nature in the hot climate of Oman, chapter 5 investigates the climatic conditions necessary to sustain the specific crop assemblages of four oases along an elevation gradient in this region, and explores the likely influences of climatic changes on this cropping system.

Besides climatic changes, oases all over Oman are also affected by transformations of an entirely different nature. Since the overthrow of Sultan Said bin Tamur by his son Qaboos bin Said in 1970, Oman has engaged in a rapid modernization process. While the country had been almost entirely closed off from the outside world and had thus remained in an almost medieval state under the rule of the previous ruler, HM Sultan Qaboos embraced progress, began building up Oman's infrastructure and loosened formerly repressive cultural and societal restrictions. The transformation process initiated by the new politics affected most aspects of life in Oman, but in the traditional oases, which had always been the backbone of Oman's economy, it was particularly consequential. The new developments evoked unprecedented changes to the agricultural systems of the oases, and the implications of these changes for the sustainability of oasis agriculture are as yet unknown. Chapter 6 investigates the effects of land use changes, brought about by infrastructural and demographic changes, on water use in the oases of Al Jabal al Akhdar, trying to evaluate the development over the past 30 years with respect to oasis sustainability.

Finally, chapter 7 will draw some conclusions from all these particular studies, summarizing the value and applicability of the applied methods and exploring the implications of all findings for the sustainability of mountain oases in Oman.

## References

- FAO (2007). AQUASTAT Database. Food and Agriculture Organization of the United Nations. Accessed on 10 Sep 2007 at <http://www.fao.org/nr/water/aquastat/dbase/index.stm>.
- Fisher M (1994). Another look at the variability of desert climates, using examples from Oman. *Global Ecology and Biogeography Letters* 4(3), 79-87.

- Gebauer J, Luedeling E, Hammer K, Nagieb M and Buerkert A (2007). Mountain oases in northern Oman: An environment for crop evolution and *in situ* conservation of plant genetic resources. *Genetic Resources and Crop Evolution* 54, 465-481.
- Glennie K (2005). The geology of the Oman Mountains: an outline of their origin. Scientific Press, Beaconsfield, Bucks, UK.
- Glennie K, Boeuf M, Hughes Clarke M, Moody-Stuart M, Pilaar W and Reinhardt B (1974). Geology of the Oman Mountains. *Verhandelingen Koninklijk Nederlands geologisch mijnbouwkundig Genootschap* 31, 1-423.
- Hall O, Falorni G and Bras RL (2005). Characterization and quantification of data voids in the shuttle radar topography mission data. *IEEE Geoscience and Remote Sensing Letters* 2(2), 177-181.
- Scholz F (1984). Höhensiedlungen am Jabal Akhdar - Tendenz und Probleme der Entwicklung einer peripheren Region im Oman-Gebirge. *Zeitschrift für Wirtschaftsgeographie* 28(1), 16-30.



## Chapter 2

*published in ISPRS Journal of Photogrammetry & Remote Sensing 62 (4), 2007,  
283-294*

# Filling the voids in the SRTM elevation model — A TIN-based delta surface approach

Eike Luedeling <sup>a</sup>, Stefan Siebert <sup>b</sup> and Andreas Buerkert <sup>a</sup>

<sup>a</sup> *Organic Plant Production and Agroecosystems Research in the Tropics and Subtropics,  
University of Kassel, Steinstr. 19, D-37213 Witzenhausen, Germany*

<sup>b</sup> *Institute of Physical Geography, University of Frankfurt, Altenhöfer Allee 1, D-60438  
Frankfurt, Germany*

---

### Abstract

The Digital Elevation Model (DEM) derived from NASA's Shuttle Radar Topography Mission (SRTM) is the most accurate near-global elevation model that is publicly available. However, it contains many data voids, mostly in mountainous terrain. This problem is particularly severe in the rugged Oman Mountains. This study presents a method to fill these voids using a fill surface derived from Russian military maps. For this we developed a new method, which is based on Triangular Irregular Networks (TINs). For each void, we extracted points around the edge of the void from the SRTM DEM and the fill surface. TINs were calculated from these points and converted to a base surface for each dataset. The fill base surface was subtracted from the fill surface, and the result added to the SRTM base surface. The fill surface could then seamlessly be merged with the SRTM DEM. For validation, we compared the resulting DEM to the original SRTM surface, to the fill DEM and to a surface calculated by the International Center for Tropical Agriculture (CIAT) from the SRTM data. We calculated the differences between measured GPS positions and the respective surfaces for 187,500 points throughout the mountain range ( $\Delta$ GPS). Comparison of the means and standard deviations of these values showed that for the void areas, the fill surface was most accurate, with a standard deviation of the  $\Delta$ GPS from the mean  $\Delta$ GPS of 69 m, and only little accuracy was lost by merging it to the SRTM surface (standard deviation of 76 m). The CIAT model was much less accurate in these areas (standard deviation of 128 m).

The results show that our method is capable of transferring the relative vertical accuracy of a fill surface to the void areas in the SRTM model, without introducing

uncertainties about the absolute elevation of the fill surface. It is well suited for datasets with varying altitude biases, which is a common problem of older topographic information.

---

## **2.1 Introduction**

The Digital Elevation Model (DEM) produced by the Shuttle Radar Topography Mission (SRTM) has set new standards for Digital Terrain Elevation Data (DTED). In the few years since this dataset has been made available to the public, it has found a wide array of applications. SRTM data has been used for purposes as diverse as hydrological modeling (Valeriano et al. 2006), vegetation surveys (Bourgine and Baghdadi 2005, Simard et al. 2006), reconstruction of prehistoric water bodies (Leblanc et al. 2006), mapping of glaciers (Berthier et al. 2006) and detection of ancient settlement sites (Menze et al. 2006).

The SRTM mission was jointly operated by NASA's Jet Propulsion Laboratory (JPL), the United States' National Imaging & Mapping Agency (NIMA; in 2003 renamed to National Geospatial-Intelligence Agency — NGA) and the German and Italian Space Agencies (DLR, ASI). Data was acquired by interferometric synthetic aperture radar (InSAR) during an 11-day flight of the Space Shuttle Endeavor in February 2000 (Kobrick 2006). The DEM derived from C-band measurements during this mission has a spatial resolution of 1", about 30 m, making it the best currently available near-global elevation model (van Zyl 2001). The highest SRTM resolution is, however, only publicly available for the United States, whereas all other areas can only be obtained at a resolution of 3", approximately 90 m.

The mission objective of SRTM was to obtain a DEM with an absolute vertical accuracy of 16 m and a relative vertical accuracy of 10 m for 90% of the data (Rodriguez et al. 2005). This means that for nine out of ten data points, the assigned elevation is within 16 m of the true elevation, and the error is within 10 m of the errors of neighboring data points. According to an internal review at JPL, the SRTM DEM meets these requirements (Rodriguez et al. 2006, Rodriguez et al. 2005).

The accuracy of the SRTM model has been confirmed by several researchers, using GPS ground truthing points, lidar data or high-accuracy small-scale DEMs for validation (Bourgine and Baghdadi 2005, Brown et al. 2005, Hofton et al. 2006, Jarvis et al. 2004, Kocak et al. 2005, Rodriguez et al. 2006, Smith and Sandwell 2003, Sun et al. 2003). Other studies found that the accuracy of the SRTM surface depended on local topography (Berthier et al. 2006, Falorni et al. 2005, Kääh 2005), with errors being much larger in mountainous terrain than on plane surfaces.

Unfortunately, the SRTM model also has large areas of data voids. According to Hall et al. (2005), these voids make up 0.3% of the total dataset analyzed in their study of the United States, but for rugged terrain, such as some regions of

Nepal, they can amount to up to 30% of the area. Most data voids are less than 5 data pixels in size (Hall et al. 2005). The larger voids belong to one of two categories. Many voids occur on flat level terrain and correspond to water bodies. Water surfaces produce radar signal scattering, which makes it impossible for the interferometer to detect meaningful reflections. The second category of large data voids coincides with steep slopes in mountainous terrain. For surface inclinations above  $20^\circ$ , the frequency of data voids increases because of radar shadowing.

One region, where radar shadowing affects a large proportion of the area, is the range of the Oman Mountains, at the eastern tip of the Arabian Peninsula. Much of this range is made up of limestone, which forms almost vertical cliffs of often more than 1000 m around the eroded center of the range. Most settlements of the region are located near these cliffs, which are the main hydrological reservoir of the region (Buerkert et al. 2005, Siebert et al. 2005). Many of these oases thus lie in SRTM data voids (Fig. 2.1), making the SRTM model unsuitable for hydrologic modeling. To improve the applicability of the SRTM surface for such purposes, several attempts have been undertaken to fill the data voids. These differ in the type of data used to fill the gap and in the methodology applied to achieve this.

### *2.1.1. Methods to fill the voids*

For small data voids, which account for the majority of holes (Hall et al. 2005), simple interpolation of the values around the edges is a reasonable strategy that has been applied successfully. For water bodies, which were prone to voids in the original dataset, the elevations of the water surface have been leveled in the release of the finished version of the SRTM DEM (Slater et al. 2006). The remaining data voids are those that arise from rugged topography. These holes are mostly too large to simply be interpolated from the edges and cannot be substituted by a surface of constant elevation.

They thus need to be filled with topographic information from other sources. Global elevation models are only available at very coarse resolution, so local or regional models have to be used. Kääb (2005) used a local DEM derived from ASTER satellite images, whereas researchers at the International Center for Tropical Agriculture (CIAT) used various local DEMs or the global SRTM30 with a 30" resolution to fill the SRTM voids (Jarvis et al. 2004). To our knowledge, all approaches to filling the voids have so far been based on digital elevation models rather than non-digital topographic maps.

The methods used to merge these auxiliary grids with the SRTM model also vary. Kääb (2005) simply replaced SRTM no data cells with values from the alternative DEM. This process cannot be recommended for most datasets, since most elevation surfaces differ from the SRTM surface by a vertical bias. A more sophisticated approach is the fill and feather technique, in which the void-specific bias of the alternative surface is removed by adding a constant, and the surfaces are then feathered at the edges to provide a seamless transition. This



method provides smooth DEMs, but has the disadvantage that it corrupts the presumably correct SRTM surface at the void edges and cannot account for varying vertical biases within the void. Such variable biases, however, are likely to occur in older elevation models or when a surface is derived by optical interpretation of stereo images. A more promising approach is the delta surface fill method, proposed by Grohman et al. (2006). The delta surface in this method is used to remove the vertical bias of the auxiliary DEM. For the central area of a void, the delta surface is assigned a mean value representing the mean vertical difference between the SRTM and the fill surface. The outer 20 to 30 pixels of the void are then interpolated from the fill surface and the edge of the SRTM outside the void. This method preserves the original values of the SRTM model, while providing a smooth transition.

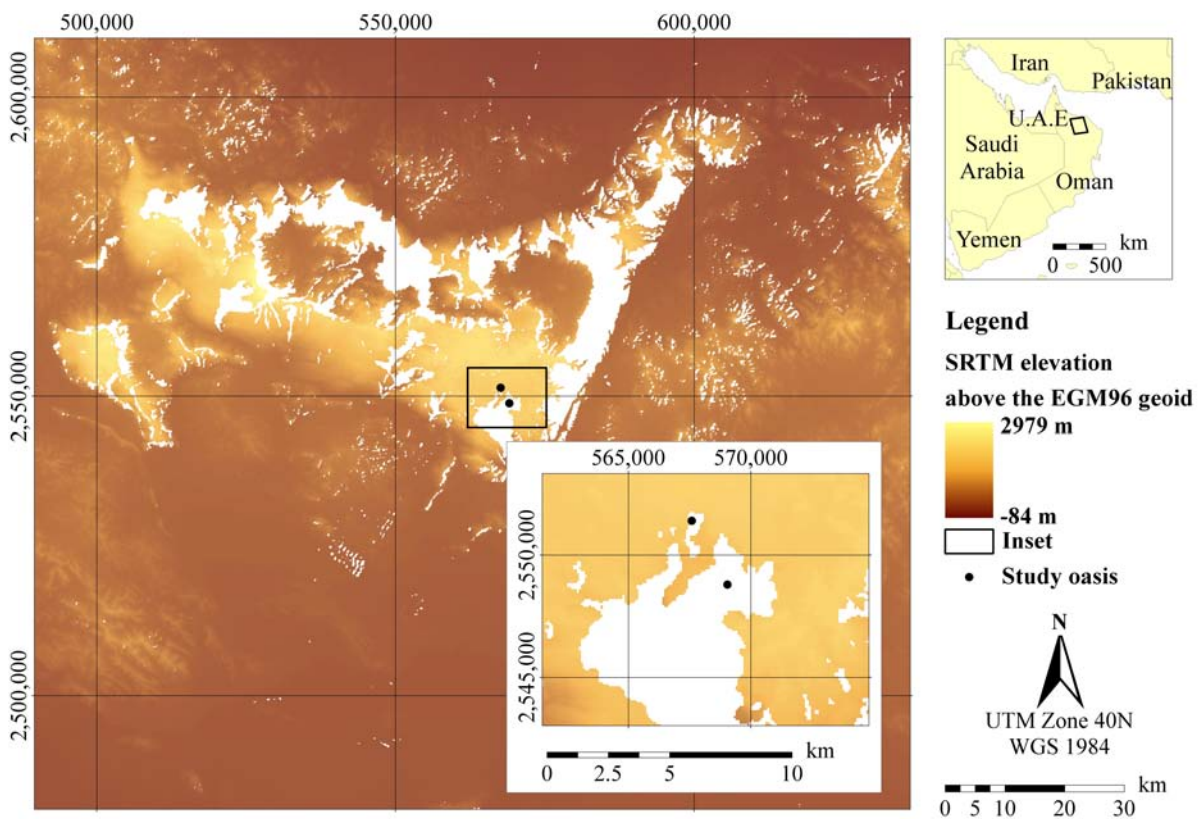


Figure 2.1. SRTM surface of the central part of the Oman Mountains, showing the data voids (white areas) and the locations of two mountain oases in these voids (magnified in the inset). The map in the upper right corner shows the location of the study area on the Arabian Peninsula.

In this study, we use a DEM derived from topographic maps, from which only the void areas were digitized to fill the SRTM voids in the Oman Mountains. To merge the SRTM surface with this auxiliary DEM, we use a method that resembles the delta surface fill method, but is based on a Triangular Irregular Network (TIN) surface to quantify the pixel-specific difference between the surfaces.



To illustrate our method description, we include two figures (Fig. 2.3 and Fig. 2.4) to clarify the sequence of processes and the functions of the various elements of the method. We use a dataset of GPS ground control points to compare the resulting DEM with the original topographic maps and the interpolated SRTM surface published by CIAT (Jarvis et al. 2006).

## 2.2 Materials

### 2.2.1. Study area

The Oman Mountains are a rugged desert mountain range forming a 600-km long arch spanning the northern part of the Sultanate of Oman and the United Arab Emirates, on the Eastern tip of the Arabian Peninsula (Fig. 2.1). The main arc of the mountain range consists of formerly plane limestone formations and underlying sediments, which were warped upwards by the opening of the Red Sea in the Eocene around 35 million years ago. Since then, erosion of the central area of the range has formed an extensive basin, around which the full thickness of the limestone formations has been exposed. The resulting rock faces, steep slopes and deep valleys present a major challenge for the SRTM approach and are the target of this study. The study area covered the entire mountain range, including the Musandam Peninsula, the Batinah Coastal Plain and part of the interior desert, ranging from 26°30'N to 21°20'N in north–south direction and from 59°50'E to 55°10'E from east to west.

### 2.2.2. SRTM data

Finished grade C-band SRTM data for the region with a resolution of 3" were obtained from the United States Geological Survey (USGS 2002). Terrain elevations specified by the SRTM surface were between – 84 and 2979 m above the EGM96 geoid. Of our area of interest, 2.6% of the total dataset of 206,823 km<sup>2</sup> was void, mostly concentrated in the interior of the mountain range, with the size of the two largest voids amounting to 255 and 225 km<sup>2</sup> (Fig. 2.1).

### 2.2.3. Russian topographic maps

Between the 1950s and 1980s, the Russian military conducted extensive mapping operations all over the world leading to a wealth of topographic information covering most of the globe at varying scales. The results of these surveys became available to the public after the demise of the Soviet Union. For the region of the Oman Mountains, we obtained 16 map sheets at a scale of 1:200,000 with elevations given as 40-m contour lines from a German distributor of these maps (Därr Expeditionsservice GmbH, Munich, Germany). All maps use the Krassowsky ellipsoid and the Pulkovo 1942 datum.

### 2.2.4. Hole-filled SRTM data from CIAT

The International Center for Tropical Agriculture (CIAT), a member of the Consultative Group for International Agricultural Research (CGIAR), has published a modified version of the SRTM data, in which all holes have been filled (CIAT 2004, Jarvis et al. 2006). For filling the voids, several local elevation models were used where available, whereas for most of the land surface, the global SRTM30 model formed the basis for filling the holes. To our knowledge, this DEM is the only SRTM product covering the full extent of the SRTM dataset, in which all holes have been filled. At this point, the CIAT model is therefore the standard, with which other void-filling efforts have to be compared.

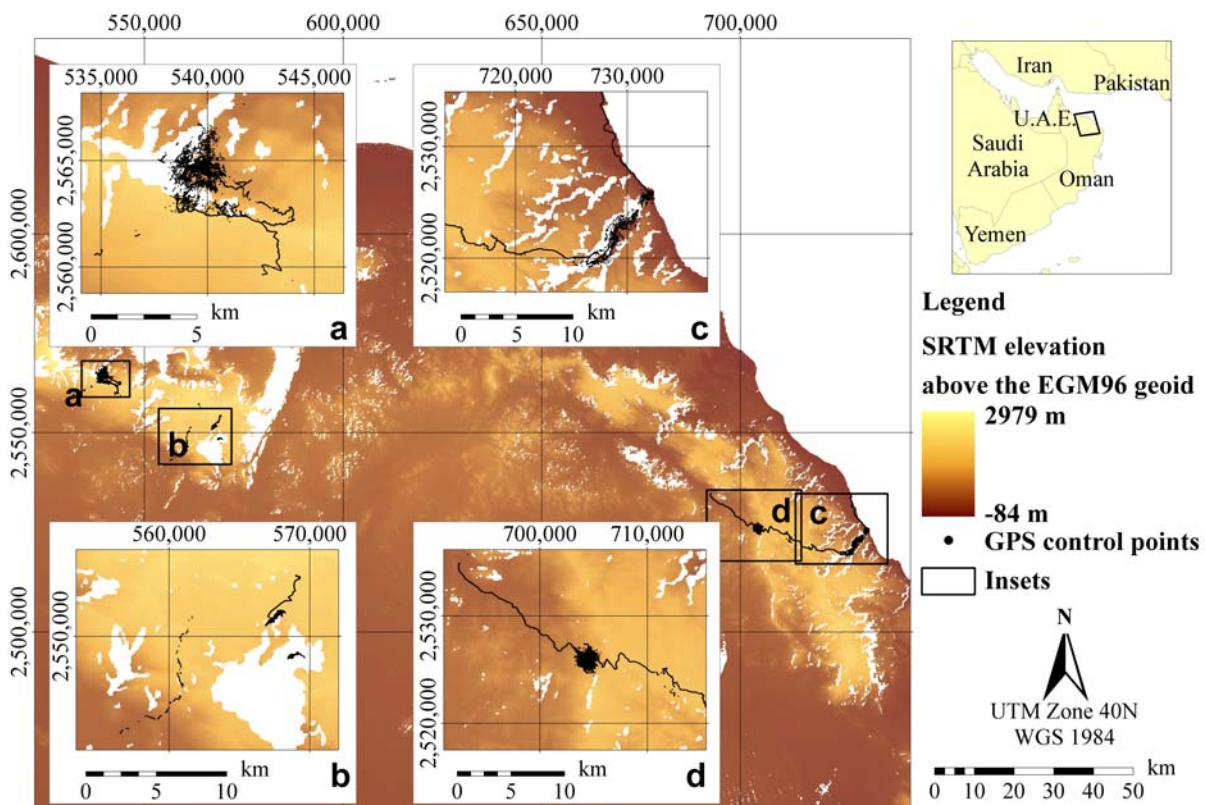


Figure 2.2. Location of the GPS control points in the Oman Mountains. The insets a–d show the surroundings of the oases, where most of the positions were recorded. The small map in the upper right corner shows the location of the large map window on the Arabian Peninsula.

### 2.2.5. GPS control points

To evaluate the accuracy of the three existing elevation models and compare them to the model derived from our new method, we used 187,500 GPS survey points collected over seven years at several sites in the Oman Mountains (Fig. 2.2). Most of these points were recorded using Differential GPS (Trimble Pro XRS and Trimble GeoExplorer II, Trimble Navigation Limited, Sunnyvale, CA, USA), while some points were measured remotely from known GPS positions,

using a Leica Vector range finder (Vecronix AG, Heerbrugg, Switzerland). These points are centered around several mountain oases, the agricultural systems of which we investigated (Buerkert et al. 2005, Luedeling et al. 2005a, Nagieb et al. 2004a), but span large parts of the mountain range both inside (13.9% of all measured points) and outside (86.1%) of SRTM data voids. The GPS points covered an elevation range from 1 to 2375 m above EGM96 sea level.

Complete coverage of such a large area with GPS positions is impossible, and finding sample locations that are representative of the entire area is very difficult. Besides, our GPS measurements were not taken primarily for the purpose of validating elevation models, but for the study of mountain oases. Consequently, the sample locations are particularly concentrated around a few settlements. Nevertheless, since the sample size is fairly large, the full range of elevations, bearings and slopes that occur in the mountains is covered by an adequate number of positions (Table 2.1), allowing a validation of the different DEMs.

## 2.3 Methods

### 2.3.1. The TIN delta surface fill method

Elevation datasets for the Oman Mountains are scarce. The region has only been mapped in the context of global mapping endeavors, such as those by the Russian military. The Russian maps, however, have two major disadvantages. They only exist as paper maps and, as can easily be seen by visual comparison, they do not correspond very well to absolute elevations specified in other sources. The reason for this is probably the kind of equipment used for mapping as well as the large extent of the survey, which might have offset accuracy at times. For the Oman Mountains, it seems that the maps accurately specify the sea surface, an obvious reference, but decrease in absolute accuracy towards the country's interior. This varying bias makes it impossible to directly replace SRTM data voids with values derived from the Russian dataset, as done by Kääh (2005), who merged SRTM and ASTER data. Unlike the absolute elevations above a fixed reference level, the elevations of topographic features relative to the surrounding area are nevertheless likely to be good approximations of the true elevations. We therefore attempted to develop a method to extract these relative elevations from the Russian maps and combine them with the more accurate absolute elevations of the SRTM model. Thereby we generated a fill surface for the SRTM data voids, which combines the absolute accuracy of the SRTM DEM with the relative accuracy of the Russian topographic maps.

This is achieved by extracting the points bordering the holes from both the Russian and the SRTM DEMs, and calculating Triangular Irregular Networks (TIN) from these points for both datasets. In the creation of a TIN, the original elevation points remain unaltered, and the spaces between them are filled by triangular planes connecting these points. By converting these TINs to rasters with the SRTM cell size, we obtain base elevations for both surfaces, the pixel-

specific difference of which represents the local vertical bias of the Russian model. Subtracting the Russian base surface from the Russian elevation model then yields the relative elevation of the Russian model above the base surface spanning the void. Adding this difference surface to the SRTM base surface results in an elevation model that accounts for the varying vertical bias within the void and can seamlessly be merged with the SRTM model (Fig. 2.3).

Table 2.1. Frequencies of different levels of elevation, slope and slope bearing (aspect) among the GPS control points and on the OmanTopo surface

	<b>GPS points (%)</b>	<b>OmanTopo (%)</b>
<i>n</i>	187,500	22,576,394
<i>Elevation</i>		
< 500 m	4.3	83.1
500–1000 m	30.9	13.0
1000–1500 m	48.2	2.6
1500–2000 m	9.5	0.9
> 2000 m	7.1	0.3
<i>Slope</i>		
Low (0–10°)	34.2	84.5
Moderate (10–20°)	44.0	8.4
Steep (20–30°)	12.8	4.8
Very steep (30–60°)	9.0	2.3
<i>Slope bearing</i>		
N	8.6	10.9
NE	13.3	12.1
E	19.5	12.1
SE	9.9	12.9
S	6.1	13.1
SW	8.5	12.8
W	22.1	13.9
NW	12.0	12.1

*n* represents the number of GPS points and the number of OmanTopo raster cells, respectively.

### 2.3.2. Detailed method description

To create the DEM for filling the voids (referred to as ‘fill’ hereafter), the Russian topographic maps were scanned and georeferenced to the Russian ellipsoid and datum specified above using ArcGIS 9.1 (ESRI, Redlands, CA, USA). We extracted the voids from the SRTM surface into a feature layer using the ArcGIS Spatial Analyst's ‘Is Null’ tool, reprojected this layer to fit the Russian datum, and manually digitized the contour lines for the area covering the data voids plus a buffer of about 500 m around each void from the Russian maps. These contours were reprojected to UTM Zone 40N, the Universal Transverse Mercator projection suitable for this longitude, and interpolated

using the ‘Topo to Raster’ tool of the ArcGIS 3D Analyst. To avoid interference patterns in the final DEM, care was taken that from the beginning all raster surfaces were created with cell sizes and cell locations corresponding exactly to those of the SRTM dataset. This was mainly achieved by adjusting the settings in ArcGIS' Analysis Environment, except for the ‘Topo to Grid’ command, which required a manual approach. For this step, a rectangle corresponding to the extent of the area of interest was extracted from the SRTM surface, converted to a polygon layer and buffered by half an SRTM cell size. This extent was then fed into the Analysis Environment.

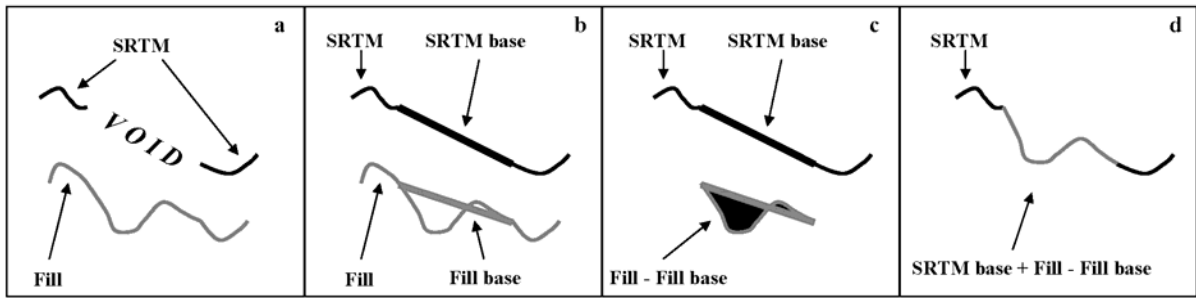


Figure 2.3. Illustration of the process used to merge the two elevation surfaces. For the void area in the SRTM model and for the corresponding region in the fill surface (a), TINs are calculated from points at the edges to create base surfaces (b). The fill base surface is then subtracted from the fill surface (c) and added on top of the SRTM base surface (d) to obtain a seamless DEM.

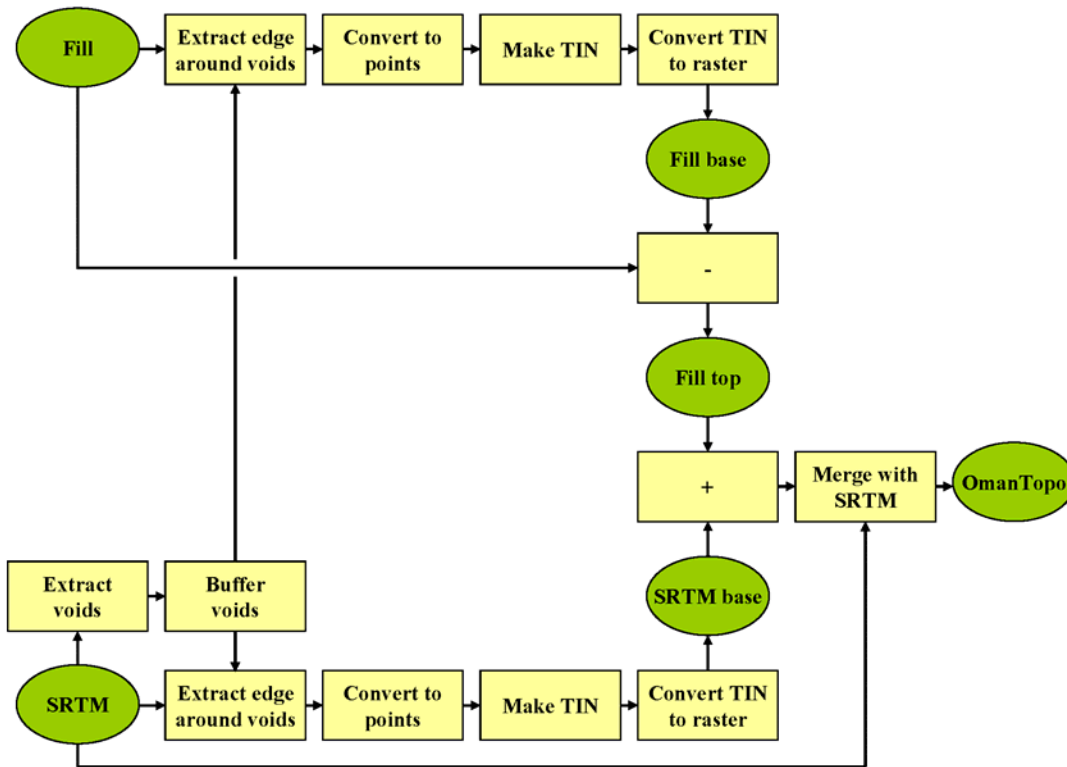


Figure 2.4. Overview of the geoprocessing operations carried out to derive the OmanTopo surface from the SRTM DEM and the fill surface derived from Russian military maps. Rectangles indicate processes, whereas ovals are used to depict important raster surfaces.

We extracted the grid cells contained in a 170-m buffer around the data voids from both the SRTM and the fill surface and converted them to points. From these points, we created TIN layers, which were transformed into grids of SRTM extent and cell size. These raster layers constitute base surfaces, which can be compared to obtain a linear approximation of the vertical bias between each pixel of the SRTM and the corresponding pixel of the fill surface.

We subtracted the fill base surface from the fill surface, obtaining a raster that describes the relative difference between the fill surface and the fill base level inside the specific data void. This relative surface was added on top of the SRTM base surface to generate an elevation surface that can seamlessly be mosaicked into the holes of the SRTM model. Subsequently, we replaced the no data cells of the SRTM surface with the values from this new surface. Finally, we replaced all data cells containing negative elevations with interpolated values to obtain the final product, which will be referred to as OmanTopo in the following. An overview of all geoprocessing operations is given in Fig. 2.4.

### 2.3.3. Validation and analysis of the DEMs

A first quality assessment of the OmanTopo DEM was done visually, based on a shaded relief calculated from the OmanTopo surface for better visualization (Fig. 2.5). For more quantitative validation of the DEM, we used our reference dataset of 187,500 differential GPS positions. For each position, we extracted the corresponding values of the SRTM DEM, the CIAT DEM, the Russian fill surface and the new OmanTopo DEM from the respective surfaces. In addition to these, slope and slope bearing (aspect) were calculated from the OmanTopo DEM and also assigned to each GPS point. We calculated the differences between each surface and the GPS elevations. These differences will be referred to as the  $\Delta$ GPS of the DEMs. We choose this term, because the GPS positions have a much higher resolution than the raster cells, and the differences thus cannot be referred to as the error of the DEM. The  $\Delta$ GPS values were then analyzed using the SPSS 12.0 statistics package (SPSS Inc., Chicago, IL, USA).

We calculated the means and standard deviations of the  $\Delta$ GPS for each surface. The mean is a good measure of the average absolute deviation from the true elevation, whereas the standard deviation describes the relative accuracy of a DEM. For CIAT and OmanTopo, we differentiated between GPS locations inside and outside the holes, whereas SRTM elevations only existed outside and fill elevations only inside the holes. Since several authors reported a bearing-specific bias of the SRTM model, we also calculated the respective means and standard deviations for each of eight bearings (N, NW, W, SW, S, SE, E, and NE).

## 2.4 Results

Visual assessment of the OmanTopo surface did not reveal major flaws (Fig. 2.5). Overlay with a hillshade often highlights topographic steps arising from



incorrect merging of DEMs. The only visual disturbance was a slight striping pattern in the shaded relief, which seems to originate from the merging of SRTM tiles from different longitudes. The SRTM tiles downloaded from USGS have slightly different cell sizes, and the resampling necessary for merging the tiles may have caused interference, which produced the striping.

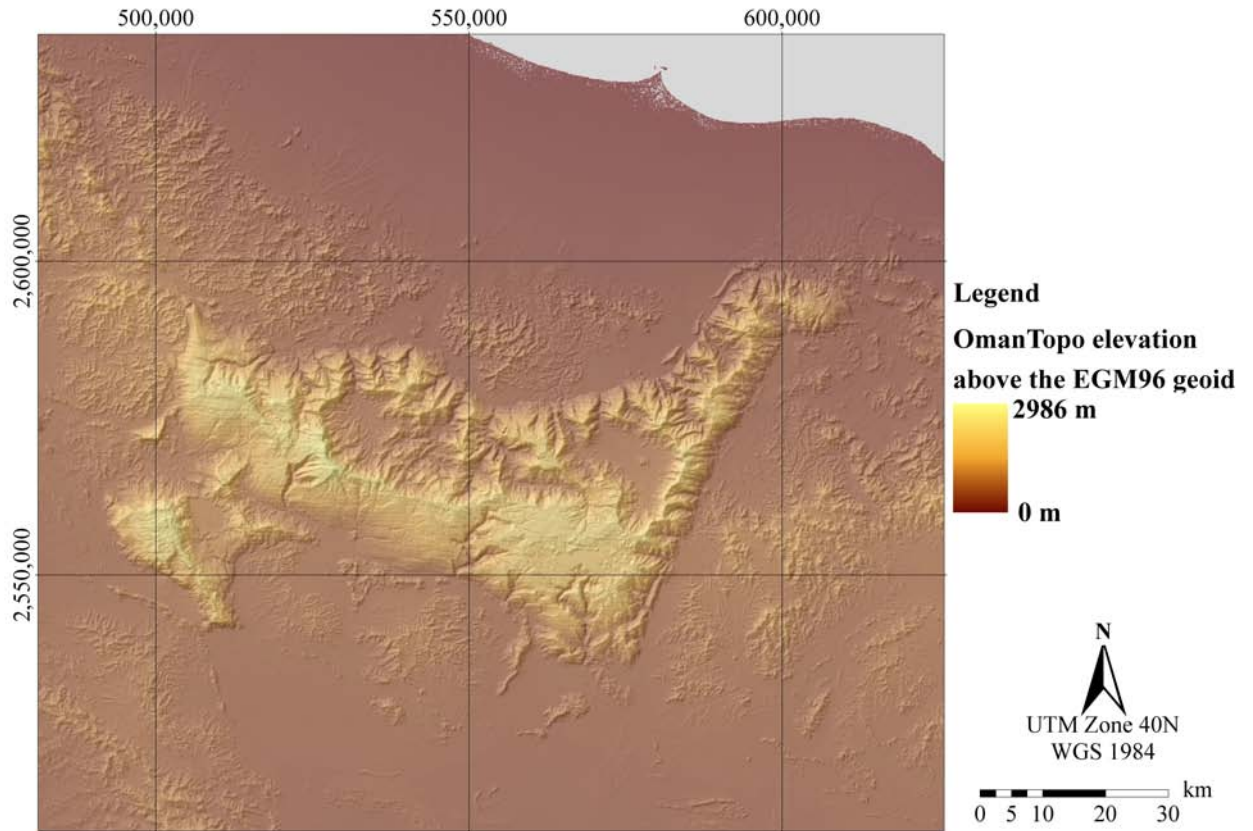


Figure 2.5. Shaded relief of OmanTopo for visual inspection.

Comparison of the mean values and standard deviations of the  $\Delta$ GPS values inside and outside of the SRTM data voids showed that the OmanTopo surface underestimated the GPS elevations by 7.8 m on average, whereas the fill DEM lay considerably above the GPS heights (+ 84.3 m) and the CIAT surface almost matched the GPS elevations (+ 2.8 m) (Table 2.2). Standard deviations of the  $\Delta$ GPS values were comparable for the OmanTopo and CIAT surfaces outside the void areas (27.7 and 24.1 m), but much lower for the fill surface (69.2 m) and OmanTopo (76.3 m) than for the CIAT DEM (128.0 m) in the areas, where the SRTM surface had no data (Table 2.2).

Analysis of the bearing-specific bias of the surfaces showed that  $\Delta$ GPS standard deviations outside the voids were between 14 and 33 m for CIAT, OmanTopo and SRTM, and tended to be highest on north and northeast facing slopes (Fig. 2.6). Inside the void areas, differences between the surfaces were much greater. The lowest  $\Delta$ GPS standard deviations occurred in the fill surface, followed closely by OmanTopo. The CIAT DEM had much larger  $\Delta$ GPS standard deviations. The bias due to bearing was strongest in north and west facing directions for CIAT and OmanTopo, and in northwest direction for the

fill surface (Fig. 2.6). The  $\Delta$ GPS values also varied according to slope, with steeper slopes leading to higher deviations from the mean values (Table 2.3).

Table 2.2. Means and standard deviations of  $\Delta$ GPS values for the DEMs derived from the method applied in this study (OmanTopo), the Shuttle Radar Topography Mission (SRTM), the SRTM-based interpolated surface released by CIAT (CIAT) and the Russian topographic map (Fill)

		OmanTopo (m)	SRTM (m)	CIAT (m)	Fill (m)
Inside void	Mean	- 16.3	-	+ 10.6	+ 84.3
	Std. dev.	76.3		128.0	69.2
Outside void	Mean	- 6.4	- 6.4	+ 1.6	-
	Std. dev.	27.7	27.7	24.1	
Total	Mean	- 7.8	- 6.4	+ 2.8	+ 84.3
	Std. dev.	38.4	27.7	52.8	69.2

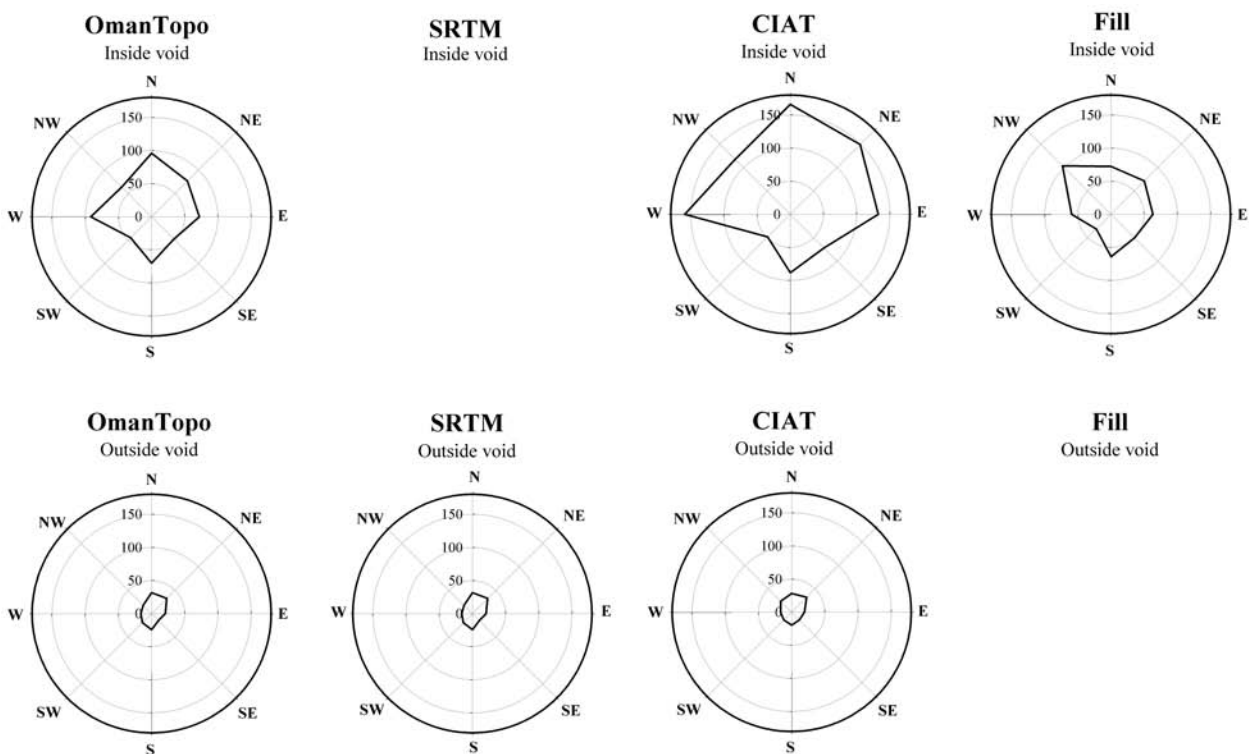


Figure 2.6. Standard deviations of the  $\Delta$ GPS values derived from the four surfaces, inside and outside the void areas in the SRTM model, according to the bearing of the slope at the GPS location.



Table 2.3. Mean values and standard deviation of the  $\Delta$ GPS values, according to steepness of slope, for the four surfaces

Slope		OmanTopo		SRTM		CIAT		Fill	
		Inside void (m)	Outside void (m)	Inside void (m)	Outside void (m)	Inside void (m)	Outside void (m)	Inside void (m)	Outside void (m)
Low (0–10°)	Mean	+ 8.2	– 6.5	–	– 6.5	+ 87.3	– 2.2	+ 11.7	–
	Std. dev.	58.8	14.1		14.1	123.8	14.7	57.3	
Moderate (10–20°)	Mean	– 10.9	– 0.1	–	– 0.1	– 15.4	+ 5.4	+ 79.7	–
	Std. dev.	43.4	20.5		20.5	97.0	18.4	42.2	
Steep (20–30°)	Mean	– 22.5	– 7.0	–	– 7.0	– 38.0	+ 7.0	+ 98.8	–
	Std. dev.	66.0	38.5		38.5	123.1	36.8	67.2	
Very steep (30–60°)	Mean	– 21.9	– 61.6	–	– 61.6	+ 60.6	+ 15.5	+ 90.1	–
	Std. dev.	106.4	58.1		58.1	140.2	57.7	87.5	

## 2.5 Discussion

The comparison of the SRTM dataset to the measured GPS elevations revealed that the absolute elevation of the SRTM DEM is 6.4 m below the surface indicated by the GPS readings (Table 2.2). This corresponds well to the absolute height error estimated for Africa (including the Arabian Peninsula) by Rodriguez et al. (2005), who determined the continental error to be 5.6 m. The absolute error of the CIAT model was + 2.8 m, suggesting that CIAT (Jarvis et al. 2006) added a correction to the original SRTM surface. Our initial impression that the Russian topographic maps overestimated the true elevation was confirmed by the analysis, which determined mean elevations of the maps to be 84 m higher than the GPS positions. Nevertheless, inside the SRTM data voids, the  $\Delta$ GPS values obtained from the fill surface showed a much lower standard deviation (69 m) than those from the CIAT surface (128 m), indicating that the fill surface represented the relative topography better than the CIAT DEM. The OmanTopo surface inherited most of the accuracy from the fill surface, resulting in a standard deviation of the  $\Delta$ GPS values of 76 m (Table 2.2). Nevertheless, for the area corresponding to the no data cells in the SRTM model, OmanTopo's  $\Delta$ GPS values had a much higher standard deviation than for the area that was covered by the SRTM. The surface developed in this study does, however, provide a much more accurate fill for the SRTM voids than the DEM published by CIAT.

In part, the fairly large  $\Delta$ GPS standard deviation might arise from the method used to calculate it. We compared point measurements with mean values for each raster cell. Since the spatial resolution of the grid was 81 m, the cell size corresponds to an area of about 0.65 ha, which is represented by only one value in the grid. Within a level raster cell, accuracy could be measured reliably by comparing a GPS position with the DEM surface. For sloping land, however, the GPS position would be at one specific elevation within the range spanned in the cell. For a slope of 14°, the average inclination of the raster cells covered by

GPS control points, the range of altitude that can be expected is about 29 m. For a slope of  $45^\circ$ , the maximum elevation range within one cell amounts to 115 m (Fig. 2.7). Consequently, we have to expect higher standard deviations of the  $\Delta$ GPS values inside the void areas, since slopes are generally steeper than outside the voids. In fact, the average slope at GPS positions outside the voids is  $13^\circ$ , compared to  $25^\circ$  inside the voids. This corresponds to potential elevation ranges per raster cell of 26 and 53 m, respectively. For the cardinal directions (N, E, S, W), these numbers are slightly lower (18 and 38 m), since the distance between the center of the square raster cell and the edge in slope direction is shorter than for the other directions (NE, SE, SW, NW).

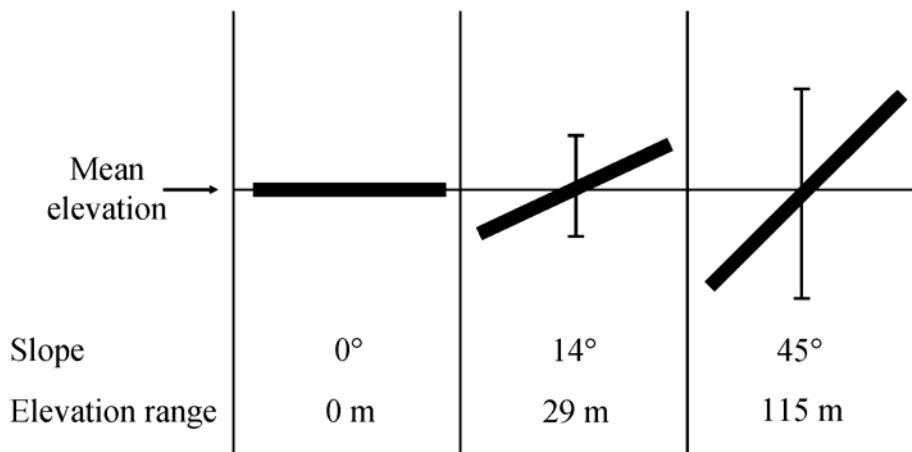


Figure 2.7. Effect of raster cell inclination (slope) on the elevation range spanned in one raster cell. The elevation ranges given apply to the directions NE, SE, SW and NW. For the cardinal directions, they are 0 m, 20 m and 81 m, respectively.

For the areas outside the SRTM voids, the bearing-specific uncertainties were small (Fig. 2.6) and distributed among the different aspects in a similar manner as reported previously (Jarvis et al. 2004). Analysis of the areas inside the data voids, however, shows the quality of our new method. Even though the size of the  $\Delta$ GPS standard deviations differs between OmanTopo and CIAT, the distribution pattern between the bearings is similar for both DEMs. The biggest standard deviations of the  $\Delta$ GPS values occur at bearings N, W, NE and E. The steepest slopes inside the voids face to the N, NE and E (on average  $36.4^\circ$ ,  $28.7^\circ$  and  $27.9^\circ$ , respectively), which makes the large standard deviation in western direction surprising. It is striking that the bearing-specific bias of the fill surface does not correspond to the DEMs derived from the shuttle mission (SRTM, CIAT, OmanTopo). It is highest in NW, N, and NE direction, but also has a strong southern component, which might originate from the Russian surveying and mapping techniques. In filling the SRTM voids with this dataset, however, the TIN-based method removed this bias, so that the bearing-specific distribution of  $\Delta$ GPS standard deviations corresponds in its shape to the respective distribution for the CIAT surface. This shows that the TIN-based delta fill surface method successfully combined the absolute elevations of the

SRTM surface with the relative elevations of the fill surface without introducing the error of the fill surface into the DEM.

The data analysis revealed that the SRTM model contains several cells in Musandam, at the northern edge of the Oman Mountains, which were assigned negative elevations between  $-1$  and  $-84$  m. Most of these cells lie directly at the coast in an area with very steep shorelines. We assume that the shoreline mask used to clip the land surface from the original SRTM dataset (Slater et al. 2006) was inaccurate in this region. For the OmanTopo surface, we corrected this.

The CIAT surface approximately retained the resolution of the unfinished SRTM dataset, which is slightly coarser than that of the finished SRTM DEM. The CIAT product is good for areas, for which the SRTM delivered reliable data. CIAT diminished the vertical bias of the SRTM DEM for the region and also took care of the anomalously low elevations in Musandam. For the areas that are void in the SRTM dataset, however, the approximation achieved by OmanTopo is much better.

This study shows that our method, which realizes the transition between the incomplete dataset and the fill surface by using TINs, yields useful results. It is particularly useful for datasets, about which only little is known. The delta fill surface method described by Grohman et al. (2006) relies on knowledge of the average difference between the incomplete DEM and the fill surface. This requires that this difference be calculated, based on a complete DEM. Digitizing topographic maps is a time-consuming process. The TIN-based approach allows us to restrict the digitizing to the areas that are to be filled plus a small buffer zone around them. The average difference between the surfaces remains unknown, but is irrelevant to this method. Knowledge of the ellipsoid or geoid, above which the fill elevations are calculated is also unimportant and complicated adjustments do not have to be carried out, since the TIN-based method only considers the relative elevations of the fill.

Moreover, it can account for varying differences between the incomplete DEM and the fill surface over the whole extent of the DEM and even within a specific void. The delta fill surface method assumes an average bias of the fill surface, or the specific void, and interpolates the values at the void edge to merge into the frame. In the case of varying biases within the hole, this can create unrealistic inclinations near the void edges. Our TIN-based approach simply uses a linear interpolation created by the TIN to realize a smooth transition between the surfaces.

For older maps, arbitrary variations in absolute height must be expected. We assume that the Russian military used aerial photographs taken by planes and manually drew contour lines using stereographic techniques. Such maps will almost unavoidably have varying biases at different map locations. If they are to be merged with other datasets, they require estimation of the pixel-specific difference between both elevation models. Our TIN-based approach provides this.

The surveys conducted by the Russian military produced a wealth of topographic information. It seems that the relative vertical accuracy of these surveys, especially in mountainous terrain, has not been matched by any other survey at that scale, the results of which are publicly available. The Russian data is relatively easily available and at least one commercial GIS data provider has begun to include DEMs derived from these maps into his stock.

## 2.6 Conclusions

The TIN-based delta surface is a versatile tool to fill the voids in the SRTM dataset, even with fill surfaces that have varying absolute elevation errors. Traditional paper maps constitute a wealth of topographic information that may for many regions be superior to all available DEMs, making such maps the most suitable datasets for filling the SRTM data voids.

The TIN delta fill method would be a valuable contribution to the CIAT dataset, which is already very accurate in the areas covered by SRTM data, but could benefit from this new method to help improve DEM quality in the SRTM voids.

## Acknowledgments

We gratefully acknowledge the help of Uta Dickhoefer, Ariane Grotz, Henning Jahn, Kristiyan Asenov and Alexander Matecki, who tirelessly digitized portions of the Russian topographic maps.

## References

- Berthier E, Arnaud Y, Vincent C and Remy F (2006). Biases of SRTM in high-mountain areas: Implications for the monitoring of glacier volume changes. *Geophysical Research Letters* 33(8).
- Bourgine B and Baghdadi N (2005). Assessment of C-band SRTM DEM in a dense equatorial forest zone. *Comptes Rendus Geoscience* 337(14), 1225-1234.
- Brown CG, Sarabandi K and Pierce LE (2005). Validation of the shuttle radar topography mission height data. *IEEE Transactions on Geoscience and Remote Sensing* 43(8), 1707-1715.
- Buerkert A, Nagieb M, Siebert S, Khan I and Al-Maskri A (2005). Nutrient cycling and field-based partial nutrient balances in two mountain oases of Oman. *Field Crops Research* 94(2-3), 149-164.
- CIAT (2004). Hole-filled seamless SRTM data v1. Accessed on 03 August 2005 at [http://gisweb.ciat.cgiar.org/sig/90m\\_data\\_tropics.htm](http://gisweb.ciat.cgiar.org/sig/90m_data_tropics.htm).
- Falorni G, Teles V, Vivoni ER, Bras RL and Amaratunga KS (2005). Analysis and characterization of the vertical accuracy of digital elevation models from the Shuttle Radar Topography Mission. *Journal of Geophysical Research-Earth Surface* 110(F2).
- Grohman G, Kroenung G and Strebeck J (2006). Filling SRTM voids: The delta surface fill method. *Photogrammetric Engineering and Remote Sensing* 72(3), 213-216.
- Hall O, Falorni G and Bras RL (2005). Characterization and quantification of data voids in the shuttle radar topography mission data. *IEEE Geoscience and Remote Sensing Letters* 2(2), 177-181.

- Hofton M, Dubayah R, Blair JB and Rabine D (2006). Validation of SRTM elevations over vegetated and non-vegetated terrain using medium footprint lidar. *Photogrammetric Engineering and Remote Sensing* 72(3), 279-285.
- Jarvis A, Reuter H, Nelson A and Guevara E (2006). Hole-filled seamless SRTM data v3. Accessed on 16 October 2006 at <http://srtm.csi.cgiar.org/>.
- Jarvis A, Rubiano J, Nelson A, Farrow A and Mulligan M (2004). Practical use of SRTM data in the tropics: Comparisons with digital elevation models generated from cartographic data. International Center for Tropical Agriculture (CIAT).
- Kääb A (2005). Combination of SRTM3 and repeat ASTER data for deriving alpine glacier flow velocities in the Bhutan Himalaya. *Remote Sensing of Environment* 94(4), 463-474.
- Kobrick M (2006). On the toes of giants - How SRTM was born. *Photogrammetric Engineering and Remote Sensing* 72(3), 206-210.
- Kocak G, Buyuksalih G and Oruc M (2005). Accuracy assessment of interferometric digital elevation models derived from the Shuttle Radar Topography Mission X- and C-band data in a test area with rolling topography and moderate forest cover. *Optical Engineering* 44(3).
- Leblanc M, Favreau G, Maley J, Nazoumou Y, Leduc C, Stagnitti F, van Oevelen PJ, Delclaux F and Lemoalle J (2006). Reconstruction of Megalake Chad using Shuttle Radar Topographic Mission data. *Palaeogeography Palaeoclimatology Palaeoecology* 239(1-2), 16-27.
- Luedeling E, Nagieb A, Wichern F, Brandt M, Deurer M and Buerkert A (2005). Drainage, salt leaching and physico-chemical properties of irrigated man-made terrace soils in a mountain oasis of northern Oman. *Geoderma* 125(3-4), 273-285.
- Menze BH, Ur JA and Sherratt AG (2006). Detection of ancient settlement mounds: Archaeological survey based on the SRTM terrain model. *Photogrammetric Engineering and Remote Sensing* 72(3), 321-327.
- Nagieb M, Häser J, Siebert S, Luedeling E and Buerkert A (2004). Settlement history of a mountain oasis in northern Oman - Evidence from land use and archaeological studies. *Die Erde* 135(1), 81-106.
- Rodriguez E, Morris CS and Belz JE (2006). A global assessment of the SRTM performance. *Photogrammetric Engineering and Remote Sensing* 72(3), 249-260.
- Rodriguez E, Morris CS, Belz JE, Chapin EC, Martin JM, Daffer W and Hensley S (2005). An assessment of the SRTM topographic products, Technical Report JPL D-31639, Jet Propulsion Laboratory, Pasadena, CA, USA.
- Siebert S, Häser J, Nagieb M, Korn L and Buerkert A (2005). Agricultural, architectural and archaeological evidence for the role and ecological adaptation of a scattered mountain oasis in Oman. *Journal of Arid Environments* 62(1), 177-197.
- Simard M, Zhang KQ, Rivera-Monroy VH, Ross MS, Ruiz PL, Castaneda-Moya E, Twilley RR and Rodriguez E (2006). Mapping height and biomass of mangrove forests in Everglades National Park with SRTM elevation data. *Photogrammetric Engineering and Remote Sensing* 72(3), 299-311.
- Slater JA, Garvey G, Johnston C, Haase J, Heady B, Kroenung G and Little J (2006). The SRTM data "finishing" process and products. *Photogrammetric Engineering and Remote Sensing* 72(3), 237-247.
- Smith B and Sandwell D (2003). Accuracy and resolution of shuttle radar topography mission data. *Geophysical Research Letters* 30(9).
- Sun G, Ranson KJ, Khairuk VI and Kovacs K (2003). Validation of surface height from shuttle radar topography mission using shuttle laser altimeter. *Remote Sensing of Environment* 88(4), 401-411.
- USGS (2002). Shuttle Radar Topography Mission (SRTM) Elevation Data Set. Accessed on 16 October at <http://seamless.usgs.gov/>.

- Valeriano MM, Kuplich TM, Storino M, Amaral BD, Mendes JN and Lima DJ (2006). Modeling small watersheds in Brazilian Amazonia with shuttle radar topographic mission-90 m data. *Computers & Geosciences* 32(8), 1169-1181.
- van Zyl JJ (2001). The Shuttle Radar Topography Mission (SRTM): A breakthrough in remote sensing of topography. *Acta Astronautica* 48(5-12), 559-565.

## Chapter 3

*published in Remote Sensing of Environment (in press)*

# Typology of oases in northern Oman based on Landsat and SRTM imagery and geological survey data

Eike Luedeling<sup>a</sup> and Andreas Buerkert<sup>a</sup>

<sup>a</sup> *Organic Plant Production and Agroecosystems Research in the Tropics and Subtropics, University of Kassel, Steinstr. 19, D-37213 Witzenhausen, Germany*

---

### Abstract

In the desert country of Oman, available water resources are scarce and scattered. In most locations where water can be accessed, this resource is harnessed by oases planted to date palms (*Phoenix dactylifera* L.) and other crops. So far, little is known about the site-specific conditions determining the existence, size and type of these oases. Remote sensing and image processing techniques were used to locate these oases, to characterize the sites according to their topographic, hydrologic and geologic characteristics and to develop a typology of oases in northern Oman.

To derive oasis positions, we calculated the Normalized Difference Vegetation Index (NDVI) of Landsat images covering all of northern Oman, subtracted a regional average NDVI, averaged the resulting grid over 3 x 3 pixels and extracted the brightest of five classes determined by a natural breaks algorithm. A buffer of six pixels was added to the oases and the vegetated area as determined by the NDVI was summarized for these polygons. The oasis detection procedure was validated using Google Earth Pro<sup>®</sup>. Topographic information was derived from data of the Shuttle Radar Topography Mission (SRTM), complemented by digitized Russian military maps, from which mean elevations and elevation range above the oases within a buffer of 2 km were extracted.

Water contributing upslope area and distance to streams with catchments of 10 km<sup>2</sup> and 100 km<sup>2</sup> were derived from the same elevation model. All geologic formations of northern Oman were assigned to one of 7 groups and tested for influence on vegetation surrounding them. Four such geologic settings were identified and described by categorical variables. All input parameters were used to define oasis types based on cluster analysis.

Our algorithm detected 2663 oases in northern Oman, of which 2428 had vegetated areas of more than 0.4 ha, the minimum size for reliable detection. The oases were

subdivided into six groups. ‘Plain Oases’ (49% of all oases) lie mostly in the plains east and west of the mountains, and are fed by groundwater flow in Quaternary sediments. ‘Foothill Oases’ (46%) are scattered over the foothills, where they draw their water from groundwater flow that is channeled by rock formations. ‘Mountain Oases’ (3%) and ‘Kawr Oases’ (0.5%) lie in the mountains, close to an unconform boundary between limestones and confining rocks. ‘Drainage Oases’ (0.3%) are the largest oases in northern Oman. They lie close to a drainage channel, which drains the entire area west of the mountains. Finally, ‘Urban Oases’ (1.7%) consist of parks and sporting facilities, which do not lie in conclusive hydrologic settings.

---

### **3.1 Introduction**

The major part of the Sultanate of Oman is made up of arid to hyperarid desert, and only a very small portion of the country is covered by more than xerophytic vegetation. Locally, however, water is concentrated in special geologic or topographic settings, where farmers have been harnessing this scarce resource for thousands of years by channeling surface flow, tapping springs or draining water-soaked subsoil (Costa 1983). Once made accessible, the water is conducted through intricate systems of irrigation channels to leveled fields, which often lie at considerable distances from the water source.

Most traditional irrigation systems, once established, operate on gravitational flow, without external energy inputs, except for some systems on the Batinah coastal plain, which traditionally used water-lifting techniques based on animal traction. Today, this latter method of water acquisition has been replaced by modern electric or diesel-powered pumping systems (Norman et al. 2001), which now irrigate extensive areas along the coast (Harris 2003). The modern methods quickly led to overuse of water and created problems of aquifer recession, intrusion of salt water into freshwater aquifers and widespread soil salinization on the coastal plain (Cookson and Lepiece 2001). The problems connected with modern pumping techniques make the traditional agricultural systems all the more remarkable, because they managed to survive without evident signs of soil degradation for hundreds or even thousands of years (Siebert et al. 2005). Unlike modern well-based agriculture, these traditional systems could only arise where water could be made accessible using the technologies available at the time of oasis formation. In recent years, these systems have received considerable attention, shedding some light on the factors that ensured the sustainability of oasis agriculture in northern Oman (Gebauer et al. 2007c, Luedeling et al. 2005a, Siebert et al. 2005, Wichern et al. 2004).

To date, however, no systematic studies have been conducted on the factors that allowed oases to form in the first place. Oases are not randomly distributed over the countryside and their existence is likely to reflect specific hydrologic, topographic or geologic conditions. We hypothesized that oasis locations in Oman can be attributed to a limited number of specific geologic, hydrologic or topographic settings, explainable by proximity to geologic units and topographic



features, as well as hydrologic catchment sizes and proximity to intermittent streams, where surface or sub-surface water accumulates. We further hypothesized that it is possible to classify oases accordingly using remote sensing techniques and spatial data processing. The objective of this study therefore was to use such techniques to determine the locations of oases with year-round cultivation in Oman and to develop an oasis typology based on topographic, hydrologic and geologic parameters.

### *3.1.1. Geology of the Oman Mountains*

The geology of northern Oman is very complex (Glennie 2005, Glennie et al. 1974) and some basic information is necessary to understand the effects that geologic setting may have on oasis formation. The following therefore provides a short overview of the mountains' genesis, explaining the origins of the main geologic units represented in the complex stratigraphic column of the mountains (Fig. 3.1).

Between the Late Permian (260-251 million years before present, Ma BP) and the end of the Early Cretaceous (100 Ma BP), the area that is now Oman was covered by a warm shallow sea, which deposited thick limestone sediments, known as the Hajar Supergroup (Robertson and Searle 1990). The Hajar unit overlays a Basement of Pre-Middle Permian age (before 271 Ma BP), which consists of several types of crystalline rocks and ancient sediments (Gass et al. 1990).

In the Campanian (Late Cretaceous, 84 to 71 Ma BP), the area that now constitutes northern Oman was subjected to the rare geologic process of obduction, in which a slab of oceanic crust was thrust upon the continent (Glennie 2005). The remains of the ancient seafloor are called ophiolites. They are present in thick layers east and west of the Oman Mountains, constituting the Samail unit. Along with the ophiolites, the Samail unit transported a large amount of other materials onto the Afro-Arabian Platform. These include sediments from former ocean basins, which were scraped off the seafloor by the overriding tectonic plate and accumulated in an accretionary wedge on the underside of the Samail layer (Ravaut et al. 1997). There is evidence that an entire microcontinent suffered the same fate and was obducted onto the continental shelf. All these materials are referred to as the Hawasina Series. It is mostly made up of sedimentary rocks, which have been intensely folded and faulted during the translocation process, except for the remains of the obducted microcontinent, which constitute the limestones of the Kawr unit (Fig. 3.1).

The obduction process ceased by the end of the mid Late Cretaceous and part of the area was once again covered by a shallow sea, resulting in the deposition of large limestone layers until the late Paleogene (35 Ma BP). Around 35 Ma BP, the opening of the Red Sea divided the Afro-Arabian Plate, separating Africa from Arabia. The pressure build-up created by this separation was partly relieved by warping the eastern margin of the Arabian Plate upwards, forming the giant anticline that now constitutes the Oman Mountains. The final structure

of the range was then determined by erosion processes, which freed some underlying rock formations from the obducted layers, and exposed large areas of Hajar limestones. These fall steeply into a central basin, the bottom of which is made up of Basement rocks.

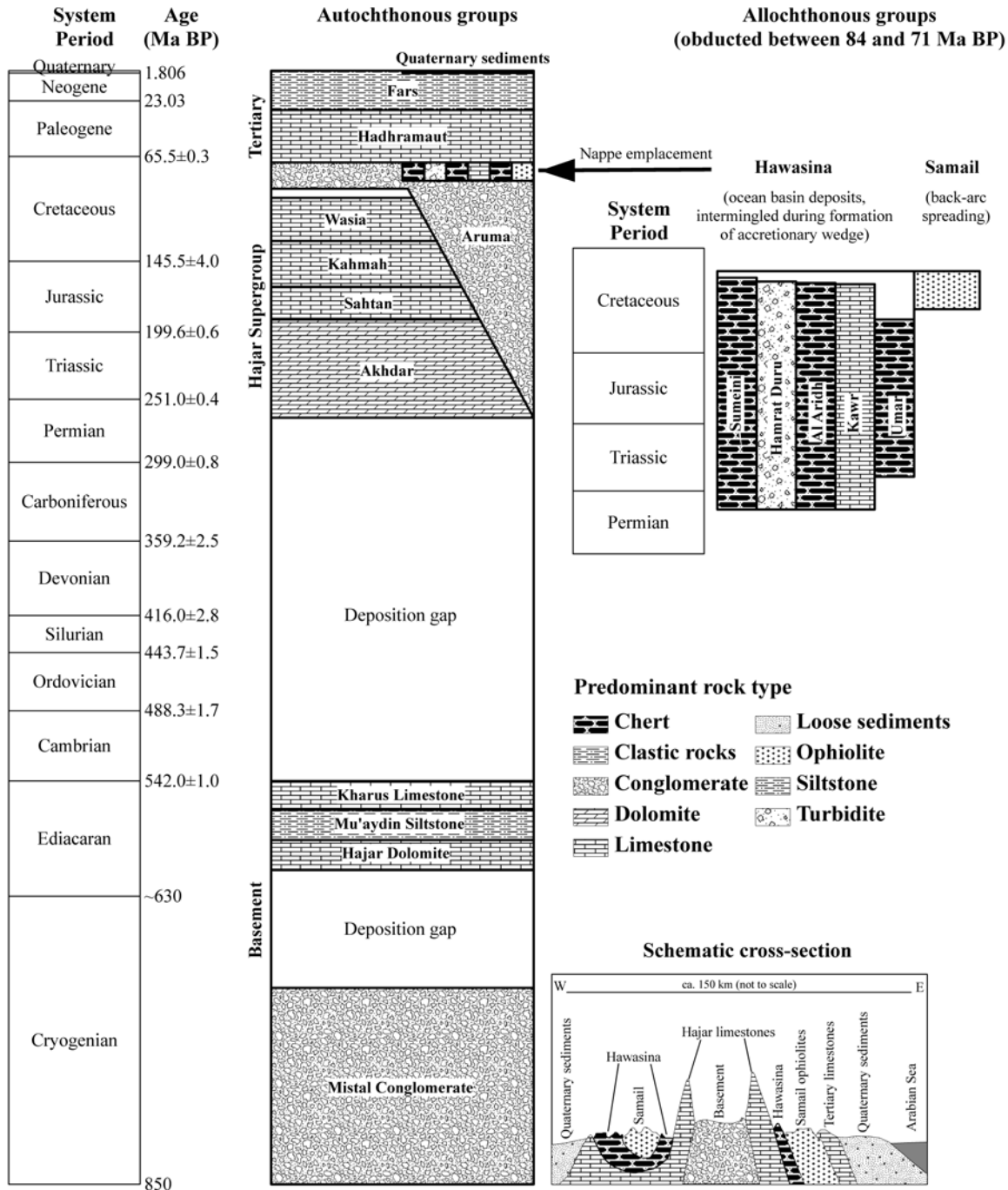


Figure 3.1. Simplified stratigraphy and cross-section of the Oman Mountains showing the main geological groups (Glennie 2005, Rabus et al. 2003). Numerical ages are according to Gradstein et al. (2004).

A cross-section through the mountain range (Fig. 3.1, bottom right) shows that, starting from the Arabian Sea inland, the first geologic feature is a large plain of Quaternary sediments, known as the Batinah coastal plain. Further

inland, it is succeeded by limestones of Maastrichtian and Paleogene origin, which in the southern part of the mountains form a large range that extends all the way to the coast. Behind the limestones, large tracts of Samail ophiolites are exposed, followed by sedimentary rocks of the Hawasina unit. These two formations form series of low weathered hills, which are mostly barren except for some vegetation at topographic lows. Hajar limestones are the next stratigraphic unit. They rise steeply from the surrounding area, forming a barrier that is only disrupted by the outlets of some steeply incised intermittent stream beds. These so-called wadis originate from a large basin of Basement rocks. It is surrounded on all sides by Hajar cliffs, which constitute the highest peaks of the mountain range. To the west of the basin, on the lower end of a long slope of Hajar limestone, lies another region characterized by remains of the obduction process. More Hawasina rocks were deposited on both sides of large outcrops of Samail ophiolites. A low range of Hajar limestones is then followed by extensive plains of Quaternary sediments.

Throughout most of the mountain range, erosion processes did not expose the full sequence of rocks described above. The Musandam Peninsula in the north of the country consists almost entirely of Hajar limestones, and between 23.5° and 25.5°N no outcrops of Hajar or Basement occur, so that the central part of the cross-section is characterized by Samail and Hawasina.

## **3.2 Area of interest and dataset description**

### *3.2.1. Study area*

The area of interest comprises the range of the Oman Mountains, at the Eastern tip of the Arabian Peninsula (Fig. 3.2). Within the range, which rises to almost 3000 m a.s.l. at its highest peak, the study was restricted to the national territory of the Sultanate of Oman, because geologic data for the United Arab Emirates were not available. The entire area is characterized by a desert climate with mean annual precipitation ranging from 75 mm in the lowlands to 300 mm in the higher reaches of the mountains (Fisher 1994). Mean annual temperatures vary between 18°C at an elevation of 2000 m a.s.l. and 29°C at sea level, creating environmental conditions that in most places do not allow for a permanent vegetation cover. Bare rock and gravel dominate the landscape, with densely vegetated patches being scattered and rarely larger than about 0.1 ha.

### *3.2.2. Vegetation dataset*

To determine the positions of oases, we used eleven cloud-free satellite images obtained from the University of Maryland's Global Land Cover Facility (GLCF 2006). These images were taken by the Enhanced Thematic Mapper Plus instrument (ETM+) of the Landsat 7 satellite between January 2000 and August 2001 and covered the entire range of the Oman Mountains (Tab. 3.1). We used ENVI 4.2 (Research Systems, Boulder, CO, USA) to merge all images. To compensate for slight differences in light intensity between the images, we used

the program's color balancing function based on the overlapping areas. ArcGIS 9.2 (ESRI, Redlands, CA, USA) was then used to calculate the Normalized Difference Vegetation Index (NDVI; Tucker and Sellers 1986) for the resulting mosaic, which had a spatial resolution of 28.5 m. This index was calculated using the Red (R) and Near Infrared (NIR) bands of the images and deriving the normalized difference as:  $NDVI = \frac{NIR - R}{NIR + R}$ .

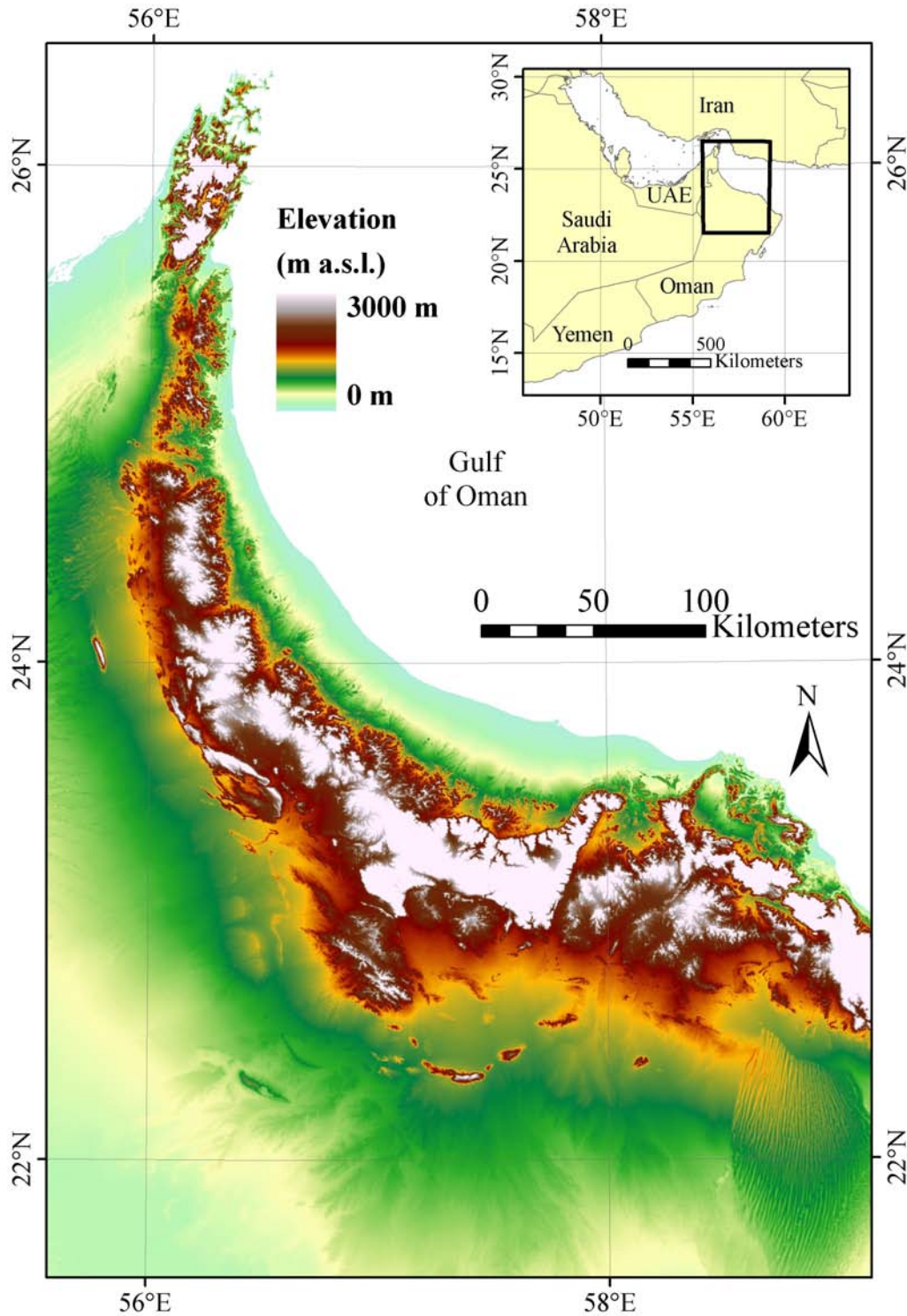


Figure 3.2. Location of the study area on the Arabian Peninsula (inset) and topographic map of the Oman Mountain Range.

### 3.2.3. Topographic dataset

For analysis of the topography around the oases, we used a Digital Elevation Model (DEM) of the Oman Mountains, which was based on the readings from NASA's Shuttle Radar Topography Mission (SRTM) (Rabus et al. 2003). For areas outside the United States, the spatial resolution of this dataset is three arc seconds. Its vertical resolution is 1 m, and for Africa (including Arabia), Rodriguez et al. (2006) determined absolute and relative height errors at 5.6 and 9.8 m, respectively. This satellite-based mission used stereo-imaging to derive surface elevations, which is known to have difficulties in very rugged terrain. These difficulties were reflected in large areas of missing data in the interior of the mountain range. These data voids were filled with elevations derived from topographic maps of the area, which were merged with the SRTM DEM using a delta-surface approach based on Triangular Irregular Networks (TINs; Luedeling et al. 2007b).

This elevation model was resampled from its original resolution of 81 m to 85.5 m, which is three times the resolution of the vegetation grid, using a nearest neighbor algorithm (Fig. 3.2).

Table 3.1. List of Landsat ETM+ scenes used in this study.

Path	Row	Acquisition date
157	44	19 Sep 2000
	45	23 Jan 2000
158	44, 45	28 Oct 2000
159	42	31 May 2001
	43, 44, 45	31 Jul 2000
160	42, 43	23 Aug 2000
	44	26 Aug 2001

### 3.2.4. Hydrologic dataset

From the same elevation model with a spatial resolution of 85.5 m, we derived hydrologic parameters for the study area using ArcHydro Tools for ArcGIS 9 version 1.1 (ESRI, Redlands, CA, USA). We estimated the flow accumulation in each pixel of the elevation grid by using the standard terrain preprocessing functions to fill sinks, derive flow direction and obtain flow accumulation. For each pixel, the resulting flow accumulation grid contains the number of upslope pixels from the DEM that drain into the pixel. This grid was multiplied by the size of one pixel ( $85.5 \times 85.5 \text{ m}^2$ ) to obtain the contributing upslope area.

From the flow accumulation grid, we defined two sets of streams using minimum contributing upstream areas of  $10 \text{ km}^2$  (1368 cells) and  $100 \text{ km}^2$  (13,679 cells) as stream definition thresholds. These two catchment sizes are meant to represent dependence on small local and large regional drainage networks. We use the term "stream" as an analogue to the terminology used in the ArcGIS extension. It should be kept in mind, however, that there are no

permanent streams in the Oman Mountains, and that the streams delineated by hydrologic modeling correspond to intermittent streams (Arab.: wadi) that only have surface flow after heavy rains.

### 3.2.5. Geologic dataset

To analyze the oases' geologic settings, we obtained a polygon dataset describing the geology of Oman according to a regional survey at a scale of 1:100,000 conducted by the French Bureau de Recherches Géologiques et Minières (BRGM, Orléans, France; Rabus et al. 2003). We summarized all geologic formations into larger geologic units according to their geologic and hydrologic characteristics. The resulting reclassification (Tab. 3.2) was mainly aligned with the stratigraphic subdivisions of the mountain range (Fig. 3.1). For the Basement, the Hajar Supergroup and the Quaternary sediments, the entire stratigraphic units were treated as one group in the analysis. All limestones not belonging to the Hajar Supergroup were agglomerated in a separate group, regardless of whether they were of Tertiary origin or part of the Kawr Group, which belongs to the Hawasina thrust sheet. This classification seemed more appropriate than treating the entire Hawasina as one unit, since limestone was expected to have a different hydrologic behavior than the sedimentary rock types that constitute the rest of the Hawasina. The remaining Hawasina formations were aggregated with the Early Cretaceous Sumeini and Late Cretaceous Aruma Groups. Even though the hydrologic properties of these formations might differ somewhat, they are expected to behave rather as confining than as water-storing units.

Table 3.2. Geologic subdivisions used in the analysis

<b>Name</b>	<b>Stratigraphic units</b>	<b>Rock type</b>	<b>Age</b>
Basement	Basement	Sedimentary, metamorphic and crystalline rocks	Pre-Middle Permian
Hajar	Hajar Supergroup	Limestone	Late Permian to Mid Cretaceous
Non-Hajar limestones	Tertiary limestones and Kawr Group of the Hawasina	Limestone	Tertiary, Late Permian to Mid Cretaceous (Kawr)
Hawasina	Hawasina excluding Kawr Group + Sumeini Group + Aruma Group	Mostly sedimentary rocks	Late Permian to Mid Cretaceous
Samail	Samail + Metamorphic sole + Tertiary listwaenite	Crystalline and metamorphic rocks	Late Cretaceous, Tertiary
Tertiary non-limestones	All tertiary formations excluding limestone	Sedimentary rocks	Tertiary
Quaternary	Quaternary sediments	Uncompacted sediments	Quaternary

The Samail Nappe was aggregated with the associated Metamorphic Sole and with the Tertiary listwaenite, since all three geologic units constitute compact rock types with low water storage capacity, and can be expected to act as barriers to surface and groundwater flow. All Tertiary formations except the Tertiary limestones were aggregated in a separate group.

The reclassified polygon feature was converted into a 85.5-m grid using the ArcGIS 9.2 standard conversion function, which assigns values to pixels based on the polygon that covers the central point of each pixel (Fig. 3.3).

### 3.3 Methods

#### 3.3.1. NDVI image enhancement

In spite of the color balancing, some variation in light intensity remained, because the images were taken during different seasons and showed areas at different elevations. Images taken during the hot summer months had much lower overall NDVI ranges than images taken during winter. Similarly, relatively abundant rainfall in the higher reaches of the Oman Mountains provided for more natural vegetation than in the lowlands. Since evapotranspiration in the high mountains is also much lower than in the lowlands, both oases and natural vegetation in the mountains had higher NDVI values than their lowland counterparts. Some lowland oases on summer images therefore had lower NDVI values than natural vegetation in the mountains on a winter image and prevented using a single threshold to isolate oases. Since everywhere in northern Oman the perennial date palm orchards are well watered throughout the year, we hypothesize that their photosynthetic activity should be much higher than that of the surrounding natural vegetation. Therefore, subtracting a regional background from the NDVI grid before applying the thresholding technique should compensate for the seasonal and altitudinal differences. Bilinear interpolation was used to resample the NDVI grid to 85.5 m resolution and to calculate the regional background NDVI using focal statistics on an area of 101 x 101 pixels (corresponding to 303 x 303 pixels of the NDVI grid). This entailed using a moving window to focus on each pixel of the grid and replacing the value of the pixel by the mean NDVI computed from the 101 x 101 neighboring pixels. This background value was then subtracted from the original NDVI mosaic, making local NDVI maxima stand out more clearly. This grid, which retained the original NDVI resolution of 28.5 m, will be referred to as the enhanced NDVI and allows better distinction between natural and oasis vegetation.

#### 3.3.2. Exclusion of natural vegetation

Finally, it was necessary to exclude natural vegetation from the classification. In contrast to oases, intense natural vegetation typically occurs in very small patches of less than three pixels, whereas most oases are much larger. We therefore applied focal statistics to the enhanced NDVI grid, computing mean



values of 3 x 3 pixels centered on each pixel of the grid. This step de-emphasized vegetation clusters of only one or few pixels. The resulting grid was then classified into five classes using a natural breaks algorithm, which ordered all values of the grid and created the class boundaries at natural jumps in the values, and the highest class was interpreted as delineating oasis cores.

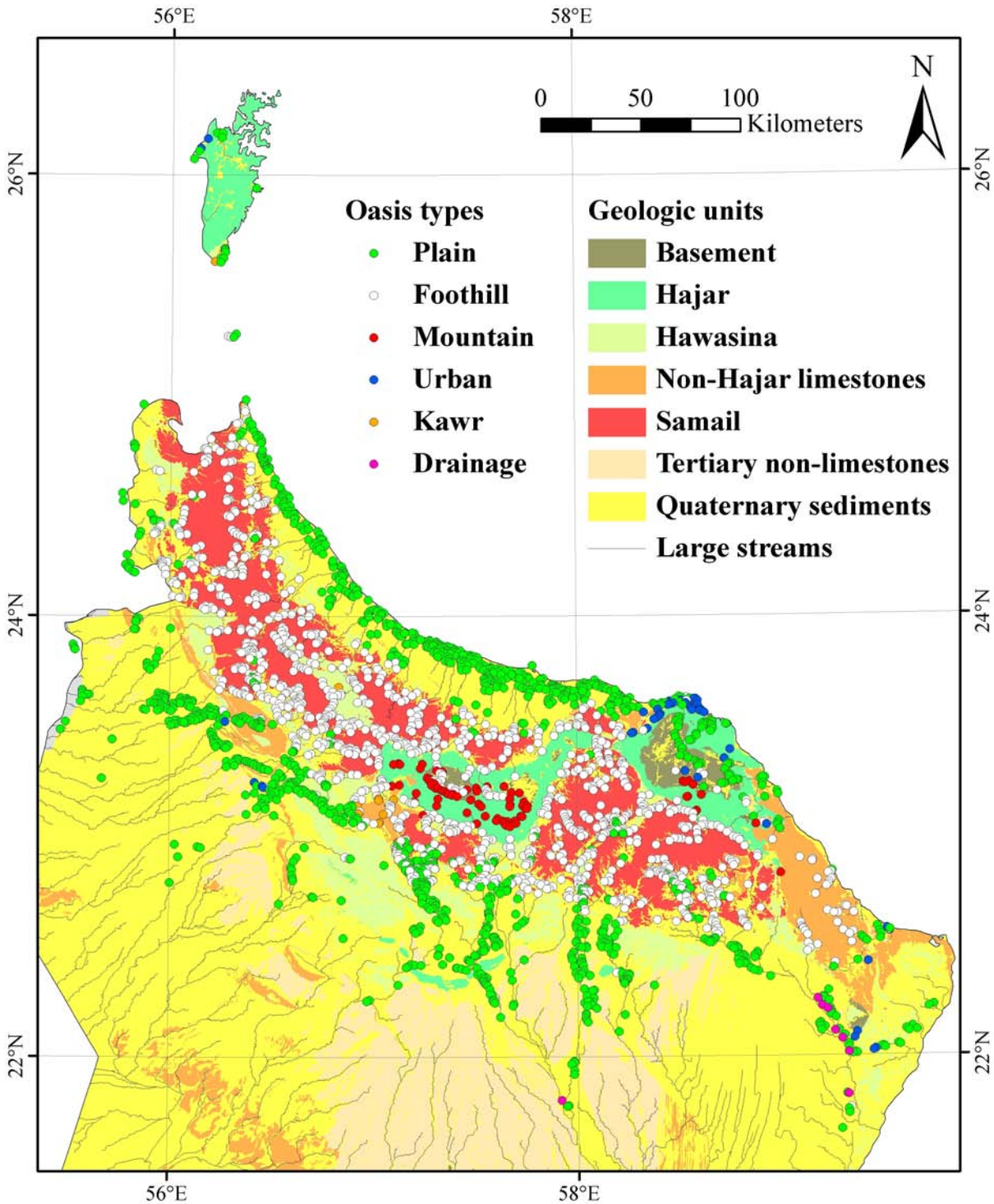


Figure 3.3. Geologic groups of northern Oman, according to the classification used in this study, and locations of oases determined by the cluster analysis. Lines in the map indicate the locations of streams fed by catchments of more than 100 km<sup>2</sup>. For illustration purposes, oasis polygons are represented by their central points.



In order to estimate how far the oases extended beyond the delineated core, we created ten buffers in increments of one pixel around the oasis cores and calculated the mean of the enhanced NDVI grid for each buffer. This analysis showed that mean NDVI was positive within a buffer of six pixels around the oasis cores (Fig. 3.4). We therefore accepted a six-pixel buffer as delineating oasis areas.

In order to estimate the vegetated area of each detected oasis, we classified the enhanced NDVI grid into five classes using again the natural breaks procedure mentioned above. The highest class was interpreted as vegetated. The result of this classification provided vegetated areas at a higher resolution than the grid used to delineate oasis cores, because the grid had not been subjected to the 3 x 3 pixel focal statistics described earlier in this section. It therefore included both small patches of cultivated vegetation and clusters of dense natural vegetation. We used the six-pixel buffer around the oasis cores to distinguish between the two vegetation types, assuming that vegetation within this buffer belonged to the corresponding oasis. For each oasis polygon, we therefore summarized the area covered by pixels classified as vegetated and used the result to estimate the vegetated area of the oasis.

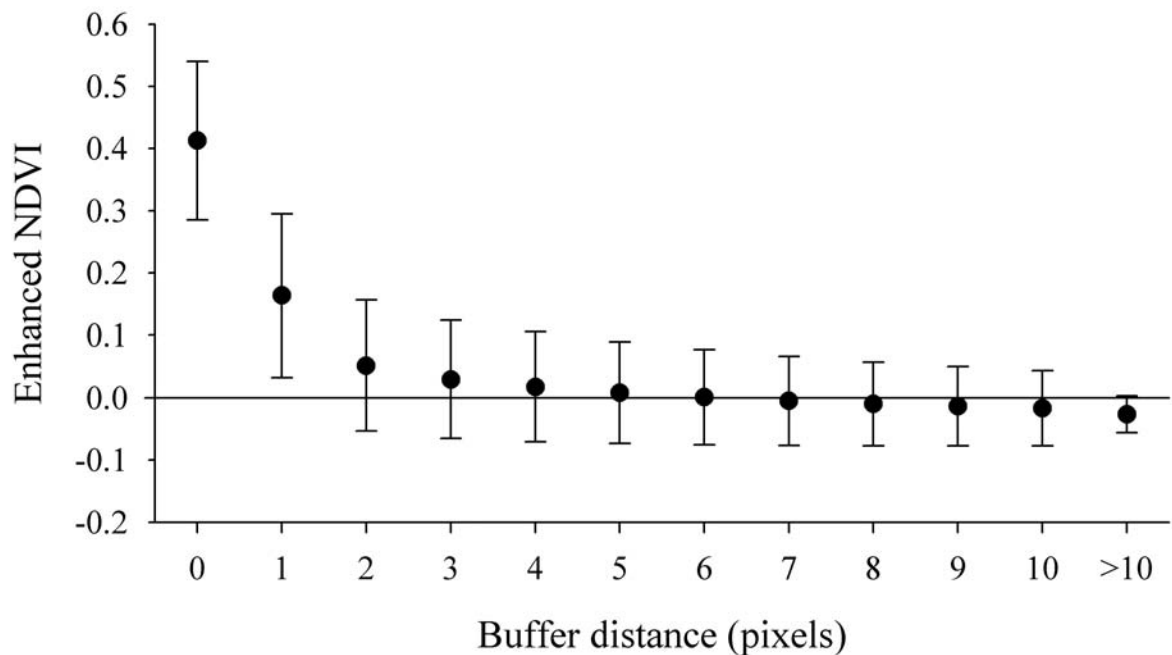


Figure 3.4. Mean enhanced NDVI within increasing buffer distances around the oasis cores. Error bars indicate  $\pm$  one standard deviation.

### 3.3.3. Classification validation

To test the quality of the classification, we created ten squares of 20 x 20 km<sup>2</sup> and distributed them randomly over the study area. We imported these squares into Google Earth Pro (Google, Mountain View, CA, USA) and shifted them slightly to overlap with areas of the Google Earth mosaic that were available in high resolution. These parts of the mosaic are based on Quickbird satellite images of submeter resolution. Even though the image resolution in Google

Earth might be somewhat lower than in the original Quickbird images, oases were clearly visible, allowing the use of the Google Earth Pro interface for validating the classification. The oasis areas were converted to polygon shapefiles and added to the Google Earth Pro view. We then visually scanned each square for oases, and registered whether the oasis was detected or missed by our algorithm. For those that were missed, we estimated the area of the corresponding palm gardens by using the program's area measuring tool. We also counted the number of polygons that were falsely classified as belonging to an oasis core.

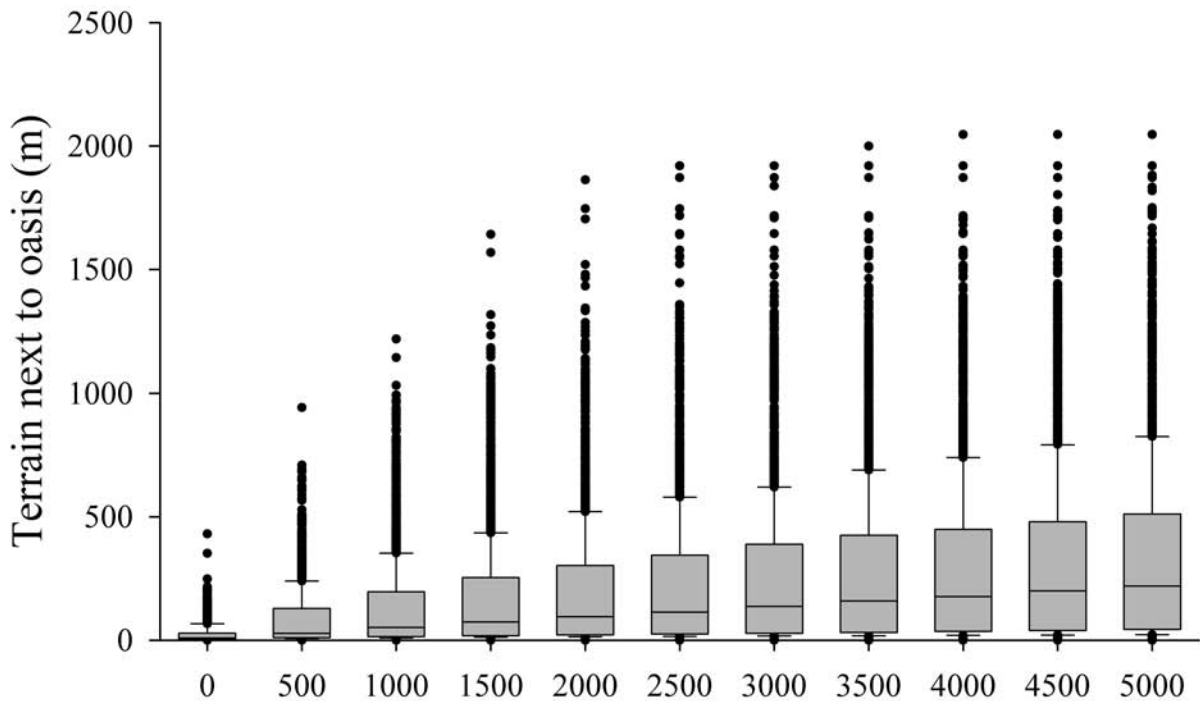


Figure 3.5. Terrain next to oases within increasing radii around the oases, calculated as the difference between the maximum elevation within the given radius and the mean elevation of the oasis.

### 3.3.4. Topographic analysis

Mean elevations of each oasis polygon were then derived using zonal statistics. As an additional topographic variable, we calculated the terrain next to each oasis, which we defined as the difference between the highest point within a given radius around the oasis and its mean elevation. To decide which radius was most appropriate, this parameter was calculated for buffer distances at 500-m increments up to 5 km around the oasis polygons. The variation of elevations next to an oasis rose steeply within 2000 m around the polygons, after which the increases leveled off (Fig. 3.5). We therefore calculated the terrain next to each oasis as the difference between the highest elevation within a 2-km buffer around each oasis and the mean elevation of the oasis polygon.

### 3.3.5. Hydrologic analysis

Since many oases do not lie directly in drainage channels, but are likely to be influenced by such channels in their vicinity, flow accumulation within a certain distance from the oases had to be considered. As described in section 3.3.4 for the terrain, we constructed buffers of increasing distance around the oases and summarized maximum flow accumulation for each buffer. The result showed that flow accumulation was almost similar for all radii above 2000 m (Fig. 3.6). We therefore included the value of the pixel with the maximum flow accumulation within a 2-km radius around the oasis as a hydrologic variable.

For each set of streams, we calculated a grid dataset containing the Euclidean distance between each grid point and the nearest stream. From these grids, we chose the minimum distance within each oasis polygon as an input variable.

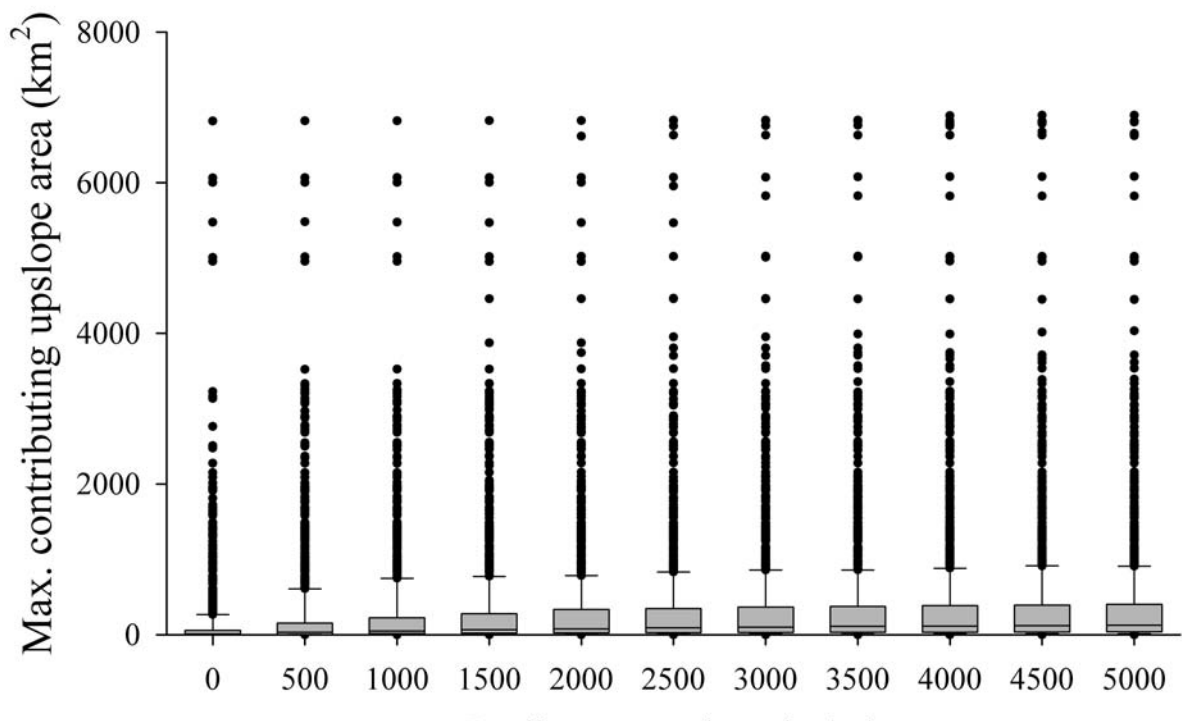


Figure 3.6. Maximum contributing upslope area of grid pixels within increasing radii around the oasis polygons.

### 3.3.6. Geologic analysis

We extracted each geologic class from the grid and calculated the Euclidean distance between each pixel of the study area and the nearest occurrence of each geologic class. We classified these distance grids into zones of increasing distance from the formation, at increments of one kilometer, and calculated the enhanced NDVI for each of these proximity zones (Fig. 3.7).

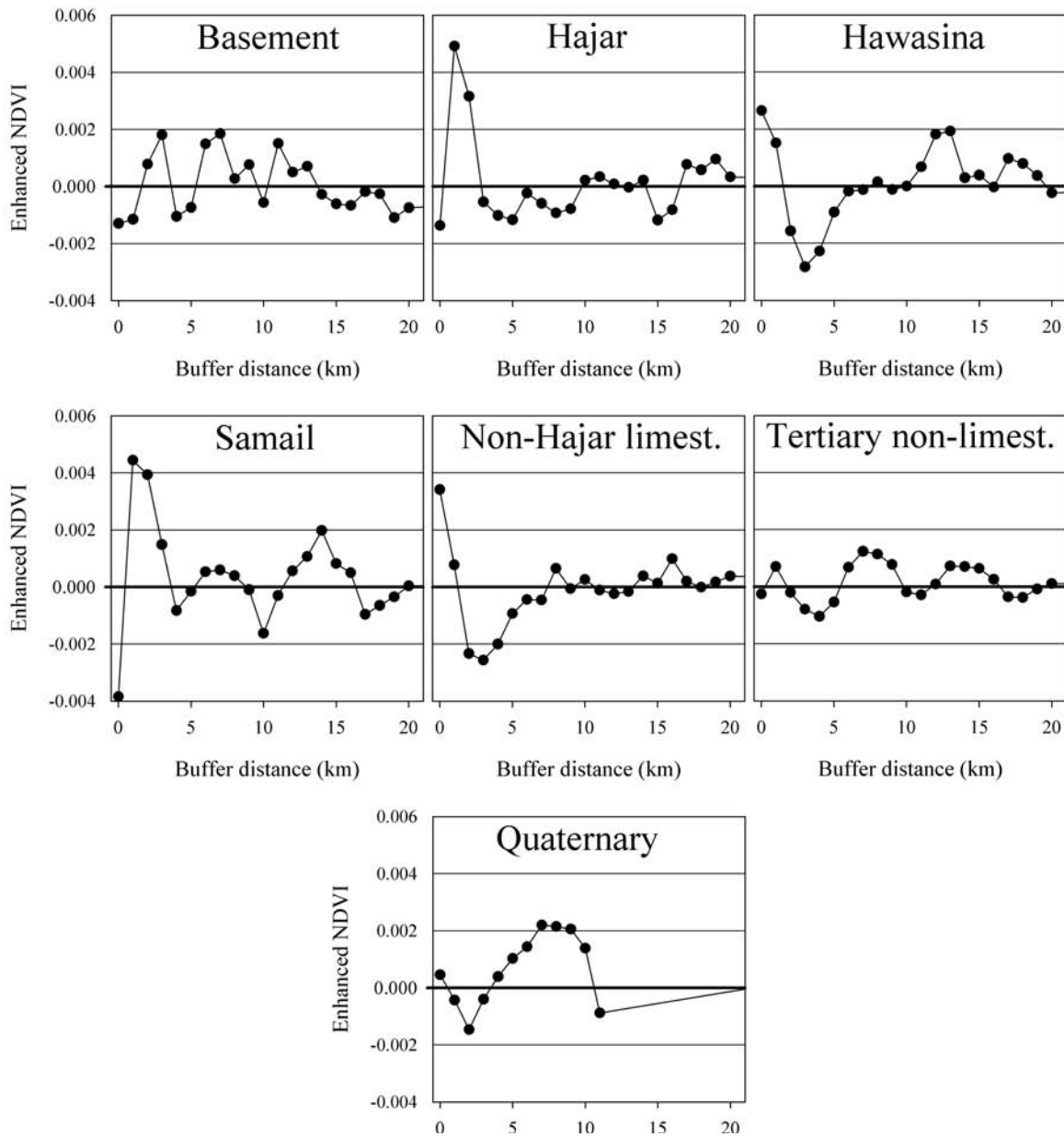


Figure 3.7. Mean enhanced NDVI at increasing buffer distances around each of the geologic classes considered in this study.

The resulting diagrams showed that the only four geologic groups that are directly correlated to the presence of vegetation were Hajar, Hawasina, Samail and Non-Hajar limestones. Moreover, the shape of the NDVI curves indicated that vegetation near these units was different from vegetation on the units themselves. The NDVI curves thus hinted at the boundaries between the respective units and the surrounding rocks as an important factor influencing vegetation. Analysis of the geologic settings of oases thus had to adequately distinguish between oases on these rock units and oases near the geologic boundaries. To achieve this, we created a new variable for each of the four rock groups, assigning a categorical value of 1, if an oasis was on a formation of the group, 0.5 for direct proximity, and 0 if the oasis was further than a certain

buffer distance from the nearest occurrence of the geologic group. According to the NDVI diagrams (Fig. 3.7), the size of the buffer was set to 3 km for Hajar, 2 km for Hawasina and Non-Hajar limestones and 4 km for Samail, reflecting the distance, at which the groups apparently influenced vegetation around them. While these categorical variables were used as inputs for the cluster analysis (Section 3.3.7), we used the distribution of distances rather than proximity categories to characterize the groups formed by the cluster analysis.

### 3.3.7. Cluster analysis

Classification of oases was done by hierarchical cluster analysis using PC-ORD 5.0 (MjM Software, Gleneden Beach, OR, USA). As input data, we used the topographic, hydrologic and geologic variables of all detected oases (Tab. 3.3). Hierarchical cluster analysis classifies all input elements based on some measure of the distance between the elements, as determined by the values of all input variables. For measuring this distance, we used a Euclidean distance measure, which calculates the distance  $d_{x,y}$  between two elements  $x$  and  $y$  as:

$$d_{x,y} = \sqrt{\sum_i (x_i - y_i)^2}, \text{ with } i \text{ being an index running through all input variables.}$$

Table 3.3. Topographic, hydrologic and geologic parameters used as input variables for the cluster analysis.

Input type	Input grid
Topographic	Mean elevation within oasis polygon Terrain height within 2 km of oasis (maximum – mean elevation)
Hydrologic	Distance to nearest stream with contributing catchment of 10 km <sup>2</sup> Distance to nearest stream with contributing catchment of 100 km <sup>2</sup> Maximum contributing upslope area within 2 km of oasis
Geologic	Proximity to nearest occurrence of Hajar <sup>a</sup> Proximity to nearest occurrence of Non-Hajar limestones <sup>a</sup> Proximity to nearest occurrence of Hawasina <sup>a</sup> Proximity to nearest occurrence of Samail <sup>a</sup>

<sup>a</sup> Geologic groups as defined in Table 3.2, proximity defined as in Section 3.2.5

Since this distance measure is sensitive to differences in scale among the input variables, giving greater weight to variables with wide ranges, we standardized all topographic and hydrologic input variables by division by the respective maximum value of the variable. To account for the skewed distribution of all variables (Fig. 3.8), the results were subjected to square-root transformation. Furthermore, since topography, hydrology and geology were assumed equally important but were represented by different numbers of variables, all variables were weighted by multiplying by factors of six (for the two topographic parameters), four (three hydrologic parameters) and three (four geologic parameters) to assign equal weights to all three categories.

A further parameter in a cluster analysis is the group linkage method, which prescribes how to calculate the distance between clusters of more than one element. For this, we used the unweighted group average method, in which the

distances between clusters are calculated from the average distance between all element pairs of the two clusters. The number of clusters was chosen so that the clustering retained just over 4% of the information in the dataset.

## 3.4 Results

### 3.4.1. Oasis locations

Our algorithm detected a total of 2663 oases, ranging in size from 0.08 to 718 ha of vegetated area. Of these 2663 oases, 2428 had vegetated areas of more than 0.4 ha, which was the minimum size for reliable detection (Section 3.4.2). Among the largest twelve oases, seven were modern agricultural schemes on the Batinah coastal plain. The largest traditional oases were Bilad Bani Bu Hasan (22.07°N, 59.28°E, 436 ha), Al Kamil (22.21°N, 59.21°E, 393 ha), Samail (23.30°N, 57.98°E, 366 ha), Nizwa (22.93°N, 57.53°E, 337 ha) and Rustaq (23.38°N, 57.42°E, 334 ha).

### 3.4.2. Verification of oasis locations

Comparing the numbers and locations of oases from the classification with the oases that were visible on the Google Earth image within the test areas indicated that the classification was quite accurate (Tab. 3.4). Instead of the 156 oases traced visually, the classification found 123 (79%) and only missed 33 (21%). The size of the missed oases ranged between 0.1 and 0.4 ha, compared to an average oasis size of 9 ha. At the Landsat resolution of 28.5 m, such small structures are difficult to distinguish from natural vegetation. In two cases, natural vegetation was interpreted as belonging to an oasis. The first test area, which lay in the Musandam Peninsula, contained several villages, which seemed to depend on rainfed agriculture and had no palm gardens. Our algorithm did not detect any of these settlements, because the corresponding satellite image was taken during the dry summer. Since our study aimed at describing oases that are located in hydrologic settings that allow year-round cultivation, the failure to detect these locations does not constitute a problem for the analysis. Perennial oases with vegetated areas of more than 0.4 ha were detected correctly in all cases that occurred in the test areas.

### 3.4.3. Distribution of input parameters

Only few oases stood out with large vegetated areas up to 718 ha, but 50% of all oases had less than 1.3 ha. (Fig. 3.8a). Mean elevations ranged from 1 to 2474 m a.s.l., with a mean at 390 m a.s.l. (Fig. 3.8b). The three highest identified oases were small patches of dense juniper vegetation near Jabal Shams (23.24°N, 57.26°E), Oman's highest mountain. The highest actual oasis was the village of Sayq (23.07°N, 57.63°E), at an elevation of 1944 m a.s.l. We identified only 15 other oases above 1500 m a.s.l. Terrain next to the oases was on average 201 m (Fig. 3.8c). For half of the oases, it was below 94 m, while the maximum was

1862 m for the small mountain village of Al Hawb just south of Jabal Shams. Half of all oases were within 86 m of a stream with a catchment of at least 10 km<sup>2</sup>, while 315 lay more than 1 km away from such streams (Fig. 3.8d).

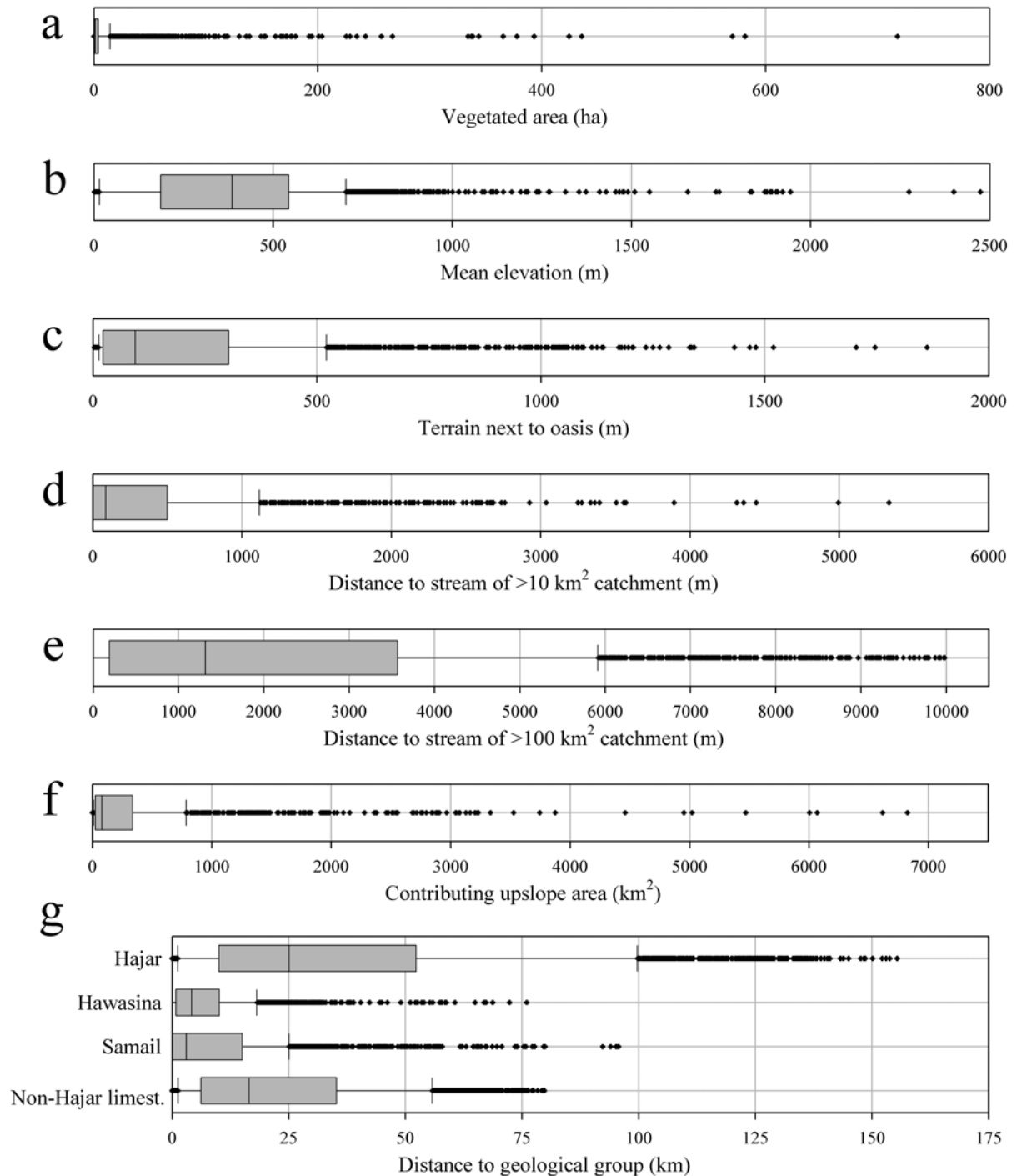


Figure 3.8. Overall distributions of all parameters assessed in this study for all 2663 oases detected in northern Oman. In the box plots, the central line represents the median of the dataset, the outer edges of the boxes are the 25% and 75% quantiles, the ends of the error bars represent the 10% and 90% quantiles and the individual points are outliers beyond these limits.

These were mostly well-based irrigation schemes or mountain oases lying directly at springs. Mean distance to larger streams (>100 km<sup>2</sup> catchment) was

2.1 km, but ranged from 0 to 10.0 km. Half of all oases were less than 1.3 km from such a stream (Fig. 3.8e). Mean contributing upstream area of the oases was 307 km<sup>2</sup>, with a median of 79 km<sup>2</sup> (Fig. 3.8f). Catchment sizes of more than 4,000 km<sup>2</sup> were only derived for eight vegetated patches around the oases of Bilad Bani Bu Hassan and Al Kamil, the largest natural oases in the region.

Hajar limestones were within 5 km of 18% of all oases, and more than 20 km away from 59%. Since the obducted geologic layers are widespread on both sides of the mountain range, most oases were relatively close to outcrops of Samail (mean distance of 9 km) and Hawasina (7 km). Non-Hajar limestones were on average 22 km from the oases (Fig. 3.8g).

Table 3.4. Verification of the classification procedure based on Quickbird images in Google Earth Pro. For each test square of 20 x 20 km<sup>2</sup>, the numbers of correctly detected oases (correct), of natural vegetation erroneously classified as oases (false) and of undetected oases are given. For undetected oases, the size range according to Google Earth Pro's measurement tool is also indicated.

Test square	Central point	Detected oases		Undetected oases	
		Correct	False	n	Size range (ha)
1	25°56'N; 56°12'E	0	0	0	-
2	22°11'N; 56°40'E	3	0	1	0.2
3	23°36'N; 56°46'E	36	0	12	0.1-0.4
4	23°14'N; 57°04'E	22	1	5	0.1-0.4
5	23°00'N; 57°39'E	14	1	0	-
6	22°44'N; 57°13'E	9	0	1	0.2
7	22°17'N; 56°31'E	0	0	0	-
8	23°24'N; 58°42'E	8	0	6	0.2-0.4
9	22°50'N; 58°42'E	29	0	6	0.1-0.3
10	22°21'N; 59°25'E	2	0	2	0.1
Total		123	2	33	0.1-0.4

#### 3.4.4. Cluster description

The cluster analysis classified the oases into six clusters, comprising between 0.3 and 48.5% of all oases (Table 3.5).

Cluster 1 contains 1291 oases, with vegetated areas ranging from 0.1 to 718 ha (1.1 ha; numbers in parentheses indicate the median of the distributions within the cluster; Fig. 3.9a). The oases of this cluster are characterized by low to moderate elevations (Fig. 3.9b) and mostly have low terrain next to them (Fig. 3.9c). Hydrologically, they lie in diverse settings, with widely varying contributing upslope areas (Fig. 3.9f) and distances to small and large streams (Figs. 3.9d and 3.9e). Cluster 1 oases are not particularly associated with any geologic groups (Figs. 3.9g-j).

The 1231 oases of cluster 2 also have widely varying vegetated areas, ranging from 0.2 to 365.7 ha (1.4 ha; Fig. 3.9a). They lie at higher elevations than cluster 1 oases (Fig. 3.9b) and have higher terrain around them (261 m; Fig. 3.9c). Most



cluster 2 oases lie very close (0 m; Fig. 3.9d) to streams fed by catchments of 10 km<sup>2</sup>. Catchment sizes are almost as variable as for cluster 1 (Fig. 3.9f). Most oases in this cluster are close to Hawasina (2 km; Fig. 3.9h) and Samail (0 km; Fig. 3.9i).

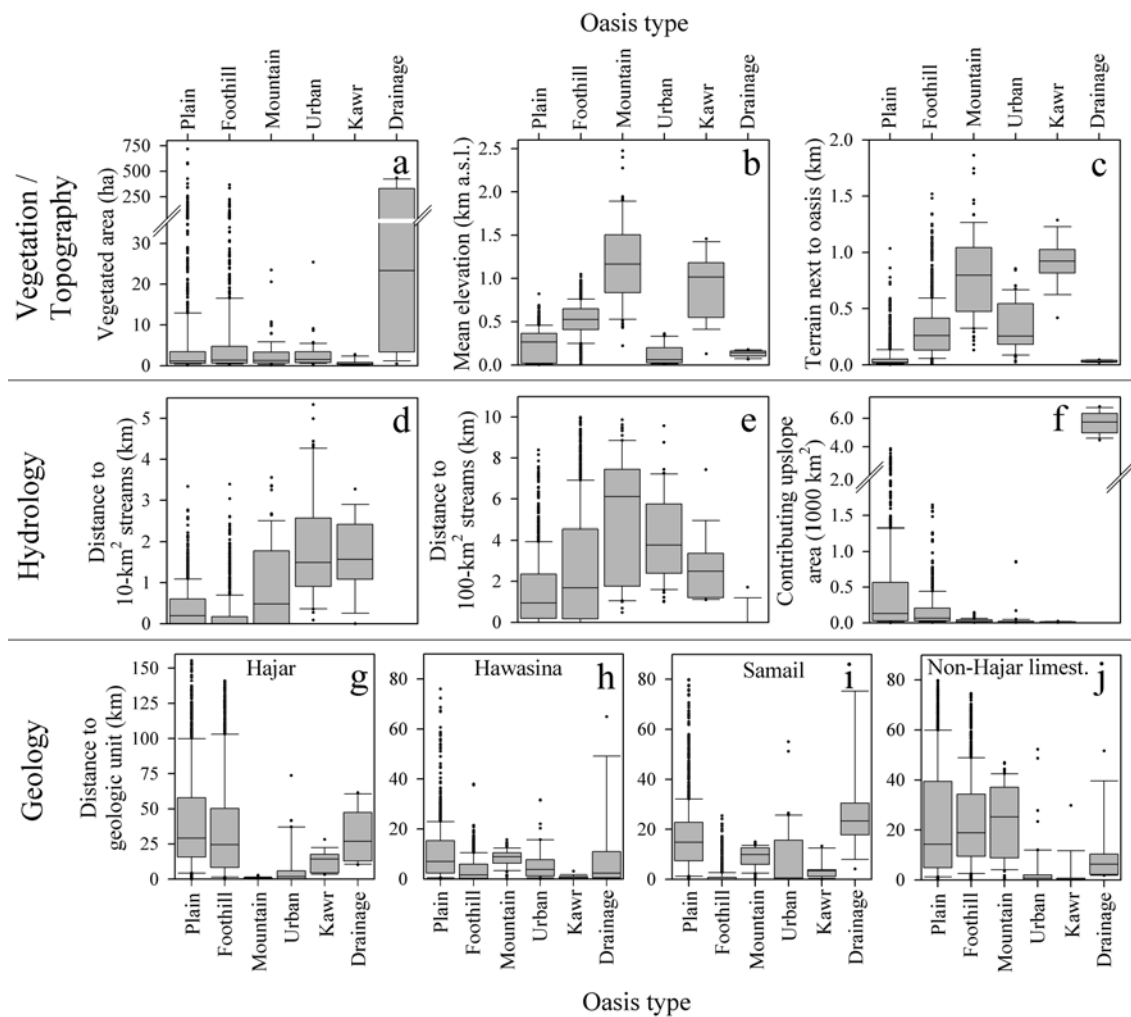


Figure 3.9. Distribution of all oasis parameters among the six clusters determined in this study of northern Oman. In the box plots, the central line represents the median of the data set, the outer edges of the boxes are the 25% and 75% quantiles, the ends of the error bars represent the 10% and 90% quantiles and the individual points are outliers beyond these limits.

Even though the 75 oases belonging to cluster 3 show a smaller variation of their vegetated areas, the median size of oases of this cluster is about the same as for clusters 1 and 2 (1.3 ha; Fig. 3.9a). They lie at high elevations (1166 m a.s.l.; Fig. 3.9b) and have high terrain around them (795 m; Fig. 3.9c). They are relatively far from small (484 m; Fig. 3.9d) and large (6.1 km; Fig. 3.9e) streams, and have small contributing areas (17 km<sup>2</sup>; Fig. 3.9f). Geologically, they are closely associated with Hajar rocks (0 km; Fig. 3.9g). In addition to the geologic units that were identified as particularly influential, oases of this cluster were closely associated with Basement rocks (0 km).

The 46 oases of cluster 4 lie at low elevations (Fig. 3.9a) and are associated with fairly low surrounding terrain (257 m; Fig. 3.9c). They are far from small

and large streams (Figs. 3.9d and 3.9e) and have small catchments (Fig. 3.9f). These oases are close to Non-Hajar limestones (Fig. 3.9j).

The 12 oases belonging to cluster 5 are the smallest (0.4 ha; Fig. 3.9a). They lie at higher elevations than cluster 4 oases (1017 m a.s.l.; Fig. 3.9b) and have the highest terrain next to them (919 m; Fig. 3.9c). They are far away from streams and have very small catchment sizes (7 km<sup>2</sup>; Fig. 3.9f). Cluster 5 oases occur in association with Hawasina (Fig. 3.9h), Samail (Fig. 3.9i) and Non-Hajar limestones (Fig. 3.9j).

Finally, the 8 oases of cluster 6 are the largest (23.4 ha; Fig. 3.9a), and all have low terrain around them (Fig. 3.9c). They are strongly associated with small and large streams (Figs. 3.9d and 3.9e) and draw their water from very large contributing areas (5737 km<sup>2</sup>; Fig. 3.9f). They are not associated with any geologic group.

Table 3.5. Results of the cluster analysis for the 2663 detected oases, including oasis types, share of oases in each cluster and general topographic, hydrologic and geologic setting of each type, as interpreted from cluster properties (Fig. 3.9) and geographic distribution (Fig. 3.3). A dash (-) indicates that a parameter category (Topography, Hydrology or Geology) was apparently unimportant for the respective oasis type.

Cluster no.	Oasis type	Share of all oases (%)	Topographic setting	Hydrologic setting	Geologic setting
1	Plain	48.5	Low, flat	Close to streams	-
2	Foothill	46.2	Medium, hilly	Close to streams	Samail, Hawasina
3	Mountain	2.8	High, steep	Natural springs	Hajar
4	Urban	1.7	-	-	-
5	Kawr	0.5	High, steep	Natural springs	Tert. limestones
6	Drainage	0.3	Low, flat	Close to streams	-

## 3.5 Discussion

### 3.5.1. Cluster characterization

The analysis showed that oases in the Oman Mountains can be found in a wide range of geologic, topographic and hydrologic settings, and that they can be grouped into six distinct categories (Fig. 3.3, Table 3.5).

Oases belonging to cluster 1 may be characterized as ‘Plain Oases’, since most of them lie in flat areas at low elevations east or west of the mountains. Virtually all oases of the Batinah coastal plain and most oases on the plain west of the mountains were assigned to this cluster. The elevation range of these oases (Fig. 3.9b) reflects the different elevations of these two flat areas. These oases are not associated with any geologic settings except for Quaternary sediments (Fig. 3.10). This indicates that the agriculture of this oasis type is not fed by springs, but either by underground wadi flow, which is tapped by branching off side channels from wadis, or by wells dug into the sediments. This cluster thus mainly comprises the modern irrigation schemes, which are not located where water was easily available in the past, but where groundwater could be accessed by pumps.

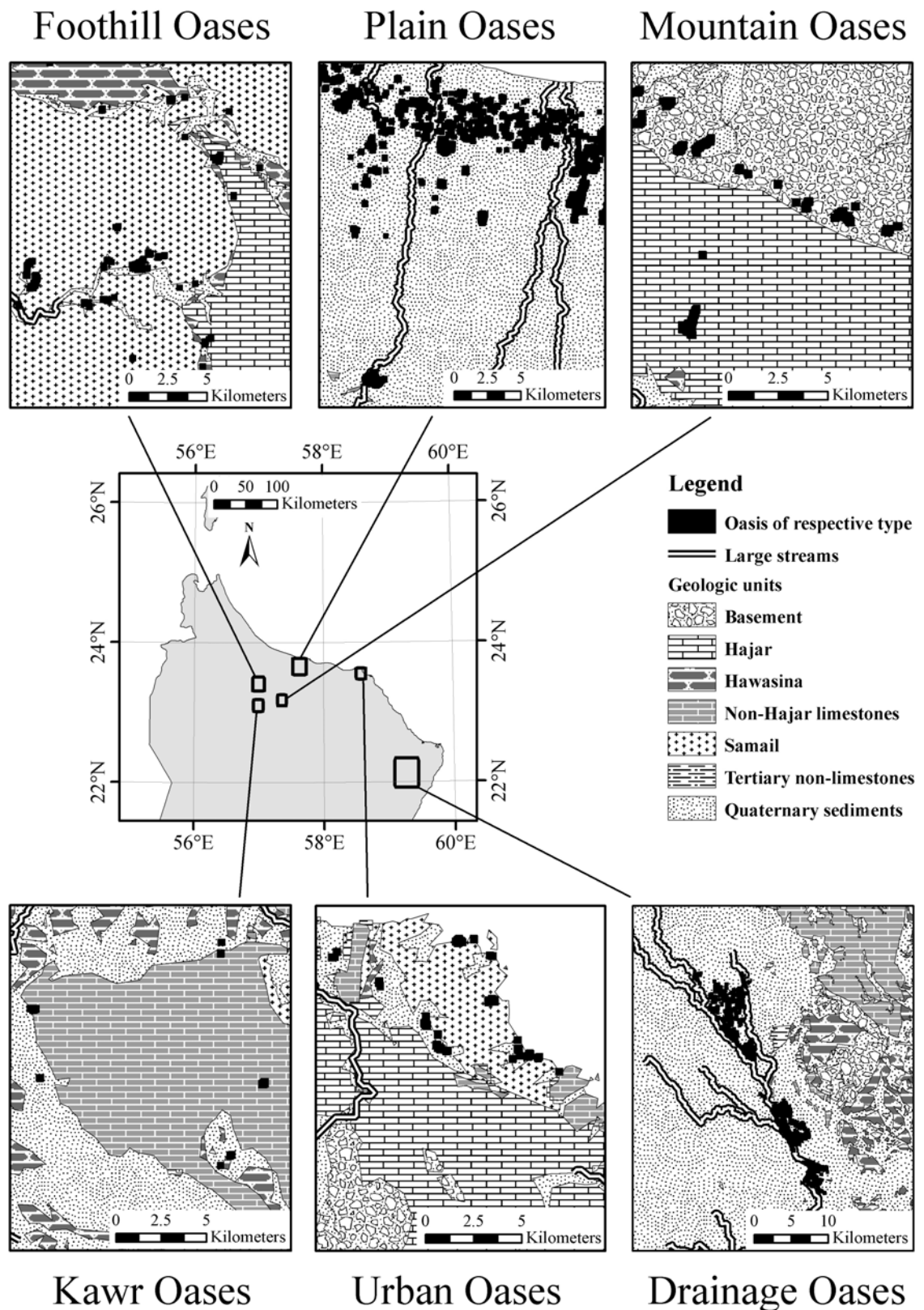


Figure 3.10. Geologic setting of the six oasis types in the Oman Mountains.

Oases of cluster 2, the ‘Foothill Oases’, are scattered over the outcrops of Hawasina and Samail on both sides of the mountains. The oases of this second large cluster lie at higher elevations than ‘Plain Oases’, close to higher terrain and closer to small streams (Figs. 3.9c and 3.9d). They therefore seem to lie in locations, where water is concentrated by local catchments and used to irrigate

small palm gardens in valleys of the Hawasina and Samail foothill ranges (Fig. 3.10). Most such oases appear to be fed by wadi groundwaters rather than by springs, even though some spring-fed oases in comparable geologic settings might also be contained in this cluster.

Oases of cluster 3 are typical ‘Mountain Oases’, lie at high elevation and are mostly in mountainous terrain. While some of these locations might also have some flow accumulation in wadi sediments, the very small catchment sizes and long distances to streams indicate that most oases in this cluster are located close to springs emerging from the geologic unconformity between Hajar and Basement (Fig. 3.9g). The Hajar limestones form the water storage rocks for these oases, and the Basement is the confining layer that makes the water surface. This unconformity is exposed at various locations throughout the inner mountains, mainly at the upper end of all wadis that penetrate the walls of the central basin and at the edge of the Sayq Plateau in Al Jabal al Akhdar. In all these locations, oases are located near springs emerging from the unconformity setting (Fig. 3.10).

Oases of cluster 4, the ‘Urban Oases’, are predominantly located in the urban areas of Muscat and Sur and consist of parks, lawn areas and soccer grounds (Fig. 3.10). Long distances from all streams and small catchment sizes combined with low elevation and flat terrain characterize this cluster (Figs. 3.9b and 3.9c), and suggest that these oases have no natural water supply. In planning sports facilities and parks, considerations about the water supply are generally not the primary concern, and consequently the parameters of this cluster do not represent any meaningful hydrologic settings. Some agricultural areas are also included in this cluster, but their grouping with the urban areas seems coincidental.

Like these ‘Urban Oases’, the twelve oases of cluster 5 are also associated with Non-Hajar limestones, but their hydrologic setting is more conclusive. They are also associated with Samail ophiolites and Hawasina (Figs. 3.9h and 3.9i), which presumably act as confining layers for an aquifer in the limestones of the Kawr group, around which 10 of the 12 oases in this cluster are grouped. These oases have very small catchment sizes and are far from streams, but the proximity to limestones and the mountainous terrain in the neighborhood indicate that they are fed by springs emerging from the limestones. Based on the locations of these oases close to the limestones of Jabal Kawr, we classify them as ‘Kawr Oases’ (Fig. 3.10).

The last cluster, the ‘Drainage Oases’ are characterized by the largest catchments of all oases in the mountain range and their locations directly at large streams. Except for outliers of clusters 1 and 2, they are also by far the largest oases in this study. These oases are located to the south-west of the mountain range, in a valley between the mountains and the extensive dune fields of the Wahiba Sands. Based purely on surface topography, this valley drains the entire area west of the mountains, channeling all water flowing towards the sea. Groundwater resources in this location should thus be very large. The

settlements of Bilad Bani Bu Hasan and Al Kamil are consequently the largest natural oases in northern Oman.

### 3.5.2. *Factors determining oasis locations*

Almost all oases are located close to Quaternary sediments. According to our classification, no oasis lies more than 10 km away from such sediments (data not shown). This is not surprising, because sediments are a necessary prerequisite for oasis formation. In Oman, cultivable soil is often as scarce as water, and it is only available where sediments accumulate or can be accumulated artificially. Even at the oases, which are far from major deposits of such sediments, farmers cultivate fields on sediment patches that are too small to appear on the 1:100,000 scale geologic map, or they collect sediments from elsewhere and transport them to the locations that are to be cultivated.

Other than close to Quaternary sediments, oases were also found in association with limestones of Kawr and Hajar rocks. These oases are associated with springs that are fed by aquifers in the limestones and emerge at the unconformity at the lower end of these storage formations. Both the Hajar and Kawr limestones rest unconformably on rocks of different types (even though from our analysis it is impossible to say if in places the aquifer extends into the thin Precambrian Kharus Group, which stratigraphically lies below the Hajar Supergroup; Fig. 3.1). The small catchment areas and the relatively large distances to streams of most oases, which lie close to these formations, indicate that their agriculture is fed by springs rather than flow accumulation in sediments. They can thus be considered geologic rather than topographic oases (Table 3.5).

Most other oases lie much closer to streams and draw their water from much larger catchments. This is particularly true for oases of cluster 2 ('Foothill Oases'). Even though these oases are closely associated with Hawasina and Samail, the hydrologic properties identify them as topographic rather than geologic oases (Table 3.5). The geologic groups in their vicinity act as channeling formations rather than storage formations, making sub-surface wadi run-off flow towards the oases, where it can be made accessible by branching off aflaj from the wadi or by digging wells.

The most spectacular examples of such topographic flow oases are the oases of the 'Drainage' cluster (Table 3.5). The very high flow accumulations of these oases, as well as the high accumulations near some streams on the Batinah Coast make it likely that underground flow leads large quantities of drainage water into the sea. While locally water resources are overextracted, leading to the intrusion of saltwater into fresh aquifers, it is not unlikely that close to the main drainage channels, additional water could be extracted.

'Plain Oases' are similar to 'Foothill Oases', in that they rely on groundwater stored in sediments rather than on springs (Table 3.5). Virtually all oases on the Batinah Coast rely on wells, and the same is true for many oases west of the mountains. In both of these settings, many oases are close to streams, but it still

seems as if flow accumulation is the deciding factor for the oases' existence. The low topographic gradient in these mostly flat areas makes any form of water acquisition other than from wells difficult to implement. Proximity to streams might thus just be an indicator of groundwater depth, and thus ease of well-digging, but does not necessarily mean that farmers harvest water from the intermittent streams.

'Urban Oases' are neither close to geologic formations that are likely to be storage rocks, nor in topographically favorable places (Table 3.5). Their locations are largely determined by city planners rather than by water availability. Parks and sports facilities are often irrigated with recycled urban waste water, water from deep wells, or water that has been transported over long distances. They thus may be located in settings, for which economic considerations would preclude irrigation for agricultural production.

Today, the water flow of all major streams in northern Oman, which are likely to correspond to the main drainage lines detected by our analysis, appears to be buried under thick layers of Quaternary sediments. When sea levels were lower during the Last Glacial Maximum (LGM, ~20 ka BP), however, the places where these streams flow into the sea might have been exposed. They may thus be candidates for the now submerged coastal oases postulated by Faure et al. (2002), which are likely to have existed on the exposed continental shelf during the LGM and during the subsequent deglaciation. At that time, the surface of the Arabian Sea was up to 120 m below current sea level (Rohling et al. 1998, Siddall et al. 2003), and even though the Arabian Peninsula is assumed to have been much drier than today (Weyhenmeyer et al. 2000), the locations where the entire flow accumulation of inland northern Oman flowed into the sea are likely to have contained perennial oases. According to Faure et al. (2002), the mouths of these streams might have been important refuges for plants and animals, including early humans.

### **3.6 Conclusions**

Cluster analysis proved a useful tool for classifying oases in northern Oman, which, if their total vegetated area was >0.4 ha, were reliably detected using Landsat imagery and image processing techniques. Our analysis discovered 2428 oases with areas above this threshold.

Based on their reliance on geologic, topographic and hydrologic parameters, Omani oases can be subdivided into six types. 'Plain Oases', 'Foothill Oases' and 'Drainage Oases' draw their irrigation water from groundwater, the accumulation of which can be explained by their topographic settings. For water acquisition, oases of these types rely on wells or sub-surface flow in wadi sediments. 'Mountain Oases' and 'Kawr Oases', in contrast, rely on springs, which emerge from the boundaries of limestone storage formations and confining layers made up of other materials. 'Urban Oases' mostly do not rely on readily available water resources, and thus are not located in hydrologically conclusive settings.

## Acknowledgments

We are indebted to Stefan Siebert for his helpful advice and to the Deutsche Forschungsgemeinschaft for funding this research (BU1308). We also acknowledge the excellent reviews of two anonymous referees, which greatly improved this paper.

## References

- Buerkert A, Nagieb M, Siebert S, Khan I and Al-Maskri A (2005). Nutrient cycling and field-based partial nutrient balances in two mountain oases of Oman. *Field Crops Research* 94(2-3), 149-164.
- Cookson P and Lepiece A (2001). Could date palms ever disappear from the Batinah? Salination of a coastal plain in the Sultanate of Oman. In: K.A. Mahdi (Ed.), *Water in the Arabian Peninsula - Problems and Policies*. Exeter Arab and Islamic Studies Series. Ithaca Press, Garnet Publishing Ltd., Reading, UK.
- Costa PM (1983). Notes on traditional hydraulics and agriculture in Oman. *World Archaeology* 14(3), 273-295.
- Faure H, Walter RC and Grant DR (2002). The coastal oasis: ice age springs on emerged continental shelves. *Global and Planetary Change* 33(1-2), 47-56.
- Fisher M (1994). Another look at the variability of desert climates, using examples from Oman. *Global Ecology and Biogeography Letters* 4(3), 79-87.
- Gass I, Ries A, Shackleton R and Smewing J (1990). Tectonics, geochronology and geochemistry of the Precambrian rocks of Oman. In: A. Robertson, M. Searle and A. Ries (Eds.), *The Geology and Tectonics of the Oman Region*. Geological Society Special Publication 49, London, UK.
- Gebauer J, Luedeling E, Hammer K, Nagieb M and Buerkert A (2007). Mountain oases in northern Oman: An environment for crop evolution and *in situ* conservation of plant genetic resources. *Genetic Resources and Crop Evolution* 54, 465-481.
- GLCF (2006). Earth Science Data Interface at the Global Land Cover Facility. Accessed on 15 October 2006 at <http://glcf.umiacs.umd.edu/index.shtml>.
- Glennie K (2005). *The geology of the Oman Mountains: an outline of their origin*. Scientific Press, Beaconsfield, Bucks, UK.
- Glennie K, Boeuf M, Hughes Clarke M, Moody-Stuart M, Pilaar W and Reinhardt B (1974). Geology of the Oman Mountains. *Verhandelingen Koninklijk Nederlands geologisch mijnbouwkundig Genootschap* 31, 1-423.
- Gradstein F, Ogg J and Smith A (2004). *A geologic time scale 2004*. Cambridge University Press, Cambridge, UK, 589 pp.
- Harris R (2003). Remote sensing of agriculture change in Oman. *International Journal of Remote Sensing* 24(23), 4835-4852.
- Korn L, Häser J, Schreiber J, Gangler A, Nagieb M, Siebert S and Buerkert A (2004). Tiwi and Wadi Tiwi: the development of an oasis on the north-eastern coast of Oman. *Journal of Oman Studies* 13, 57-90.
- Luedeling E, Nagieb A, Wichern F, Brandt M, Deurer M and Buerkert A (2005). Drainage, salt leaching and physico-chemical properties of irrigated man-made terrace soils in a mountain oasis of northern Oman. *Geoderma* 125(3-4), 273-285.
- Luedeling E, Siebert S and Buerkert A (2007). Filling the voids in the SRTM Elevation Model - A TIN-based delta surface approach. *ISPRS Journal of Photogrammetry and Remote Sensing* 64(4), 283-294.
- Norman WR, Al-Ghafri AS and Shayya WH (2001). Water-use performance and comparative costs among surface and traditional irrigation systems in northern Oman. In: K.A. Mahdi

- (Ed.), *Water in the Arabian Peninsula - Problems and Policies*. Exeter Arab and Islamic Studies Series. Ithaca Press, Garnet Publishing Ltd., Reading, UK.
- Rabu D, Nehlig P and Roger J (1993). Stratigraphy and structure of the Oman Mountains. Bureau de recherches géologique et minières (BRGM), Orléans, France, 262 pp.
- Rabus B, Eineder M, Roth A and Bamler R (2003). The shuttle radar topography mission - a new class of digital elevation models acquired by spaceborne radar. *ISPRS Journal of Photogrammetry and Remote Sensing* 57(4), 241-262.
- Ravaut P, Bayer R, Hassani R, Rousset D and Al Yahya'ey A (1997). Structure and evolution of the northern Oman margin: gravity and seismic constraints over the Zagros-Makran-Oman collision zone. *Tectonophysics* 279, 253-280.
- Robertson A and Searle M (1990). The northern Oman Tethyan continental margin: stratigraphy, structure, concepts and controversies. In: A. Robertson, M. Searle and A. Ries (Eds.), *The Geology and Tectonics of the Oman Region*. Geological Society Special Publication 49, London, UK.
- Rodriguez E, Morris CS and Belz JE (2006). A global assessment of the SRTM performance. *Photogrammetric Engineering and Remote Sensing* 72(3), 249-260.
- Rohling EJ, Fenton M, Jorissen FJ, Bertrand P, Ganssen G and Caulet JP (1998). Magnitudes of sea-level lowstands of the past 500,000 years. *Nature* 394(6689), 162-165.
- Siddall M, Rohling EJ, Almogi-Labin A, Hemleben C, Meischner D, Schmelzer I and Smeed DA (2003). Sea-level fluctuations during the last glacial cycle. *Nature* 423(6942), 853-858.
- Siebert S, Häser J, Nagieb M, Korn L and Buerkert A (2005). Agricultural, architectural and archaeological evidence for the role and ecological adaptation of a scattered mountain oasis in Oman. *Journal of Arid Environments* 62(1), 177-197.
- Tucker CJ and Sellers PJ (1986). Satellite Remote-Sensing of Primary Production. *International Journal of Remote Sensing* 7(11), 1395-1416.
- Weyhenmeyer CE, Burns SJ, Waber HN, Aeschbach-Hertig W, Kipfer R, Loosli HH and Matter A (2000). Cool glacial temperatures and changes in moisture source recorded in Oman groundwaters. *Science* 287(5454), 842-845.
- Wichern F, Luedeling E, Müller T, Joergensen RG and Buerkert A (2004). Field measurements of the CO<sub>2</sub> evolution rate under different crops during an irrigation cycle in a mountain oasis of Oman. *Applied Soil Ecology* 25(1), 85-91.



## Chapter 4

*submitted to Journal of Hydrology*

# Hydrological sustainability of mountain oases in northern Oman

Eike Luedeling <sup>a</sup>, Hany El-Gamal <sup>b</sup>, Werner Aeschbach-Hertig <sup>c</sup>, Rolf Kipfer <sup>d</sup>, Maher Nagieb <sup>a</sup> and Andreas Buerkert <sup>a</sup>

<sup>a</sup> *Organic Plant Production and Agroecosystems Research in the Tropics and Subtropics, University of Kassel, Steinstr. 19, D-37213 Witzenhausen, Germany*

<sup>b</sup> *Physics Department, Faculty of Science, Assiut University, Assiut, Egypt*

<sup>c</sup> *Institute of Environmental Physics, University of Heidelberg, D-69120 Heidelberg, Germany*

<sup>d</sup> *Isotope Geology and Mineral Resources, ETH Zurich, CH-8092 Zurich, Switzerland, and Eawag, Swiss Federal Institute of Aquatic Science and Technology, CH-8600 Dübendorf, Switzerland*

---

### Abstract

In the hyperarid desert environment of the Oman Mountains, natural precipitation is scarce and erratic, confining agriculture to oases where irrigation water is available. Oasis farmers cultivate perennial orchards of date palm (*Phoenix dactylifera* L.) and other fruit trees, as well as various field crops, which are irrigated with water from natural springs or from tunnels carved into water-bearing rock formations. To date, little is known about the flow stability of the oases' springs and about the retention time of rainwater in the storage rocks, both of which are major determinants of the oases' hydrological sustainability.

To fill this knowledge gap, we determined the flow rates of four irrigation channels at Balad Seet over 34 months, 22 channels at Maqta over 31 months, and two channels at Al 'Ayn over 19 months. Water ages were derived from the concentrations of hydrological dating tracers in water samples taken from two springs at Balad Seet, six springs at Maqta, and one spring each at Hat, Al 'Ayn, As Sumayiyah and Nakhl. For this, we used the <sup>3</sup>H-<sup>3</sup>He method, which is based on the radioactive decay of tritium,

and the SF<sub>6</sub> method, which infers residence times from the concentrations of the anthropogenic trace gas sulfur hexafluoride.

Total water flow varied between 22 and 58 m<sup>3</sup> h<sup>-1</sup> at Balad Seet, between 4 and 9 m<sup>3</sup> h<sup>-1</sup> at Maqta, and between 25 and 61 m<sup>3</sup> h<sup>-1</sup> at Al ‘Ayn. During drought periods, spring flow decreased exponentially by 11.7% per year at Balad Seet and by 29.8% at Maqta.

Estimated water ages ranged from 2 to 10 years for Balad Seet, from 2 to 8 years for Maqta (except for one spring with older water), and were around 8 years for the samples from Hat, As Sumayiyah and Al ‘Ayn. Large amounts of radiogenic helium in the sample from Nakhl precluded <sup>3</sup>H-<sup>3</sup>He dating, but the SF<sub>6</sub> concentrations indicated an age of 16 years. All age determinations were complicated by difficult sampling conditions, which might have led to gas exchange during sampling, and low tritium concentrations. Potential water flow through caves in the limestone storage rock formations added uncertainty. Three SF<sub>6</sub> samples indicated negative water ages, hinting at the presence of natural SF<sub>6</sub>.

Our analyses indicated that the water supply of most of the studied oases is stable enough to allow crop cultivation during drought periods of several years, but not during dry spells of ten or more years. The springs of Maqta were least reliable, with relatively low ages and high flow decrease rates. This condition likely explains the semi-nomadic lifestyle of the inhabitants of this oasis, who rely much more on pastoral activities than the farmers at all other oases of this study.

---

## 4.1 Introduction

Almost the entire land area of the Sultanate of Oman consists of hyperarid desert. Throughout most of the country, mean annual rainfall ranges between 40 and 100 mm (Fisher 1994), as opposed to a mean annual evapotranspiration in excess of 2000 mm (Siebert et al. 2007). The only parts of the country with higher precipitation are the southern region of Dhofar and the upper reaches of the Oman Mountains, but even there the long-term average of annual rainfall does not exceed 350 mm (Fisher 1994). In addition to the general aridity, rainfalls are very erratic. Droughts of several years are common and often ended by torrential rainstorms.

Given these climatic conditions, virtually all agriculture in Oman relies on irrigation. Traditional farming systems have therefore developed in geological or topographic settings, where water was readily available or could easily be accessed (Luedeling and Buerkert 2008b). At some of these locations, permanent agricultural settlements have existed for thousands of years (Korn et al. 2004b, Nagieb et al. 2004b), with no evidence of natural resource depletion. Most of these villages are scattered within or around the main ridge of the Oman Mountains. Oasis farmers derive their irrigation water either from natural springs, from tunnels carved manually into the rocks or from the beds of intermittent streams (Arabic: wadi) flowing out of the mountain range (Costa 1983). From the source, the water is then conveyed through an intricate system of channels (Arabic: aflaj, singular: falaj) to irrigate the crops, which in the mountains are generally grown on small terraced fields (Luedeling et al. 2005a). Omani oasis farmers grow a large array of different crops (Gebauer et al. 2007a),

with much of the cultivated area dedicated to groves of date palm (*Phoenix dactylifera* L.), pomegranate (*Punica granatum* L.), lime (*Citrus aurantiifolia* (L.) Swingle), peach (*Prunus persica* L.), mango (*Mangifera indica* L.) and other fruit trees. In addition to these, farmers cultivate field crops, such as alfalfa (*Medicago sativa* L.), wheat (*Triticum aestivum* Desf. and *Triticum durum* L.), maize (*Zea mays* L.), sorghum (*Sorghum bicolor* (L.) Moench), onion (*Allium cepa* L.) and garlic (*Allium sativum* L.).

Perennial and annual crops have very different water demand patterns. While fruit orchards require uninterrupted water supply all year round over decades, water consumption by field crops is restricted to the crops' growing period, and it is possible to adjust the cultivated area from year to year depending on the amount of available water. In most oases, farmers grow perennial fruit trees on some terraces, annual crops on others, and typically a certain proportion of the oasis is left uncultivated. Since dates and other fruits are the most valuable agricultural products of the oases, farmers strive to put as much area under perennial crops as the reliable long-term water flow permits. The ratio of annual vegetation and fallow terraces to perennial crops may thus indicate the perceived long-term risk of a decline in water flow during a prolonged drought (Korn et al. 2004b, Norman et al. 1998a, Siebert et al. 2007).

To date, little is known about the stability of the water supply in mountain oases of Oman, which is complicated by the complex geology of these places and unknown characteristics of their water storage bodies. Information about the stability of the oases' water resources, however, is essential for evaluating their long-term hydrological sustainability.

The main parameters, from which such information can be derived, are the outflow dynamics of the springs and the rocks' ability to store and gradually dispense the water, which is supplied by the rare rainfall events. To fill the described knowledge gaps, we measured spring flows at three oasis systems in the Oman Mountains, and determined the water retention time in the rocks from water samples taken at six oases throughout the mountain range.

## 4.2 Materials and Methods

### 4.2.1. Study sites

The study was conducted in seven mountain oases in Oman (Fig. 4.1). Agricultural areas of Balad Seet, Maqta and Al 'Ayn were determined by detailed surveys using Differential GPS and aerial photography (Buerkert et al. 1996). Palm grove and field areas for Hat, As Sumayiyah and Nakhil were estimated using the area measurement tool of Google Earth Pro (Google, Mountain View, CA, USA).

In the oasis of Balad Seet (23°11'N, 57°23'E, 985 m a.s.l.), all springs emerge at the bottom of a 1000-m cliff made up of limestones of the Late Permian to Early Cretaceous (260 to 100 million years before present) Hajar Supergroup, which forms an extensive elevated plateau just south of the oasis (Glennie et al.

1974). From the springs, water is conducted through aflaj of up to 1 km length to 9 ha of orchards and 5 ha of fields, which are located around a rock outcrop holding the traditional settlement (Nagieb et al. 2004b).

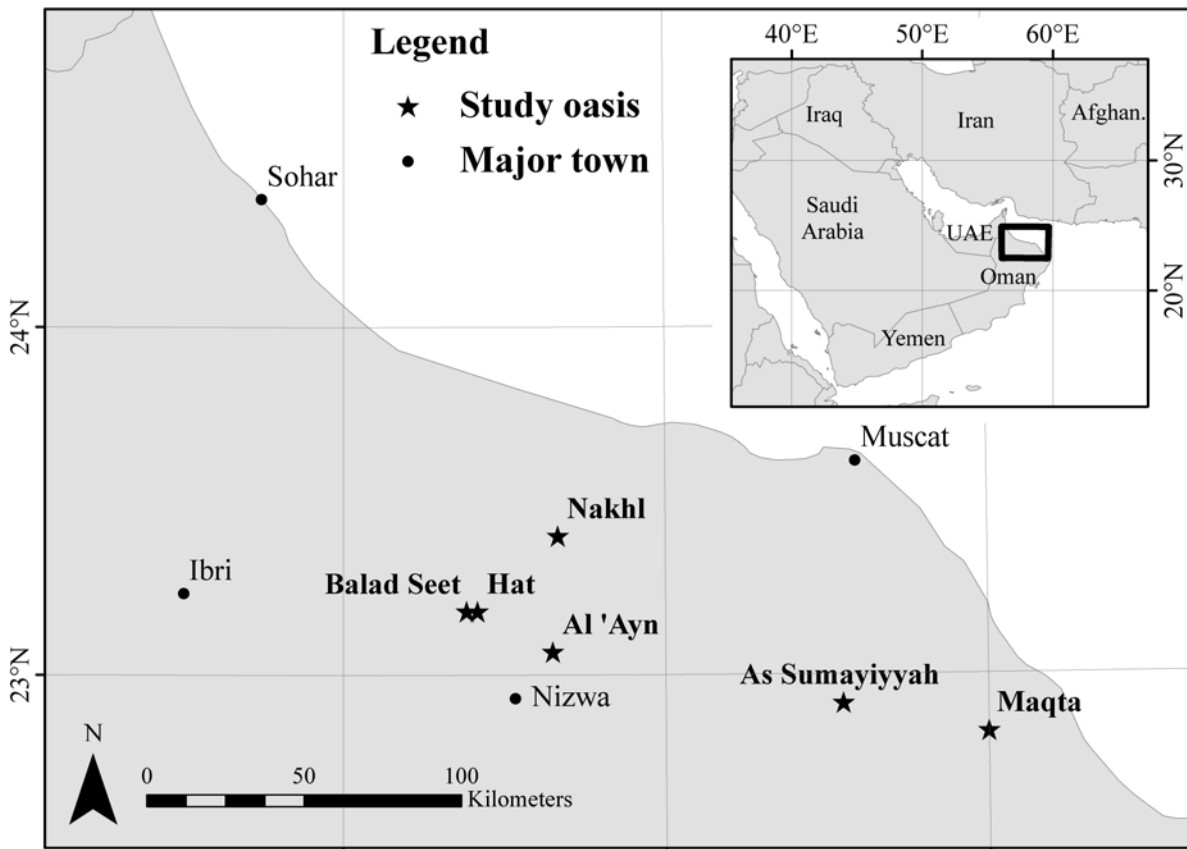


Figure 4.1. Locations of the study oases in northern Oman.

The oasis of Hat ( $23^{\circ}11'N$ ,  $57^{\circ}25'E$ , 1115 m a.s.l.) lies in a similar geological setting, but its agriculture is only fed by one major spring. From this, the irrigation water is conducted through a 0.7-km long falaj to about 4 ha of palm groves and 4 ha of field crops.

In contrast, the 22 springs of Maqta ( $22^{\circ}50'N$ ,  $59^{\circ}00'E$ , 1050 m a.s.l.) are scattered over an area of approximately  $1 \text{ km}^2$  and arise from diverse geological settings, with springs emerging from limestones, ophiolites or loose gravel. Because of the crumbly nature of the rocks around Maqta, no extended falaj network exists in this oasis, and all water is used in separate terrace systems built close to the springs. The agricultural area consists of 3 ha of date palm and 1 ha of annual fields (Siebert et al. 2005).

At the oasis of As Sumayiyah ( $22^{\circ}55'N$ ,  $58^{\circ}53'E$ , 450 m a.s.l.), the main spring emerges at the foot of a large Hajar limestone outcrop and is directed via a short falaj to extensive palm gardens covering an area of 35 ha and to about 8 ha of annual fields.

The spring at Nakhl ( $23^{\circ}24'N$ ,  $57^{\circ}40'E$ , 295 m a.s.l.) emerges at the stratigraphically upper end of the Hajar limestone formation, which steeply drops into the ground close to the spring. The water emerges at a temperature of

38°C, indicating some deep water circulation, and is used to irrigate about 151 ha of palm groves and 12 ha of field crops.

The agricultural terraces of the high mountain oasis of Al 'Ayn (23°04'N, 57°39'E, 1930 m a.s.l.) and the adjacent villages of Ash Sharayjah, Al 'Aqr and Qasha' are fed by two springs emerging below the edge of a high mountain plateau made up of Hajar limestones (Scholz 1984). The springs feed about 13 ha of orchards and two ha of field crops.

#### 4.2.2. Spring flow

To monitor the oases' water supply, the flow of the aflaj at Balad Seet and Maqta was measured at irregular intervals over a period of 34 months at Balad Seet (36 occasions, from Nov 15<sup>th</sup>, 2000 to Sep 29<sup>th</sup>, 2003) and over 31 months at Maqta (18 occasions, from Mar 15<sup>th</sup>, 2001 to Oct 1<sup>st</sup>, 2003). At Balad Seet, we measured the flow of the four main aflaj and recorded rainfall using a standard rain gauge. At Maqta, 20 of the oasis' 22 springs were measured regularly, while the small flow of the two remaining springs could only be estimated.

All flow measurements were carried out by collecting the water flowing through the irrigation channels in containers of known volume. For small flows a 2 L measuring cup was used, whereas the water of the stronger-flowing springs was collected in a barrel of 200 L. Water losses by leakage were avoided as much as possible by means of cloth or flexible plastic, which were used to channel the water. The time needed to fill the containers was registered and allowed the calculation of the spring's flow rate.

Between November 10<sup>th</sup>, 2005 and June 5<sup>th</sup>, 2007, spring flow was additionally measured at two springs in the oasis of Al 'Ayn in the mountains of Al Jabal al Akhdar. Falaj gradients in this oasis are much smaller than in the other settlements, and the falaj networks are more ramified, so that it was difficult to collect the entire spring flow anywhere in the system. For measuring flow rates, we therefore located a straight and even stretch of falaj of known length and made a styrofoam device float along the falaj. Given the straight nature of the cemented channels, dividing the volume of water along the floating course by the time needed to float the distance was accepted as an approximation of the flow rate. To make measurements more comparable and less prone to errors caused by wind or by the inevitably turbulent flow conditions, we changed the measurement method in October 2006. Close to the springs, we channeled all water from the falaj into a pipe of 5 m length, kept the pipe in a near horizontal position, and collected all water at the end of the pipe, where it dropped back into the falaj. Unfortunately, this method could not be applied to the largest falaj in the area, which conducts large amounts of water over a distance of more than one kilometer to the oasis of Ash Sharayjah. The gradient of this falaj is small and cannot easily be raised artificially. However, the water flow in this falaj is very smooth and runs in a channel that is well

protected from wind. We therefore consider the styrofoam floating method acceptable for this falaj.

Since no detailed information on the structure of the aquifers was available, we described spring flow recession according to linear reservoir theory (Malvicini et al. 2005, Peters et al. 2005) as

$$Q_t = Q_0 e^{-at},$$

with  $Q_t$  being the spring flow at time  $t$  (in years),  $Q_0$  being the base flow,  $t$  denoting time in years, and  $a$  being a spring-specific recession factor. No recharge term was added to this model, because we had no information on rainfall in the recharge areas during the study period. Therefore, our analysis of flow recession rates was restricted to periods of drought. Based on our repeated measurements of  $Q_t$ , we used SigmaPlot 7.0 (SPSS Inc., Chicago, IL, USA) to calculate two parameter exponential decay regressions for all springs at Balad Seet and Maqta, yielding the recession factor  $a$ . For Balad Seet, the longest period without significant precipitation was from Nov 15<sup>th</sup>, 2000 to Mar 15<sup>th</sup>, 2003, while for Maqta this period comprised Mar 15<sup>th</sup>, 2001 to Mar 6<sup>th</sup>, 2003. At Al ‘Ayn, rainfall was too frequent to calculate recession functions at any time during the study period.

#### 4.2.3. Water age

We used two methods to determine the retention time of rainwater in the subsurface. The  $^3\text{H}$ - $^3\text{He}$  method (Kipfer et al. 2002, Schlosser et al. 1988, Schlosser et al. 1989, Solomon and Cook 2000) has successfully been applied to study shallow groundwater in wells (Beyerle et al. 1999, Holocher et al. 2001) and natural springs (Rademacher et al. 2001). The principle behind this method is the radioactive decay of universally occurring atmospheric tritium ( $^3\text{H}$ ) in water into its stable decay product, the light helium isotope  $^3\text{He}$ . With a half-life of 12.32 years (4500 days, Lucas and Unterweger 2000), the tritium decay can be used for the determination of water ages younger than 50 years.

The  $^3\text{H}$  concentration in precipitation exhibited a sharp peak in the early 1960s due to  $^3\text{H}$  release by atmospheric thermonuclear bomb tests, but has since then returned to almost natural levels originating from cosmic-ray induced production in the atmosphere. As long as surface water is exposed to the atmosphere, constant gas exchange keeps the  $^3\text{He}$  concentration at its atmospheric equilibrium value, but as soon as the water infiltrates into the ground, the exchange is cut off and the concentration of  $^3\text{He}$  rises, as tritium decays. Measurement of the concentrations of  $^3\text{H}$  and the produced tritiogenic  $^3\text{He}$  at any time thus allows the calculation of its residence time in the rocks or the ‘water age’. As for all dating methods based on gas tracers, this age reflects the time since isolation of the water from contact with the atmosphere, and it has to be interpreted as an apparent age, because it can deviate from the true mean age of a mixed water mass.

To accurately quantify the amount of tritiogenic  $^3\text{He}$ , it is necessary to separate it from the background  $^3\text{He}$ , which originates from dissolution of

atmospheric  $^3\text{He}$  in meteoric water, and from accumulated radiogenic He in the subsurface. The calculation of the  $^3\text{He}$  derived from the atmospheric solubility equilibrium requires knowledge of air pressure, mainly determined by altitude, and soil temperature prevailing at the location and time of infiltration. Atmospheric  $^3\text{He}$  is also present in the ‘excess air’ fraction of a sample, an over-saturation of the water with atmospheric gases, which results from the dissolution of air bubbles during infiltration (Heaton and Vogel 1981). The size of the excess air fraction is often estimated from the Ne concentration and expressed as the excess of Ne relative to the equilibrium resulting from the solubility of air in water ( $\Delta\text{Ne}$ ).

The presence of radiogenic He, produced by  $\alpha$ -emitting isotopes of the uranium (U) and thorium (Th) decay series and subsequent nuclear reactions in the rocks, further complicates the calculation of tritiogenic  $^3\text{He}$ . The radiogenic  $^4\text{He}$  can be determined from the difference of the measured total and calculated atmospheric He concentration, and the respective  $^3\text{He}$  component is usually estimated using a typical crustal  $^3\text{He}/^4\text{He}$  ratio of  $2 \times 10^{-8}$ . If a significant radiogenic He component is present, this correction adds uncertainty to the calculated tritiogenic  $^3\text{He}$  and hence the  $^3\text{H}$ - $^3\text{He}$  ages. On the other hand, radiogenic He provides additional qualitative age information, with high concentrations indicating old waters that accumulated He over extended periods of time (Kipfer et al. 2002).

The calculation of the tritiogenic  $^3\text{He}$  was performed using the above described He and Ne balance equations as given by Schlosser et al. (1989) and Kipfer et al. (2002), with slight modifications to include additional information derived from the analysis of the other noble gases. The concentrations of the four stable atmospheric noble gases Ne, Ar, Kr, and Xe were used to estimate the equilibration temperature and to check and, if necessary, correct the assumption that the atmospheric He/Ne ratio can be used to estimate the excess air component of He.

The atmospheric noble gases provide information about the solubility equilibrium at infiltration, which can be used to infer recharge conditions (Aeschbach-Hertig et al. 1999, Stute and Schlosser 1993). Temperature and altitude are correlated parameters, such that one of them can be determined reliably if the other one is known (Aeschbach-Hertig et al. 1999). Infiltration altitudes at the study sites were estimated from the topography of the locations, whereas temperatures were inferred from these estimates and the noble gas data.

The noble gases are also crucial for determining the composition of the ‘excess air’ component. We considered two models, which describe how excess air is formed. The unfractionated excess air model (UA-model) assumes that entrapped air bubbles are dissolved completely, which leads to an excess air component that has the same composition as air. The closed-system equilibration model (CE-model) describes excess air with a composition that is fractionated relative to air (i.e., has a slightly lower He/Ne ratio) as a result of solubility equilibrium between entrapped bubbles and water under closed-system conditions (Aeschbach-Hertig et al. 2000).

All samples were collected in special containers, consisting of copper tubes fixed in aluminum racks that could be shut airtight by steel pinch-off clamps mounted on both sides of the rack. Every effort was made to prevent air contact of the samples during sampling to avoid degassing. To this end, flexible PVC-tubing was inserted as deeply as possible into the spring outlets and tightly connected to the copper tubes. The analyses for  $^3\text{H}$ ,  $^3\text{He}$  and noble gases were carried out at the noble gas laboratory of ETH Zurich, Switzerland, using the mass spectrometer setup described by Beyerle et al. (2000).  $^3\text{H}$ - $^3\text{He}$  samples were taken from 12 springs in the oases of Balad Seet (2 springs), Hat, Maqta (6 springs), As Sumayiyah, Nakhl and Al 'Ayn (Table 4.1).

Table 4.1. List of all springs, from which water samples were dated in this study.

Spring	Oasis	Spring description	Geographic coordinates	Elevation (m)
BS6	Balad Seet	Spring 6	23°10'55"N, 57°23'30"E	1115
BS13	Balad Seet	Spring 13	23°11'14"N, 57°23'39"E	980
Hat	Hat	Main spring	23°10'36"N, 57°24'35"E	1305
Maqta-1	Maqta	F1293	22°49'44"N, 58°59'09"E	1008
Maqta-2	Maqta	F1779	22°49'52"N, 58°59'32"E	1055
Maqta-3	Maqta	Mwezen	22°49'58"N, 58°59'11"E	958
Maqta-4	Maqta	F2680	22°49'52"N, 58°59'12"E	957
Maqta-5	Maqta	F1789	22°49'46"N, 58°59'56"E	1196
Maqta-6	Maqta	F2449	22°49'53"N, 58°59'13"E	965
Sumayiyah	As Sumayiyah	Main spring	22°55'07"N, 58°53'05"E	439
Nakhl	Nakhl	Main spring	23°22'32"N, 57°49'40"E	149
Al 'Ayn	Al 'Ayn	Al 'Ayn spring	23°04'26"N, 57°39'48"E	1936

As tritium concentrations in the samples from the first sampling campaign turned out to be rather low, leading to low amounts of tritiogenic  $^3\text{He}$  and consequently large uncertainties in the calculated water ages, we also used an alternative dating method, based on the concentration of sulfur hexafluoride ( $\text{SF}_6$ ) in the water samples (Bauer et al. 2001, Busenberg and Plummer 2000, Hofer et al. 2002). The atmospheric concentration of this gas, which is commonly used as an electric insulator in high-voltage switches, has been rising exponentially across the globe since the 1960s (Bauer et al. 2001, Busenberg and Plummer 2000, Zoellmann et al. 2001), making it an ideal dating tracer. Like any other gas,  $\text{SF}_6$  dissolves in meteoric water at known solubility equilibrium. Due to the rising atmospheric concentration, this equilibrium has been rising steadily since the 1950s. The reaction of  $\text{SF}_6$  with other substances is negligible, and it does not adsorb to surfaces nor biodegrade (Busenberg and Plummer 2000). Its concentration in ground water therefore remains constant over time. Measuring the  $\text{SF}_6$  concentration of spring water samples and correcting for the excess air contribution based on the noble gas data thus reveals the concentration that was set by equilibration with the atmosphere at the time of infiltration. The high increase rate of the atmospheric  $\text{SF}_6$  concentration of about 7% p.a. (Busenberg



and Plummer 2000) makes this method a very sensitive tool for dating young groundwaters.

SF<sub>6</sub> samples were taken in 500 ml stainless steel bottles (El-Gamal 2005) once from spring BS6 at Balad Seet, three times from the spring at Hat, once from three springs at Maqta (Maqta-4, Maqta-5 and Maqta-6) and once from the springs at As Sumayiyah and Nakhl (Table 4.1). Samples taken in 2002 and January 2003 were analyzed in the chromatographic trace gas laboratory of Eawag (Duebendorf, Switzerland) using a gas chromatograph equipped with an electron capture detector (ECD), as described by Hofer et al. (2002) and Aeschbach-Hertig et al. (2007). All later samples were measured at the Institute of Environmental Physics, University of Heidelberg, Germany. The water samples were transferred from the steel containers to special glass bottles as outlined by El-Gamal (2005), followed by injection of the headspace into a GC-ECD system described by von Rohden and Ilmberger (2001). For all water samples, water temperature was measured on site, and the approximate mean recharge altitude was estimated based on local topography.

## 4.3 Results

### 4.3.1. Spring flow

Oasis farmers at Balad Seet obtained most of their irrigation water from falaj Kabir, which is fed by six springs and accounted for 72% of the oasis' water supply in November 2000. The aflaj of Miban (one spring, 13% of irrigation water), Hidhan (one spring, 9%) and Litl (one spring, 6%) contributed relatively little water. In the absence of rainfall events, the outflow of all aflaj declined exponentially over time (Fig. 4.2). The flow of the aflaj Kabir and Litl was relatively stable, with decreases of 9.4 (R<sup>2</sup>=0.79) and 6.9% (R<sup>2</sup>=0.44) per year (p.a.) between November 2000 and March 2003, whereas the aflaj Hidhan (-20.8% p.a., R<sup>2</sup>=0.93) and Miban (-22.9% p.a., R<sup>2</sup>=0.97) lost much larger proportions of their flow during this time span. The overall water supply amounted to 30 m<sup>3</sup> h<sup>-1</sup> in November 2000, and 22.3 m<sup>3</sup> h<sup>-1</sup> in March 2003. In March and April 2003, several days of strong rains temporarily more than doubled the spring flow at Balad Seet to 58 m<sup>3</sup> h<sup>-1</sup>, but within a few days after the rains, falaj flows stabilized at only slightly higher rates than before the rains (Fig. 4.2).

At Maqta, overall spring flow was much lower at 8.99 m<sup>3</sup> h<sup>-1</sup> in March 2001 (Fig. 4.3). The largest springs were F1778 (21.4% of overall water supply in March 2001), F1777 (16.7%) and F2449 (15.0%). None of the other 19 springs contributed more than 6.4% of total irrigation water (Table 4.2). The annual decrease rates of spring flow were much higher than at Balad Seet, ranging from 1.7% to 73.7% per annum. Total available water in the oasis decreased by 29.8% per year (R<sup>2</sup>=0.91), as opposed to 11.7% at Balad Seet (R<sup>2</sup>=0.87). Some springs could not be described by an exponential decay function, which was due to construction measures on the falaj, such as further excavation of a spring,

which temporarily boosted falaj flows. Responses of falaj flow to rainfall varied widely between springs (Fig. 4.3). At Maqta, rainfall could not be recorded, but records from Ibra, 48 km west of the oasis (NCDC 2007), indicated that some aflaj, such as F1751 reacted almost immediately to rainfall events, whereas others (e.g. F1293) barely seemed affected (Fig. 4.3).

For the two springs emerging at Al ‘Ayn, overall output ranged between 24.6 and 61.0  $\text{m}^3 \text{h}^{-1}$  over the observation period (Fig. 4.4). Each of the springs is channeled in a separate falaj, with water from one spring flowing towards the gardens of Ash Sharayjah, and water from the other spring being distributed among the fields of Al ‘Ayn, Al ‘Aqr and Qasha’, according to the villages’ traditional water rights. Flow dynamics of the two aflaj differed markedly, with the falaj to Al ‘Ayn seeming more responsive to rainfall events than the Ash Sharayjah falaj. These different responses to rainfall caused the contribution of the Al ‘Ayn spring to overall spring flow to vary between 22 and 42%. Towards the end of the study period, both springs dramatically increased their flow, even though no major rainfall event was recorded by the nearby weather station at Saiq (NCDC 2007).

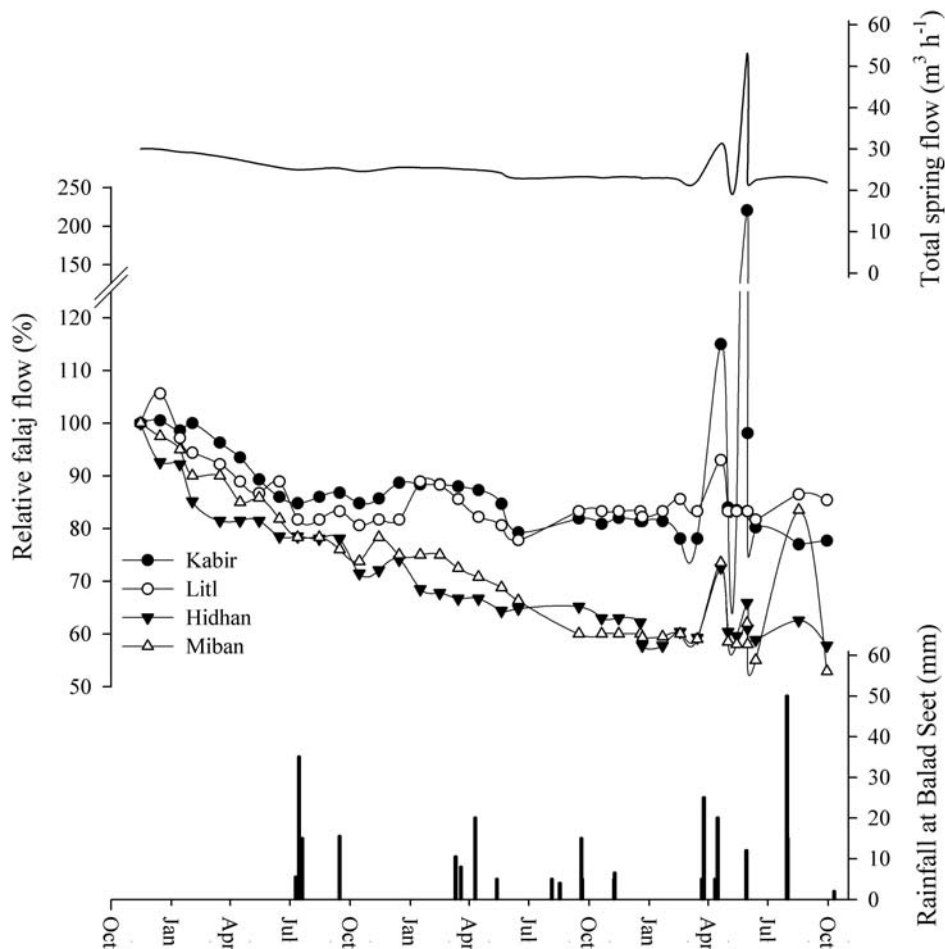


Figure 4.2. Total spring flow, flows of the four main aflaj (Kabir, Litl, Hidhan and Miban, relative to the flow on November 15<sup>th</sup> 2000) and rainfall recorded at Balad Seet, Oman, between November 2000 and September 2003.

Since the last significant rainfall before this increase happened five months before, and such a late response seems unlikely, we assume that the cause of this increase was unrecorded rainfall in a different part of the large catchment. Drought effects on spring flow could not be calculated for either of the springs, because in the high mountains dry spells are generally short and our sampling intervals were too long to reliably detect systematic decreases in spring flow.

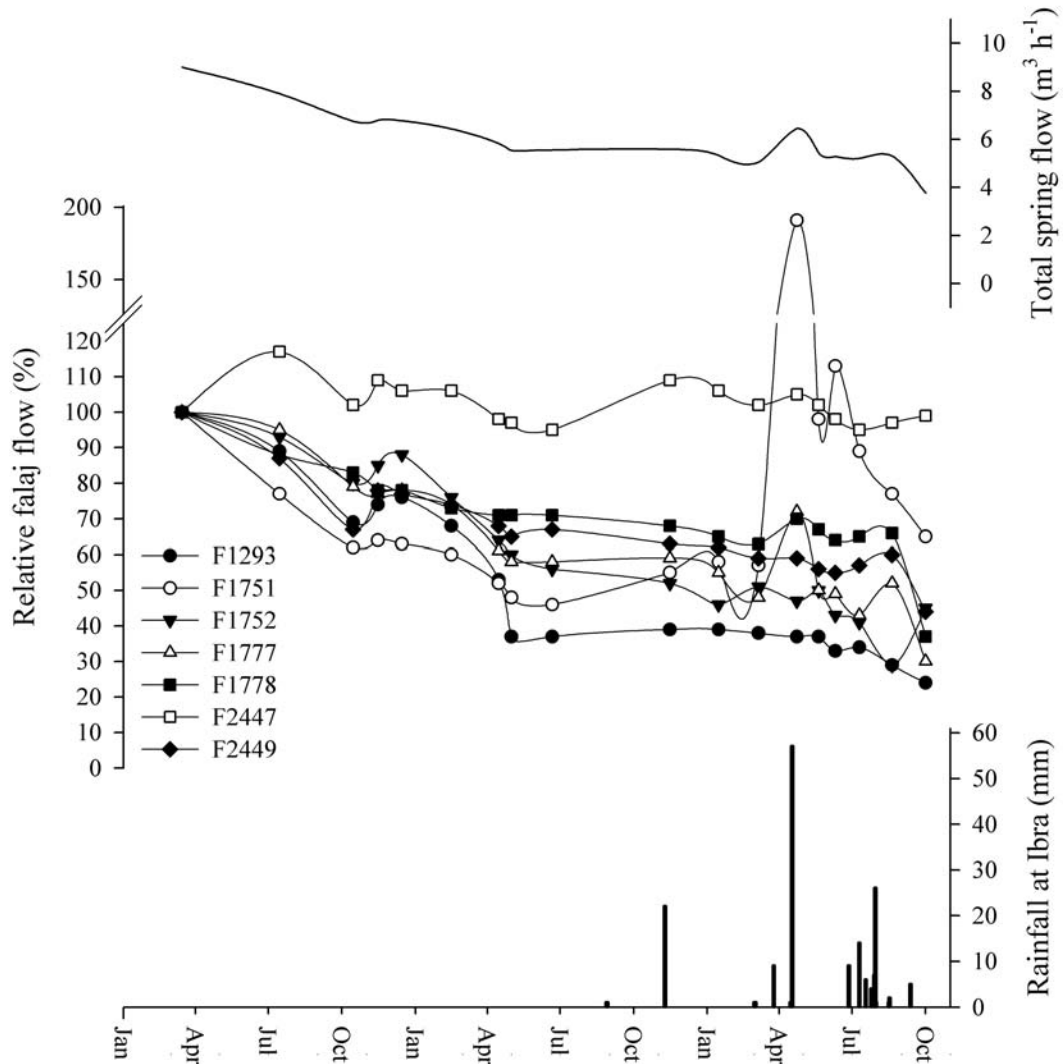


Figure 4.3. Total spring flow and flows of the seven main aflaj (relative to the flow on March 15<sup>th</sup> 2001) recorded at Maqta, Oman, between March 2001 and September 2003. In the rainfall records from Ibra, 48 km west of Maqta, data for Feb-Dec 2002 are mostly missing (NCDC 2007), but oasis farmers stated that no rain fell at Maqta during this time period.

#### 4.3.2. Water ages

For most of the sampled springs, water temperatures varied between 23 and 28°C (Table 4.3), which corresponds roughly to the mean annual temperature of the spring locations or can be explained by the influence of cooler temperatures in the higher recharge areas. Notable exceptions were spring Maqta-5 at Maqta,

which emerged at a temperature of only 15°C, and the thermal springs of As Sumayiyah (35°C) and Nakhl (38°C).

Table 4.2. Spring flow (in March 2001), contribution to the overall oasis water supply, annual flow change during times of drought and fit to an exponential decay regression for all springs at Maqta, Oman.

<b>Spring</b>	<b>Flow in March 2001 (m<sup>3</sup> h<sup>-1</sup>)</b>	<b>Contribution to oasis water supply (%)</b>	<b>Annual change during drought (%)</b>	<b>R<sup>2</sup> of exponential regression</b>
F1293	0.54	6.0	-59	0.88
F1751	0.32	3.6	-33	0.60
F1752	0.11	1.2	-41	0.91
F1754	0.27	3.0	-31	0.73
F1755	0.20	2.2	-33	0.81
F1758	0.02	0.2	-75	0.94
F1777	1.50	16.7	-38	0.92
F1778	1.93	21.4	-23	0.92
F1779	0.19	2.2	-30	0.92
F1780	0.39	4.3	-74	0.70
F1786	0.09	1.0	-59	0.84
F1788	0.24	2.6	-11	0.47
F1789	0.20	2.2	-28	0.86
F1790	0.19	2.1	-39	0.87
F2375	0.12	1.3	-	0.00
F2376	0.07	0.8	-	0.00
F2447	0.13	1.5	-2	0.03
F2448	0.36	4.0	-21	0.59
F2449	1.35	15.0	-25	0.82
Mwezen	0.58	6.4	-41	0.77
Qabel	0.03	0.3	-56	0.73
Sharr	0.18	2.0	-11	0.42

Attempts to derive the recharge altitudes of the aquifers from the concentrations of dissolved noble gases in the water samples (Aeschbach-Hertig et al. 1999, Manning and Solomon 2003) did not yield satisfactory results. This was not unexpected because the high correlation of the parameters temperature and pressure (elevation) makes reliable deduction of both parameters difficult. Age and recharge temperature determinations thus had to be based on estimates of the recharge altitude, which were derived from a Digital Elevation Model of the oases' surroundings (Luedeling et al. 2007a, Table 4.3). If a strict chi square test of the models used to fit the noble gas data was applied (Aeschbach-Hertig et al. 1999), the UA or the CE-model was acceptable for only 10 of the 16 samples. However, given the difficult sampling conditions of open springs, the complex hydrogeological settings and the uncertain recharge elevations, such a strict chi square approach did not seem appropriate. Thus, for most of the samples the simple UA-model was used, except for three of the four samples from Balad Seet (BS6-a, BS13-a, BS13-b), where the CE-model provided significantly better fits (Table 4.3). Four samples (BS6-a, BS6-b, Hat-a and

Maqta-4) had too high chi square values to rely on the calculated recharge temperature, thus the recharge temperature was assumed to be better represented by the sampling temperature. With regard to the final  $^3\text{H}$ - $^3\text{He}$  ages, the uncertainties resulting from the assumptions about recharge temperatures and altitudes, as well as excess air models, are generally small compared to the effect of analytical errors, in particular of the  $^3\text{He}/^4\text{He}$  ratio and the  $^3\text{H}$  concentration.

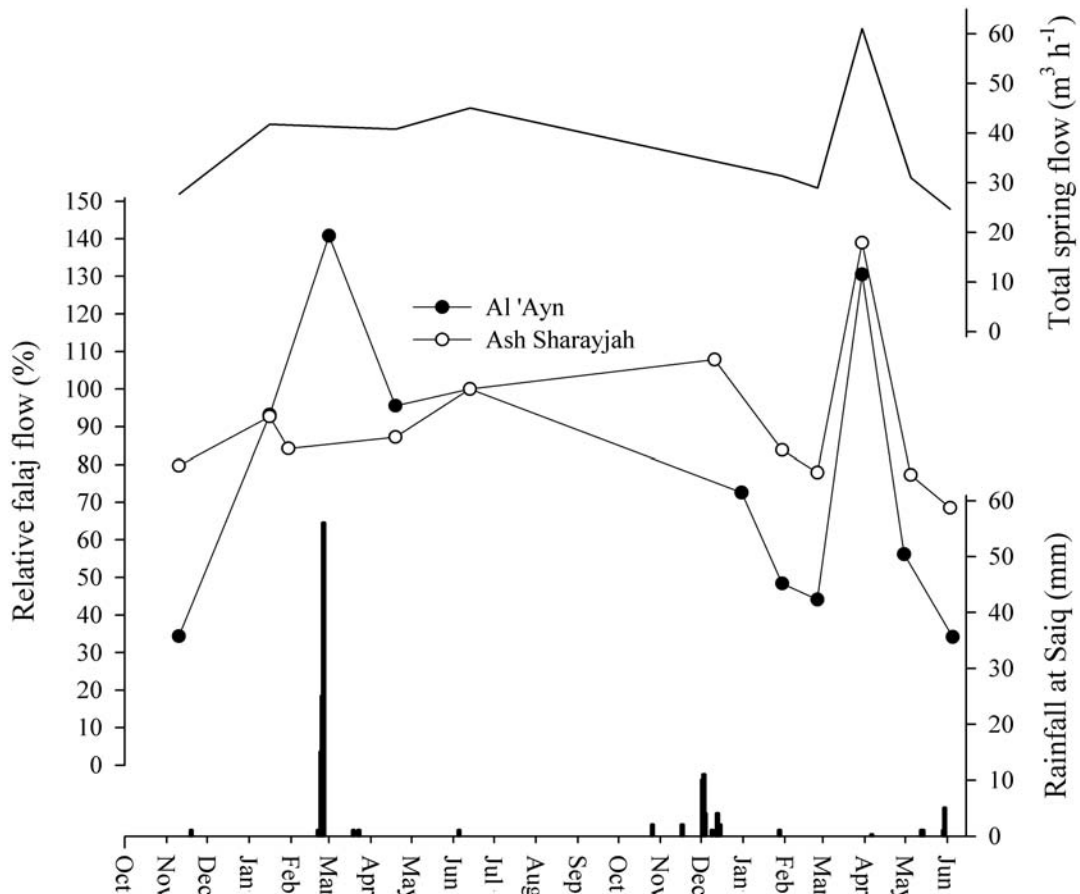


Figure 4.4. Total spring flow, and flows of the two aflaj conducting the water of the two springs emerging at Al 'Ayn, Oman, to the terraces of Al 'Ayn and Ash Sharayjah (relative to the flow on June 13<sup>th</sup> 2006), measured between November 2005 and June 2007. Rainfall records are from the weather station at Saiq, Oman, which is located within 5 km of the springs.

The size of the excess air component, as expressed by the  $\Delta\text{Ne}$  value, ranged from virtually zero at Al 'Ayn to 80% at Nakhl (Table 4.4). For one sample (Maqta-1), the Ne fraction was lost during analysis, so that  $\Delta\text{Ne}$  could not be calculated. The amount of radiogenic  $^4\text{He}$ , which increases the experimental errors for the  $^3\text{H}$ - $^3\text{He}$  ages, was below 10% of the atmospheric solubility equilibrium concentration for all samples from Balad Seet, Maqta and Al 'Ayn, high (37 to 47%) for samples from Hat and As Sumayiyah, and extremely high for the sample from Nakhl (29000%). For the Nakhl sample, the radiogenic component was so high that it precluded the calculation of a reliable age.

Table 4.3. Sampling date, sampling temperature, estimated mean recharge altitude, kind of samples taken, model fits of different excess air models to explain noble gas concentrations, and recharge temperatures for spring water of oases in northern Oman. UA is the ‘unfractionated excess air model’, CE is the ‘closed-system equilibration model’. Chi square ( $\chi^2$ ) is the sum of the squared and error weighted deviations between model and observed concentrations. The ‘model accepted’ was used to estimate the He/Ne ratio in the age calculation and the recharge temperature, except for a few samples with high chi-squares, where the recharge temperature was assumed to equal the sampling temperature.

Sample	Sampling Date	Sampling Temperature (°C)	Estimated mean recharge altitude (m a.s.l.)	Samples taken	UA-model $\chi^2$	CE-model $\chi^2$	Model accepted	Recharge temperature (°C)
BS6-a	09 Mar 2002	23	1900	<sup>3</sup> H-He	73.7	32.8	CE	23.3*
BS6-b	25 Nov 2002	23	1900	<sup>3</sup> H-He, SF <sub>6</sub>	97.0	111.8	UA	23.0*
BS13-a	19 Mar 2002	26	1900	<sup>3</sup> H-He	3.8	0.0	CE	22.9
BS13-b	25 Nov 2002	26	1900	<sup>3</sup> H-He	9.4	4.0	CE	27.1
Hat-a	15 Jan 2003	17	1900	<sup>3</sup> H-He, SF <sub>6</sub>	69.7	86.5	UA	18.0*
Hat-b	12 Jun 2003	24	1900	<sup>3</sup> H-He, SF <sub>6</sub>	5.9	5.7	UA	17.8
Hat-c	18 Aug 2003	24	1900	<sup>3</sup> H-He, SF <sub>6</sub>	7.7	7.7	UA	17.8
Maqta-1	12 Mar 2002	25	1400	<sup>3</sup> H-He	0.0	0.0	UA	23.6
Maqta-2	13 Mar 2002	26	1400	<sup>3</sup> H-He	0.1	0.1	UA	24.5
Maqta-3	13 Mar 2002	26	1400	<sup>3</sup> H-He	1.0	0.4	UA	26.3
Maqta-4	29 Nov 2002	26	1400	<sup>3</sup> H-He, SF <sub>6</sub>	131.0	158.1	UA	26.0*
Maqta-5	15 Jan 2003	15	1400	<sup>3</sup> H-He, SF <sub>6</sub>	17.6	31.9	UA	19.3
Maqta-6	10 Jun 2003	28	1400	<sup>3</sup> H-He, SF <sub>6</sub>	3.9	2.8	UA	24.8
Sumayiyah	09 Jun 2003	35	1400	<sup>3</sup> H-He, SF <sub>6</sub>	13.9	11.1	UA	25.3
Nakhl	11 Jun 2003	38	800	<sup>3</sup> H-He, SF <sub>6</sub>	8.3	3.4	UA	25.8
Al ‘Ayn	13 Jun 2003	23	2150	<sup>3</sup> H-He, SF <sub>6</sub>	8.4	7.9	UA	20.1

\*Sampling temperature used for calculations.

Tritium concentrations in the samples ranged from 0.3 TU for Maqta-5 to 2.4 TU for Maqta-2, with most concentrations between 1.5 and 2.0 TU (Table 4.4). The corresponding  $^3\text{H}$ - $^3\text{He}$  ages were between 1.7 and 10.1 years at Balad Seet, between 8.4 and 13.6 years at Hat, between 1.7 and 34.5 years at Maqta, 5.8 years at As Sumayiyah and 8.0 years at Al ‘Ayn.

$\text{SF}_6$  concentrations in the samples were between 0.80 and 1.73 femtomole  $\text{L}^{-1}$ , yielding water ages between 2.3 and 16.2 years. For three samples, the  $\text{SF}_6$  concentrations were above the modern equilibrium leading to apparently negative ages. It should be noted, however, that  $\text{SF}_6$  ages indicate minimum ages only. The formal uncertainties of about 0.5 years for the  $\text{SF}_6$  ages (Table 4.4), derived solely from the experimental errors of the  $\text{SF}_6$  analysis, do not reflect possible biases due to sample contamination or exposure to natural  $\text{SF}_6$ .

Table 4.4. Indication of excess air presence ( $\Delta\text{Ne}$ ), size of the radiogenic  $^4\text{He}$  fraction relative to the  $^4\text{He}$  concentration expected at equilibrium ( $\Delta^4\text{He}_{\text{rad}}$ ), tritium and  $\text{SF}_6$  concentrations, and respective age estimates for spring water samples taken from mountain oases in northern Oman.

Sample	$\Delta\text{Ne}$ (%)	$\Delta^4\text{He}_{\text{rad}}$ (%)	$^3\text{H}$ (TU)	$\text{SF}_6$ ( $10^{-15} \text{ mol L}^{-1}$ )	$^3\text{H}$ - $^3\text{He}$ age (yr)	$\text{SF}_6$ age (yr)
BS6-a	8.7	1.8	1.80±0.08	-	1.7±2.3	-
BS6-b	35.4	-3.2	1.70±0.06	1.041±0.031	3.0±2.1	8.4±0.5
BS13-a	10.8	1.7	1.48±0.05	-	8.9±2.7	-
BS13-b	15.8	3.8	1.74±0.07	-	10.1±2.3	-
Hat-a	42.6	45.1	1.46±0.30	0.810±0.024	8.4±5.0	14.2±0.4
Hat-b	18.1	41.1	1.54±0.30	1.510±0.023	13.6±3.4	2.3±0.5
Hat-c	15.8	37.2	1.38±0.30	1.892±0.034	11.8±4.0	<0 <sup>c</sup>
Maqta-1	lost	5.7	2.27±0.12	-	4.7±5.6	-
Maqta-2	11.3	1.1	2.42±0.10	-	1.7±2.4	-
Maqta-3	5.4	1.5	1.39±0.04	-	8.3±3.0	-
Maqta-4	32.0	0.2	2.00±0.30 <sup>a</sup>	1.079±0.032	5.1±3.3	7.3±0.5
Maqta-5	62.2	9.0	0.32±0.05	1.734±0.052	34.5±5.5	7.0±0.5
Maqta-6	9.6	1.2	1.87±0.30	1.393±0.025	3.4±3.9	<0 <sup>c</sup>
Sumayiyah	31.6	46.9	1.19±0.30	1.010±0.021	5.8±6.6	8.9±0.5
Nakhl	79.1	29175	1.49±0.30	0.932±0.028	- <sup>b</sup>	16.2±0.4
Al ‘Ayn	-0.4	4.2	1.92±0.30	1.571±0.035	8.0±1.7	<0 <sup>c</sup>

<sup>a</sup> Estimated tritium concentration

<sup>b</sup>  $^3\text{H}$ - $^3\text{He}$  age could not be calculated because of high radiogenic component

<sup>c</sup> Negative apparent  $\text{SF}_6$  age because of the presence of non-atmospheric  $\text{SF}_6$

## 4.4 Discussion

### 4.4.1. Spring flow

The flow of most springs at Balad Seet and Maqta could be approximated by an exponential decay function, indicating that in times of drought future spring flow can be anticipated quite reliably, allowing farmers to adjust their cropping area at the beginning of the season. At Balad Seet, the four main aflaj at Balad Seet, Hidhan and Miban have much higher decrease rates than Kabir and Litl and were also less responsive to rainfall events during the observation period.

The former two aflaj emerge from separate wadis in the northern part of the oasis, and appear to originate from a different reservoir than the other two aflaj, which are located further to the south. Falaj Kabir combines the waters of six springs, one of which (BS6) lies relatively high in the rock wall and seems to be particularly responsive to rainfall events.

The intricate water distribution system at Balad Seet allows farmers to compensate for shortfalls of individual springs. In former times, terrace systems were located closer to the springs of falaj Miban and to one of the springs of falaj Kabir, making them vulnerable to fluctuations of the respective aflaj (Nagieb et al. 2004b). With the improvement of the falaj system and the construction of additional distribution basins, these terraces were abandoned, in favor of a larger contiguous area further downstream, which could be irrigated with water from all springs.

At Maqta, such a water distribution system could not arise because of the crumbly nature of the rocks, and the rugged topography made construction of long aflaj impossible. Consequently, the individual terrace systems, each of which is fed by its own spring, are much more vulnerable to drought. While some springs had only small decrease rates allowing farmers to maintain a relatively stable cultivated area, the cropped area of other systems has to be adapted from year to year to the available water flow. In 2003, after several years of drought, farmers attempted to compensate for the shortcomings of their falaj network by using plastic tubes to conduct water from one system to another. Before modern materials became available, however, Maqta must have been even more susceptible to drought than today, probably explaining its much shorter settlement record compared to Balad Seet (Siebert et al. 2005). Assuming mean decline rates for falaj flow of 11.7% for Balad Seet and 29.8% for Maqta, typical droughts of five years would decrease spring flow at Balad Seet by 46%, while farmers at Maqta would be hit by a loss of 83% of their irrigation water. This situation probably explains the semi-nomadic lifestyle of Maqta's population, which relies to a much greater extent on their livestock than the more sedentary farmers of Balad Seet (Nagieb et al. 2004b, Siebert et al. 2005).

At Al 'Ayn, more frequent rainfalls alleviate the consequences of long dry spells and hint at a much more stable water supply than in the two other oases. Mean annual rainfalls of 312 mm (Fisher 1994), and the location at the edge of the Saiq Plateau, which constitutes a large water catchment area, allow the cultivation of extensive orchards, with little evidence of long-term drought periods. The proportion of the agricultural area that is covered by perennial crops is at 87% much higher than at Balad Seet (66%) and Maqta (64%). Expansions of the orchard area at the expense of cereal production since the 1980s indicate that at least a few decades ago, water was relatively abundant in these high-mountain systems. The presence of large numbers of terraced fields on the steep slopes at the edge of the oases may further indicate that crop cultivation at Al 'Ayn and Ash Sharayjah was traditionally limited by space



rather than water. It is possible that the relative flow stability of the Ash Sharayjah falaj compared to the falaj running to Al ‘Ayn at least partly reflects the effects of the floating method used to measure falaj flow, which incompletely accounts for the fact that water flow in the falaj is not homogeneous, but tends to be slowed by friction at the falaj edges.

In all cases, analyzing the effects of rainfall events on spring flow is hampered by the fact, that rainfall was measured at the oases or at nearby weather stations rather than in the catchment areas feeding the springs. Rainfall in Oman is notoriously variable in time and space and tends to be more frequent and heavier in the mountains (Fisher 1994). Precipitation in the oases, which invariably lie in valleys, can therefore be expected to be substantially lower than rainfall in the mountainous catchments.

#### 4.4.2. *Water age*

Age determination of the water samples from the Oman Mountains was complicated by several factors. Compared to most previous studies of water bodies that were clearly cut off from the atmosphere between the time of recharge and the collection of the samples, our samples were taken under not well-controlled conditions. In the limestone-dominated Oman Mountains, it cannot be excluded that groundwater gets in contact with air pockets or even caves on its flow path through the rocks. It is also possible that samples have partially degassed or re-equilibrated during sampling from open springs, which is more susceptible to such problems than sampling from closed boreholes. Even though we made every effort to take the samples directly at the outlet from the rocks, the spring channel might in some cases have been exposed to the atmosphere at an invisible point before the obvious outlet. For samples that were adequately described by the excess air model, we expect these effects to be negligible, but for the others, equilibration or degassing processes are likely explanations of the bad fits.

Calculated errors for all ages were relatively large. One reason for this was that the recharge altitudes were uncertain because of the diverse topography of the catchment areas. A further source of error were the low  $^3\text{H}$  concentrations. Although they could still be measured quite accurately by mass spectrometry, the resulting amounts of tritiogenic  $^3\text{He}$  are very small, leading to larger errors of the  $^3\text{H}$ - $^3\text{He}$  age. The observed  $^3\text{H}$  concentrations of about 2 TU are in agreement with local precipitation, as indicated by the few available data from the nearest monitoring station in Bahrain (IAEA/WMO 2004). Such values are typical of low-latitude sites, as compared to 5 to 10 TU at higher latitudes, reflecting the latitudinal variation of  $^3\text{H}$  production (Masarik and Beer 1999).

For  $^3\text{H}$ - $^3\text{He}$  dating of samples with high radiogenic components, it was unfortunate that the  $^3\text{He}/^4\text{He}$  ratio of helium produced by the rocks could not be well confined. Most studies use the average crustal ratio of  $2 \times 10^{-8}$ , but the water sample from Nakhl, whose He fraction was dominated by radiogenic helium, indicated a much higher ratio of  $1.22 \times 10^{-7}$ . The geologic setting of Nakhl,

however, differs strongly from all other oases, so that this value cannot be considered representative of the whole mountain range. We therefore used the crustal average value for the radiogenic helium isotope ratio, which might have had an effect on the samples from Hat and As Sumayiyah with high radiogenic components. Using the isotopic ratio from Nakhil would make these samples younger.

For the SF<sub>6</sub> method, the high recharge temperatures led to unusually low equilibrium concentrations of SF<sub>6</sub> in the water samples, which, in combination with the often large excess air components, increased the errors of the age determination. Our analyses underscore the importance of analyzing noble gases parallel to the SF<sub>6</sub> dating to account for the effects of excess air and recharge temperature.

Some surprisingly young or even apparently negative SF<sub>6</sub> ages indicate the presence of excess SF<sub>6</sub>. Explanations such as contamination of samples during sampling or elevated SF<sub>6</sub> concentrations in the local atmosphere appear unlikely. In contrast, natural SF<sub>6</sub> released from aquifer rocks has been observed in various environments (Harnisch and Eisenhauer 1998, Mitchell et al. 2007). All apparently affected springs in our study originate from Hajar limestones. In an overview of known natural sources of SF<sub>6</sub>, Harnisch and Eisenhauer (1998) did not mention limestones, but found high SF<sub>6</sub> contents in fluorite minerals. There is evidence that geothermal processes can lead to a replacement of calcite in limestones by fluorite (Jin et al. 2006). Since the Hajar limestones of Oman were subject to obduction by the Samail ophiolite suite in the Late Cretaceous, which exposed the rocks to large amounts of geothermal energy, such processes are not unlikely to have occurred in Oman. A fluorite component in the Hajar rocks would explain the presence of elevated natural SF<sub>6</sub> in the water samples from Hat, Al 'Ayn and Maqta-6 at Maqta, all of which emerge from or in association with Hajar limestone rocks. It is also possible that such effects influenced SF<sub>6</sub> ages from other samples, which were still positive but in some cases substantially younger than the <sup>3</sup>H/<sup>3</sup>He-ages.

One such example is spring Maqta-5, for which an estimated <sup>3</sup>H/<sup>3</sup>He-age of 34.5 years contrasted with an SF<sub>6</sub> age of only 7 years. The <sup>3</sup>H/<sup>3</sup>He-age of this sample, however, is relatively unreliable, because of its very low <sup>3</sup>H concentration (0.32 TU). As the apparent age indicates an origin shortly after the bomb peak, a much higher concentration would be expected. The most likely interpretation of this sample is therefore that it represents a mixture between a young component and a substantial contribution of pre-bomb origin.

Maqta-5 also stood out from all other samples with its low sampling temperature of only 15°C, which, given the much higher air and soil temperatures of today, is difficult to explain. Calculated recharge temperatures of all other samples, except the thermal springs of Nakhil and As Sumayiyah, were about 2-3°C higher than the average air temperatures expected in the recharge areas. A likely explanation for this difference is that the soil temperatures, which are recorded by the noble gases, are significantly higher

than the mean annual air temperatures in the region. Similarly enhanced soil and noble gas temperatures have been observed in Niger, a site with a comparable warm and arid climate (Beyerle et al. 2003).

#### 4.4.3. Hydrological sustainability of the oases

At Balad Seet, there is a surprising difference between the  $^3\text{H}$  and  $\text{SF}_6$  ages of spring BS6, whereas the two ages are similar for BS13. It is doubtful whether either of the two springs truly represents the oasis' hydrology, because the outflow of spring BS13 is very low, and BS6 emerges from higher up in the rock wall than most other springs. Since all other springs at Balad Seet could not be sampled without risk of atmospheric contamination, we chose BS6 for sampling, but the low  $^3\text{H}$ - $^3\text{He}$  age of about 2-3 years does not correspond well with the average flow decrease of only 12% per year. We assume that the water of BS6 took a shortcut through the rocks and emerged from a large but more superficial reservoir than most other springs. This is supported by its position in a deeply incised wadi, which conducts a lot of surface run-off during rainfall events.

The three water samples collected at Hat were surprisingly different in age. While the  $^3\text{H}$ - $^3\text{He}$  age of the sample collected before the summer rains of 2003 indicated an age of 8 years, the rains lifted the apparent age to 14 and 12 years. At the same time, the  $\text{SF}_6$  age decreased from 14 years to negative ages. This apparent contradiction might be due to the subsidence of the limestone storage formation deeper into the ground close to the oasis. We hypothesize that the aquifer extends deep into the ground, and that the rainfalls raised the water level in the aquifer to the point, where a substantial proportion of deeper, older water got mixed into the spring water. If the limestones have really been fluoritized and thus emit natural  $\text{SF}_6$ , one would expect this gas to accumulate in water over time. Older water would thus have lower  $^3\text{H}$  concentrations, but higher concentrations of  $\text{SF}_6$ , explaining both the older  $^3\text{H}/^3\text{He}$ -ages and the younger  $\text{SF}_6$  ages.

There seems to be no clear relationship between the calculated water ages and the annual flow decrease rates determined from the falaj flow measurements (Table 4.5). Low water ages were not necessarily correlated with high flow decrease rates, although the high uncertainties of some age estimates have to be taken into account. An explanation for the missing correlation might be that not all spring water infiltrated at the time indicated by the apparent water ages, but that the water is always a mixture of waters of different ages. The proportions of young and old components are unknown and likely to change over time. The flow decrease rates may also vary during periods of drought. Aquifers might discharge water homogeneously, until the hydrologic head of the spring water has dropped to near zero, with spring flow diminishing rapidly, as soon as this level is reached. During this later stage, old water age might coincide with moderate or even high decrease rates, as seems to be the case for sample Maqta-5. Additionally, water flowing through a karstic environment might still experience gas exchange with cave air, leading to water ages that are younger

than the latest rainfall event. This process might be responsible for the young age of sample Maqta-2.

Such processes are likely to be of greater importance at Maqta than in the other oases, because the topographic gradients are not very steep, flow decrease rates are fairly high and the geology is very complicated. At all other oases, most notably at Balad Seet and Hat, the aquifer seems much more homogeneous and the hydrologic head should be greater and more stable, leading to a presumably closer correlation of water age and flow decrease rate. At least for Maqta, the decrease rate of the spring flow appears to be a better indicator of hydrological sustainability than the water age.

Table 4.5. Water ages and annual flow decrease rates for the springs at Maqta, for which water samples were dated.

Sample name	Spring name	$^3\text{H}$ - $^3\text{He}$ age	$\text{SF}_6$ age	Annual decrease rate (%)
Maqta-1	F1293	4.66±5.57	-	-59%
Maqta-2	F1779	1.68±2.38	-	-30%
Maqta-3	Mwezen	8.32±3.02	-	-41%
Maqta-4	F2680	5.09±3.31	7.25±0.50	Not measured
Maqta-5	F1789	34.50±5.54	7.02±0.47	-27%
Maqta-6	F2449	3.39±3.87	<0	-25%

For As Sumayiyah and Nakhl, no spring flow measurements were carried out, but the large proportions of the agricultural area that were covered by date plantations (81% at As Sumayiyah and 93% at Nakhl) indicate a water flow that is strong and stable enough to irrigate perennial crops. At these two settlements, the moderate to old water ages also hint at a high stability of the water flow. The spring waters at Nakhl emerge from an extensive limestone aquifer that is inclined towards the oasis, providing an effective buffer against spring flow decline.

The moderate water age of about 8 years for Al ‘Ayn indicates a fairly stable water supply, which is complemented by relatively frequent and abundant rainfall. Farmers at Al ‘Ayn and the adjacent villages can thus dedicate most of their available area (87%) to perennial crops. In spite of the generally high rainfalls, relatively dry years have been reported for the mountain areas, but the presumably large aquifer under the extensive limestone catchment of the Sayq Plateau might help to provide sufficient irrigation water even during periods of drought.

## 4.5 Conclusions

Falaj flow in the oases of Balad Seet and Maqta declined strongly in times of drought, whereas for Al ‘Ayn rainfall during the observation period was too frequent to derive such information. In conjunction with the water ages of between 5 and 12 years that were derived for most springs, this indicates that the hydrological stability of most oases is ensured for only a few years after a major

rainfall rather than for several decades, and that many villages are thus vulnerable to droughts lasting for more than about five years.

Water ages of the Omani oasis springs were difficult to measure, due to the complicated sampling conditions and the unsaturated flow likely to occur in the rocks of this arid region.  $^3\text{H}$ - $^3\text{He}$  sampling was additionally hampered by very low tritium concentrations in the precipitation of Oman, whereas  $\text{SF}_6$  dating might have been affected by natural sources of  $\text{SF}_6$  in the limestone storage rocks. The conditions encountered in this study are close to the applicability limits of the employed tracer methods.

Water ages and proportion of the agricultural land under perennial crops indicate that Nakhl and As Sumayiyah have the most sustainable water supply of all oases analyzed in this study. Al 'Ayn, Hat and Balad Seet rely on relatively large limestone aquifers with slowly declining discharge. The water supply of Maqta appears to be the least sustainable. With rapidly decreasing spring flows and limited opportunities to redistribute water within the oasis, farmers of Maqta rely to a greater extent on livestock herding than the inhabitants of the other oases.

## Acknowledgments

We thankfully acknowledge the help of Uta Dickhoefer and Matthias Klais with falaj flow measurements in Al 'Ayn, the cooperation of the Extension Center at Al Jabal al Akhdar of the Ministry of Agriculture and Fisheries of Oman and the infrastructural support provided by the College of Agriculture and Marine Sciences, Sultan Qaboos University, Muscat. We thank M. Hofer for performing the  $\text{SF}_6$  analyses at Eawag. The authors are also indebted to the Deutsche Forschungsgemeinschaft (DFG) for funding (BU1308).

## References

- Aeschbach-Hertig W, Holzner CP, Hofer M, Simona M, Barbieri A and Kipfer R (2007). A time series of environmental tracer data from deep, meromictic Lake Lugano, Switzerland. *Limnology and Oceanography* 52(1), 257-273.
- Aeschbach-Hertig W, Peeters F, Beyerle U and Kipfer R (1999). Interpretation of dissolved atmospheric noble gases in natural waters. *Water Resources Research* 35(9), 2779-2792.
- Aeschbach-Hertig W, Peeters F, Beyerle U and Kipfer R (2000). Palaeotemperature reconstruction from noble gases in ground water taking into account equilibration with entrapped air. *Nature* 405(6790), 1040-1044.
- Bauer S, Fulda C and Schäfer W (2001). A multi-tracer study in a shallow aquifer using age dating tracers  $^3\text{H}$ ,  $^{85}\text{Kr}$ , CFC-113 and  $\text{SF}_6$  - Indication for retarded transport of CFC-113. *Journal of Hydrology* 248(1-4), 14-34.
- Beyerle U, Aeschbach-Hertig W, Hofer M, Imboden DM, Baur H and Kipfer R (1999). Infiltration of river water to a shallow aquifer investigated with  $^3\text{H}/^3\text{He}$ , noble gases and CFCs. *Journal of Hydrology* 220(3-4), 169-185.
- Beyerle U, Aeschbach-Hertig W, Imboden DM, Baur H, Graf T and Kipfer R (2000). A mass spectrometric system for the analysis of noble gases and tritium from water samples. *Environmental Science & Technology* 34(10), 2042-2050.

- Beyerle U, Rueedi J, Leuenberger M, Aeschbach-Hertig W, Peeters F, Kipfer R and Dodo A (2003). Evidence for periods of wetter and cooler climate in the Sahel between 6 and 40 kyr BP derived from groundwater. *Geophysical Research Letters* 30(4), 1173.
- Buerkert A, Mahler F and Marschner H (1996). Soil productivity management and plant growth in the Sahel: Potential of an aerial monitoring technique. *Plant and Soil* 180(1), 29-38.
- Busenberg E and Plummer LN (2000). Dating young groundwater with sulfur hexafluoride: Natural and anthropogenic sources of sulfur hexafluoride. *Water Resources Research* 36(10), 3011-3030.
- Costa PM (1983). Notes on traditional hydraulics and agriculture in Oman. *World Archaeology* 14(3), 273-295.
- El-Gamal H (2005). Environmental tracers in groundwater as tools to study hydrological questions in arid regions, PhD Thesis, Ruperto-Carola University, Heidelberg, Germany, 151 pp.
- Fisher M (1994). Another look at the variability of desert climates, using examples from Oman. *Global Ecology and Biogeography Letters* 4(3), 79-87.
- Gebauer J, Luedeling E, Hammer K, Nagieb M and Buerkert A (2007). Mountain oases in northern Oman: An environment for crop evolution and *in situ* conservation of plant genetic resources. *Genetic Resources and Crop Evolution* 54, 465-481.
- Glennie K, Boeuf M, Hughes Clarke M, Moody-Stuart M, Pilaar W and Reinhardt B (1974). Geology of the Oman Mountains. *Verhandelingen Koninklijk Nederlands geologisch mijnbouwkundig Genootschap* 31, 1-423.
- Harnisch J and Eisenhauer A (1998). Natural CF<sub>4</sub> and SF<sub>6</sub> on Earth. *Geophysical Research Letters* 25(13), 2401-2404.
- Heaton THE and Vogel JC (1981). "Excess air" in groundwater. *Journal of Hydrology* 50, 201-216.
- Hofer M, Peeters F, Aeschbach-Hertig W, Brennwald M, Holocher J, Livingstone DM, Romanovski V and Kipfer R (2002). Rapid deep-water renewal in Lake Issyk-Kul (Kyrgyzstan) indicated by transient tracers. *Limnology and Oceanography* 47(4), 1210-1216.
- Holocher J, Matta V, Aeschbach-Hertig W, Beyerle U, Hofer M, Peeters F and Kipfer R (2001). Noble gas and major element constraints on the water dynamics in an alpine floodplain. *Ground Water* 39(6), 841-852.
- IAEA/WMO (2004). Global Network of Isotopes in Precipitation. The GNIP Database. Accessed on 15 Jun 2004 at <http://isohis.iaea.org>.
- Jin Z, Zhu D, Zhang X, Hu W and Song Y (2006). Hydrothermally fluoritized Ordovician carbonates as reservoir rocks in the Tazhong area, Central Tarim Basin, NW China. *Journal of Petroleum Geology* 29(1), 27-40.
- Kipfer R, Aeschbach-Hertig W, Peeters F and Stute M (2002). Noble gases in lakes and ground waters. *Reviews in Mineralogy and Geochemistry* 47, 615-700.
- Koh DC, Plummer LN, Busenberg E and Kim Y (2007). Evidence for terrigenous SF<sub>6</sub> in groundwater from basaltic aquifers, Jeju Island, Korea: Implications for groundwater dating. *Journal of Hydrology* 339(1-2), 93-104.
- Korn L, Häser J, Schreiber J, Gangler A, Nagieb M, Siebert S and Buerkert A (2004). Tiwi and Wadi Tiwi: the development of an oasis on the north-eastern coast of Oman. *Journal of Oman Studies* 13, 57-90.
- Lucas LL and Unterwieser MP (2000). Comprehensive review and critical evaluation of the half-life of tritium. *Journal of Research of the National Institute of Standards and Technology* 105(4), 541-549.
- Luedeling E and Buerkert A (2008). Typology of oases in northern Oman based on Landsat and SRTM imagery and geological survey data. *Remote Sensing of Environment* in press.

- Luedeling E, Nagieb M, Wichern F, Brandt M, Deurer M and Buerkert A (2005). Drainage, salt leaching and physico-chemical properties of irrigated man-made terrace soils in a mountain oasis of northern Oman. *Geoderma* 125(3-4), 273-285.
- Luedeling E, Siebert S and Buerkert A (2007). Filling the voids in the SRTM Elevation Model - A TIN-based delta surface approach. *ISPRS Journal of Photogrammetry and Remote Sensing* 62(4), 283-294.
- Malvicini CF, Steenhuis TS, Walter MT, Parlange JY and Walter MF (2005). Evaluation of spring flow in the uplands of Matalom, Leyte, Philippines. *Advances in Water Resources* 28(10), 1083-1090.
- Manning AH and Solomon DK (2003). Using noble gases to investigate mountain-front recharge. *Journal of Hydrology* 275(3-4), 194-207.
- Masarik J and Beer J (1999). Simulation of particle fluxes and cosmogenic nuclide production in the Earth's atmosphere. *Journal of Geophysical Research-Atmospheres* 104(D10), 12099-12111.
- Nagieb M, Siebert S, Luedeling E, Buerkert A and Häser J (2004). Settlement history of a mountain oasis in northern Oman - evidence from land-use and archaeological studies. *Die Erde* 135(1), 81-106.
- NCDC (2007). Global surface summary of the day data, version 7. National Climatic Data Center (NCDC) of the National Oceanic and Atmospheric Administration (NOAA). Accessed on 15 Apr 2007 at <http://www.ncdc.noaa.gov/oa/land.html>.
- Norman W, Shayya W, Al-Ghafri A and McCann I (1998). Aflaj irrigation and on-farm water management in northern Oman. *Irrigation and Drainage Systems* 12, 35-48.
- Peters E, van Lanen HAJ, Torfs P and Bier G (2005). Drought in groundwater - drought distribution and performance indicators. *Journal of Hydrology* 306(1-4), 302-317.
- Rademacher LK, Clark JF, Hudson GB, Erman DC and Erman NA (2001). Chemical evolution of shallow groundwater as recorded by springs, Sagehen basin; Nevada County, California. *Chemical Geology* 179(1-4), 37-51.
- Schlosser P, Stute M, Dorr H, Sonntag C and Munnich KO (1988). Tritium  $^3\text{He}$  Dating of Shallow Groundwater. *Earth and Planetary Science Letters* 89(3-4), 353-362.
- Schlosser P, Stute M, Sonntag C and Münnich KO (1989). Tritiogenic  $^3\text{He}$  in shallow groundwater. *Earth and Planetary Science Letters* 94, 245-256.
- Scholz F (1984). Höhengiedlungen am Jabal Akhdar - Tendenz und Probleme der Entwicklung einer peripheren Region im Oman-Gebirge. *Zeitschrift für Wirtschaftsgeographie* 28(1), 16-30.
- Siebert S, Häser J, Nagieb M, Korn L and Buerkert A (2005). Agricultural, architectural and archaeological evidence for the role and ecological adaptation of a scattered mountain oasis in Oman. *Journal of Arid Environments* 62(1), 177-197.
- Siebert S, Nagieb M and Buerkert A (2007). Climate and irrigation water use of a mountain oasis in northern Oman. *Agricultural Water Management* 89(1-2), 1-14.
- Solomon D and Cook P (2000).  $^3\text{H}$  and  $^3\text{He}$ . In: P. Cook and A. Herczeg (Eds.), *Environmental tracers in subsurface hydrology*. Kluwer Academic Publishers, Boston, MA, USA.
- Stute M and Schlosser P (1993). Principles and applications of the noble gas paleothermometer. In: P.K. Swart, K.C. Lohmann, J. McKenzie and S. Savin (Eds.), *Climate Change in Continental Isotopic Records*. AGU Geophysical Monograph Series. American Geophysical Union, Washington, DC.
- von Rohden C and Ilmberger J (2001). Tracer experiment with sulfur hexafluoride to quantify the vertical transport in a meromictic pit lake. *Aquatic Sciences* 63, 417-431.
- Zoellmann K, Kinzelbach W and Fulda C (2001). Environmental tracer transport ( $^3\text{H}$  and  $\text{SF}_6$ ) in the saturated and unsaturated zones and its use in nitrate pollution management. *Journal of Hydrology* 240(3-4), 187-205.





## Chapter 5

*submitted to Field Crops Research*

# Climate change affects traditional high-altitude fruit production systems in Oman

Eike Luedeling <sup>a</sup>, Jens Gebauer <sup>a</sup> and Andreas Buerkert <sup>a</sup>

<sup>a</sup> *Organic Plant Production and Agroecosystems Research in the Tropics and Subtropics, University of Kassel, Steinstr. 19, D-37213 Witzenhausen, Germany*

---

### Abstract

The high-altitude fruit production systems of Al Jabal al Akhdar in Oman are unique in that they represent the only horticultural systems of the country, where farmers successfully grow temperate and cold-loving subtropical tree and shrub crops. To characterize the climatic conditions prevailing in the oases of this region, we investigated four oases along an elevation gradient from 1030 to 1950 m.a.s.l. At the oases of Al ‘Ayn, Qasha’ and Masayrat ar Ruwajah, temperatures were measured at half-hourly intervals over two full cropping years, and interpolated for Salut, a fourth settlement at an intermediate altitude. At all oases all trees were counted and classified according to species, climate preference and approximate chilling requirement.

We correlated temperature measurements at the oases with hourly temperatures recorded at the nearby weather station at Saiq, and used this correlation to estimate chilling hours at each oasis. Correlating these with minimum temperatures from Saiq, which are available since 1983 allowed deduction of the numbers of chilling hours during 20 of the 24 winters between 1983 and 2007.

Temperatures varied strongly with altitude, with mean annual temperatures of 24.7°C at the lowest and 18.7°C at the highest oasis. The lowest system was dominated by date palms (*Phoenix dactylifera* L.) and tropical species, whereas at the highest location pomegranates (*Punica granatum* L.) and roses (*Rosa damascena* Mill.) prevailed. Long-term temperature records indicated that the number of chilling hours decreased markedly over the past 24 years. In our view this decline is the most likely cause for the almost complete crop failure of pomegranate, peach (*Prunus persica* L.) and apricot (*Prunus armeniaca* L.) in the

oases at intermediate altitude and very low yields of peach and apricot at Al ‘Ayn during the season of 2005/06. The rate of decline in chilling hours is alarming, with the annual total decreasing on average by 17.4 hours per year at Al ‘Ayn from 1047 hours in 1983/84 to less than 350 hours in all winters between 2003 and 2007.

---

## 5.1 Introduction

In the Sultanate of Oman, the range of tree and shrub crops that can be cultivated is mostly restricted to species that tolerate very hot summer temperatures and do not require cold temperatures for fructification. Mean annual temperatures in Oman vary between 25 and 30°C, summer peaks often reach 45°C and even in winter, mean monthly temperatures below 20°C are rare (Fisher 1994). The range of fruit trees that can be cultivated throughout most of Oman is therefore limited to tropical species, such as mango (*Mangifera indica* L.) or papaya (*Carica papaya* L.), or subtropical species without chilling requirement, such as date palm (*Phoenix dactylifera* L.) or lime (*Citrus aurantiifolia* [L.] Swingle).

There is only one part of the country, where the cultivation of temperate crops and subtropical crops with chilling requirement is possible (Scholz 1984). In the region of Al Jabal al Akhdar, the ‘Green Mountain’, farmers cultivate pomegranates (*Punica granatum* L.), peaches (*Prunus persica* L.) and apricots (*Prunus armeniaca* L.), as well as walnuts (*Juglans regia* L.) and apples (*Malus domestica* Borkh.). These fruits are produced in mountain oases fed by permanent springs (Nagieb et al. 2004b), which originate from extensive limestone aquifers, allowing farmers to defy the scarcity and irregularity of rainfall typical of northern Oman (Fisher 1994). In the mountains’ interior, all important springs arise from a major geological unconformity, where limestones of the Hajar Supergroup are underlain by rocks of the Permian and Pre-Permian Basement (Glennie et al. 1974, Luedeling and Buerkert 2008a). Over thousands of years, farmers have developed techniques of gathering and directing spring water in concrete channels, called aflaj (sing.: falaj) in Arabic, and in some cases, they even carved tunnels into the rocks to tap sub-surface aquifers (Costa 1983, Norman et al. 1998b). In most of the mountains, the hydrologically critical unconformity lies at an elevation of approximately 1000 m.a.s.l., and the oases that formed along it are characterized by the cultivation of date palms and lime trees. Only in the mountains of Al Jabal al Akhdar, the unconformity rises up to about 2000 m.a.s.l.

The eroded center of Al Jabal al Akhdar contains oases at different levels of elevation, which differ markedly in character, with the gardens of Masayrat ar Ruwajah resembling those of low-land oases, whereas at Al ‘Ayn the crop community is dominated by pomegranate trees and rose bushes (*Rosa damascena* Mill.), cultivated for the distillation of rose water. Two settlements at intermediate altitudes (Salut and Qasha’) complete an elevation gradient that stretches over 1000 m, providing ideal conditions to obtain

information about the climatic requirements of temperate and subtropical perennials in Oman.

The study of elevation gradients has become a common tool for ecologists and botanists describing ecosystems and their characteristics (Jobbagy and Jackson 2000, Kluge et al. 2006, Lookingbill and Urban 2005, Vetaas 2002, Watkins et al. 2006). In pomiculture, such studies are lacking, and the altitudinal distribution of fruit species is poorly understood. Several authors have discussed the potential and limitations of fruit production at high altitudes (Fischer and Lüdders 1995, Khoshbakht and Hammer 2006, Lüdders and Wernke 2003), but systematic surveys of fruit species distribution among elevation gradients have not been conducted. In such surveys, altitude itself is rarely the driving force behind species distribution (Lookingbill and Urban 2005). It is rather a proxy for other parameters that vary with elevation, such as temperature or precipitation.

Temperature is of particular importance for many fruit trees, which require a certain period of cold conditions, referred to as their chilling requirement, for breaking of dormancy and initiation of fructification. The calculation of the chilling hours of a site has been widely discussed in the literature (Francis et al. 2003, Kozłowski and Pallardy 2002). Many models are fairly elaborate and specific to certain fruit species or varieties (Richardson et al. 1974, Shaltout and Unrath 1983). Several authors suggest that the chilling requirement is not necessarily fulfilled by a specific number of hours below a given threshold. Warm temperatures might compensate for earlier chilling hours (Lüdders and Wernke 2003, Shaltout and Unrath 1983), or the breaking of bud dormancy might happen in two phases (Erez and Couvillon 1987). Since our analysis is not species-specific, and most information about chilling requirements of tree crops specifies 7.2°C as the critical threshold, we choose this limit for our analysis. This approach might not completely reflect the complex nature of the dormancy-breaking process, but it serves as a proxy for the range of chilling hours in the mountain oases studied here. Moreover, lists of species-specific chilling requirements lack for most species and the best overview available (Noel 2007) only refers to chilling hours as the accumulated time below 7.2°C (Table 5.1).

To our knowledge, no study of elevation gradients has investigated chilling hours. Often, temperature information were only available as monthly (Vetaas 2002) or annual (Koyuncu et al. 2004) averages, or estimated using data from weather stations at different altitudes (Ghazanfar 1991). Since the chilling requirement of fruit trees is generally measured in hours rather than days or months (Fischer and Lüdders 1995) and depends strongly on local conditions, such information is of limited applicability for the estimation of chilling hours.

Since global warming has been reported to be potentially threatening to horticultural systems producing fruit trees with chilling requirements (Blanke 2008, Cannell et al. 1989, Seguin 2003), we correlated our high-resolution but short term data with long-term climate records of a nearby weather station to

explore, whether recent climatic changes may have influenced fruit production in Al Jabal al Akhdar or are likely to do so in the future.

Table 5.1. Chilling requirements of temperate and subtropical fruit species found in the study oases (Noel 2007). An asterisk (\*) in front of a value means that low-chill varieties exist, which need less chilling.

Temperate species		Subtropical species	
Species	Chilling requirement (h)	Species	Chilling requirement (h)
Apple	* 400-1800	Almond	400-700
Pear	600-1500	Apricot	* 350-1000
Plum	700-1800	Fig	100-500
Walnut	* 400-1500	Grape	100-500
		Peach	* 200-1200
		Pomegranate	100-200

## 5.2 Materials and Methods

### 5.2.1. Study sites

The study was conducted in four mountain oases along an elevation gradient in Al Jabal al Akhdar, Oman (Fig. 5.1). These oases were Masayrat ar Ruwajah at 1030-1060 m.a.s.l., Salut (1430-1450 m.a.s.l.), Qasha' (1620-1640 m.a.s.l.) and a contiguous agricultural area surrounding the oases Al 'Ayn, Al 'Aqr and Ash Sharayjah (referred to only as Al 'Ayn in the following; 1750-1930 m.a.s.l.).

For Masayrat ar Ruwajah, Qasha' and Al 'Ayn, aerial photographs were taken using a remotely-operated model plane equipped with a digital camera (Schäper 2006). All images were georeferenced using a differential GPS (Pathfinder ProXRS, Trimble Navigation Ltd., Sunnyvale, CA, USA) and rectified using ERDAS IMAGINE 8.5 (Leica Geosystems GIS & Mapping LLC., Norcross, GA, USA).

### 5.2.2. Tree counts

Based on the aerial images, all cultivated fruit trees and perennial shrubs of all oases were counted in the field, classified according to species and entered into a Geographical Information System, using ArcMap 9.2 (ESRI Inc., Redlands, CA, USA). For Salut, no aerial photograph was available because the village was too far away from the take-off sites of the plane at Al 'Ayn and Masayrat ar Ruwajah. The gardens of Salut are, however, relatively small and the tree count could be done without an image for orientation. For mapping purposes, the location and shape of Salut's gardens were sketched using an aerial image downloaded from Google Earth (Google, Mountain View, CA, USA), which was georeferenced by the location of the other oases.

For each oasis, species diversity was assessed using the Shannon index  $H'$

(Magurran 1988), calculated as  $H' = -\sum_i^s p_i \cdot \ln p_i$ , where  $p_i = \frac{n_i}{N}$ ,  $s$  equals the total number of species,  $n_i$  is the number of individuals belonging to species  $i$  and  $N$  is the total number of individuals of all species. Species evenness was

calculated as  $E = \frac{H'}{\ln s}$ , with  $H'$  being the Shannon index and  $s$  the number of species present in the oasis under study.

### 5.2.3. Temperature measurements

For collection of weather data, HOBO Pro climate loggers (Onset Computer Corp., Bourne, MA, USA) were installed in the gardens of Al 'Ayn, Qasha' and Masayrat ar Ruwajah. These loggers recorded temperatures and absolute and relative air humidity at half-hourly intervals between 21 February 2005 and 21 April 2007 at Al 'Ayn, from 19 April 2005 to 17 April 2006 and 28 September 2006 to 23 April 2007 at Qasha' and between 7 March 2005 and 5 April 2007 at Masayrat ar Ruwajah. Loggers were placed in standard wooden boxes designed for weather stations and positioned 1.5 m above terraces cropped with alfalfa (Al 'Ayn and Masayrat ar Ruwajah) or annual fodder grass (Qasha').

To allow a long term assessment of the data, additional weather data were taken from an official weather station at Saiq (World Meteorological Station No. 412540), which is located only a few kilometers from the study area at an altitude of approximately 1950 m.a.s.l. Hourly temperature measurements from this station between 1 January 2004 and 30 June 2007 were obtained from the Directorate General of Civil Aviation and Meteorology, Oman. Linear regressions between this dataset and the data collected in the oases revealed that the Saiq temperature records are a reliable proxy for the temperatures in our study oases (Fig. 5.2). From these regressions, we estimated the chilling hours for Salut by linearly interpolating slope and y axis intercept as functions of elevation. This allowed us to estimate the regression equation for Salut and to calculate Salut temperatures based on the values measured at Saiq.

Before 2004, temperature records from Saiq were only available as daily summaries. In order to estimate long-term chilling hour dynamics, we calculated the daily numbers of hours below 7.2°C at each oasis based on hourly data from Saiq since January 2004 and the regression equations. Subsequently, we correlated the estimated daily numbers of chilling hours with the daily temperature minima from the weather station (Fig. 5.3). The regression equation derived from this correlation allowed to estimate past daily chilling hours from daily minimum temperature records from Saiq.

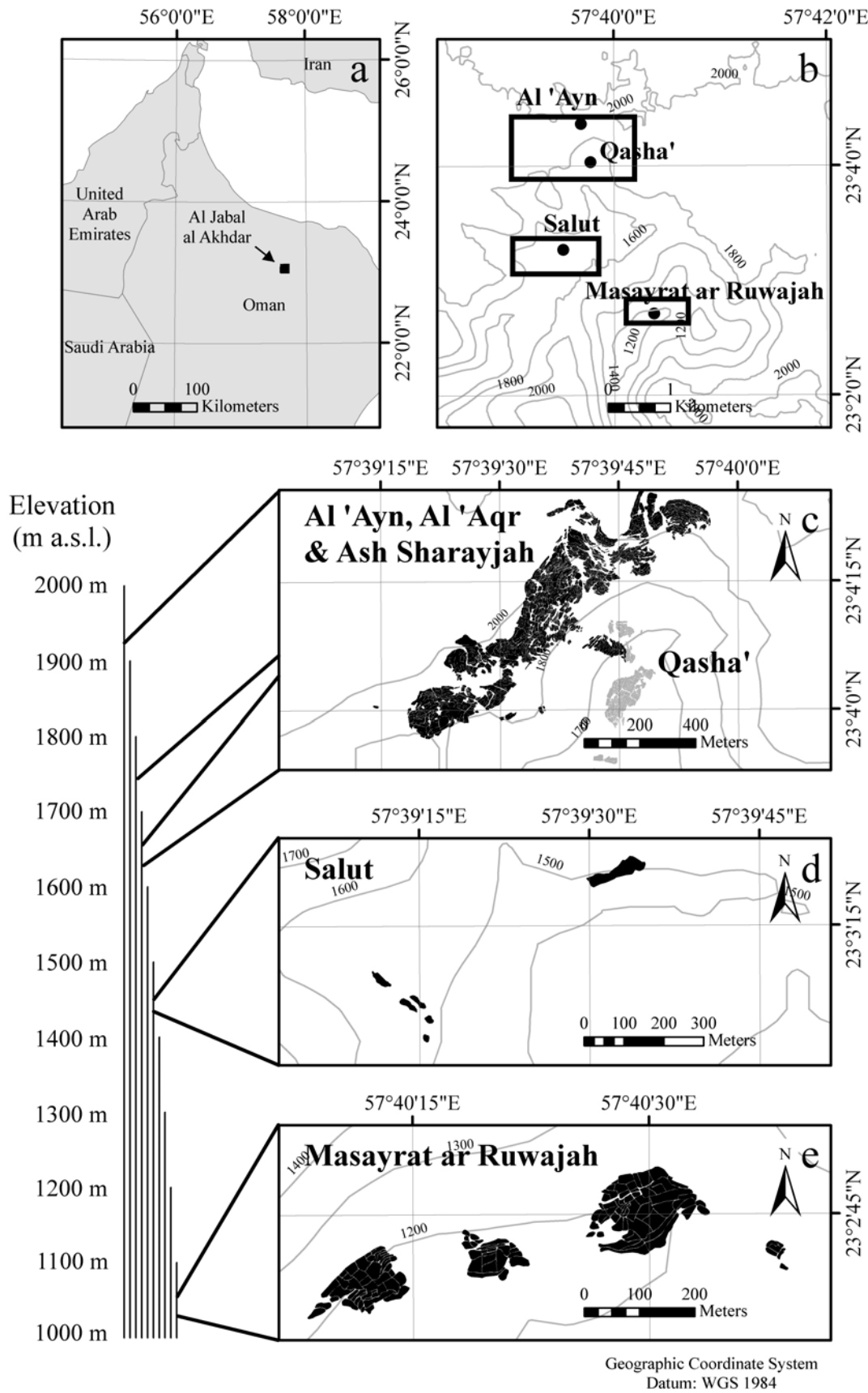


Figure 5.1. Maps showing the location of Al Jabal al Akhdar on the Arabian Peninsula (a), the locations of the study oases in Al Jabal al Akhdar (b) and the fields of Al 'Ayn, Qasha' (c, fields drawn in black belong to Al 'Ayn, gray areas to Qasha'), Salut (d) and Masayrat ar Ruwajah (e) and their position in the context of the elevation gradient.

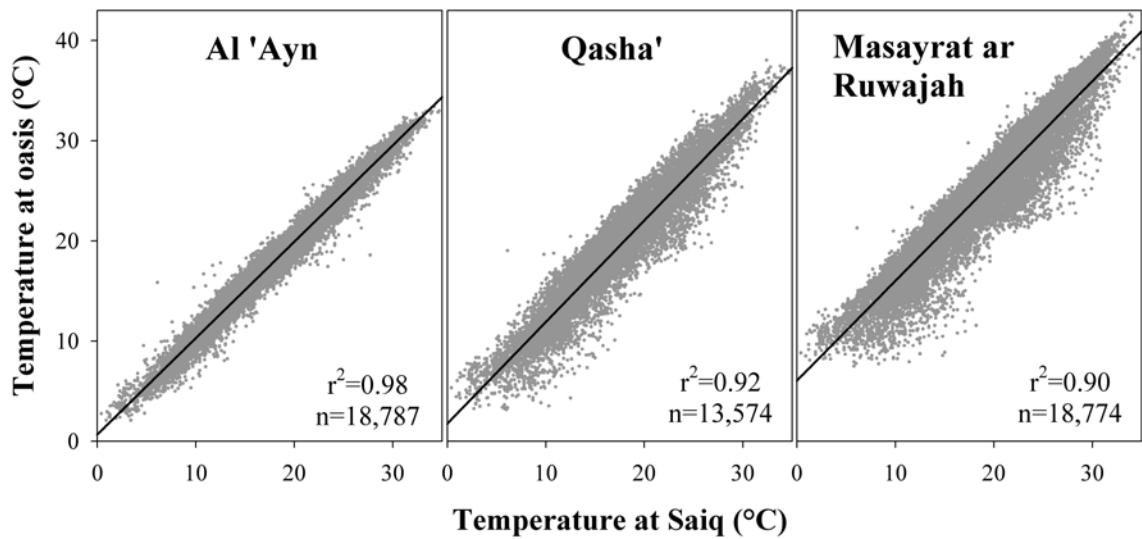


Figure 5.2. Linear regressions between hourly temperature records from the weather station at Saiq and temperatures measured in the oases of Al 'Ayn, Qasha' and Masayrat ar Ruwajah.

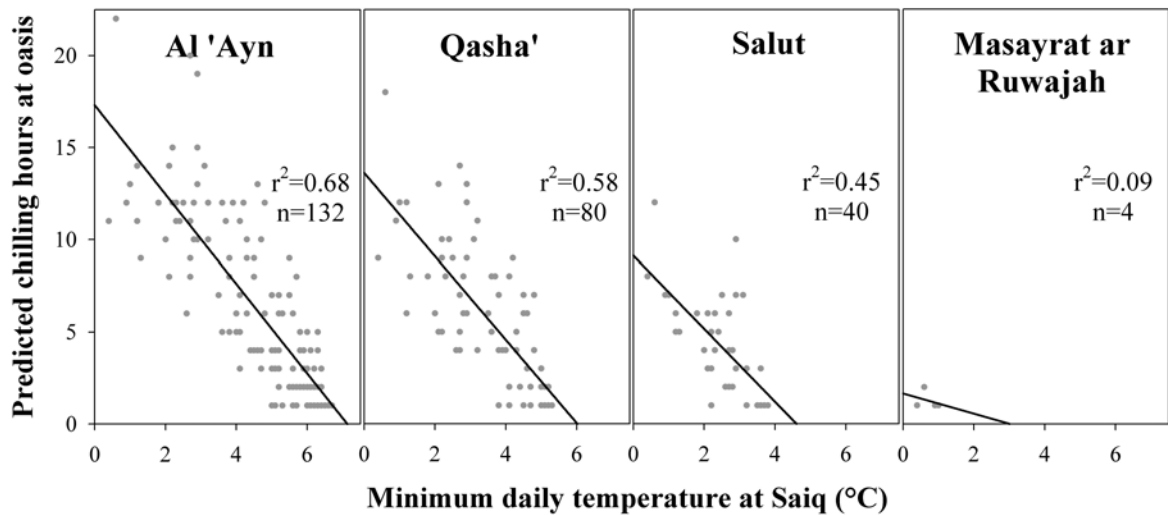


Figure 5.3. Linear regressions between minimum daily temperatures at Saiq and chilling hours calculated from hourly measurements from the same station for the oases of Al 'Ayn, Qasha', Salut and Masayrat ar Ruwajah.

#### 5.2.4. Long-term temperature data

For analysis of the long-term dynamics of chilling hours in the oases, we used a dataset of daily minimum temperatures recorded at the station of Saiq between 1979 and 2007. These data were obtained from the National Climatic Data Center (NCDC 2007) of the US National Oceanic and Atmospheric Administration (NOAA). Since the dataset was not continuous, gaps in the record were interpolated linearly from minimum temperatures measured on days before and after the gaps. Years, during which more than 50 days were missing during the winter season (November to April), were excluded from further analysis. This was the case for the winters of 1979/80 through 1982/83, 1984/85, and 1988/90 through 1990/91 (Fig. 5.4).

We used the equations derived from the hourly records to estimate daily chilling hours at each oasis and to calculate the total chilling hours for each winter. Rather than calculating chilling hours during a calendar year, which would be meaningless for plant physiology, we summed up the chilling hours for time spans ranging from July of one year to June of the following year. Linear regressions from the chilling hour records for all years were used to determine long-term trends in chilling dynamics.

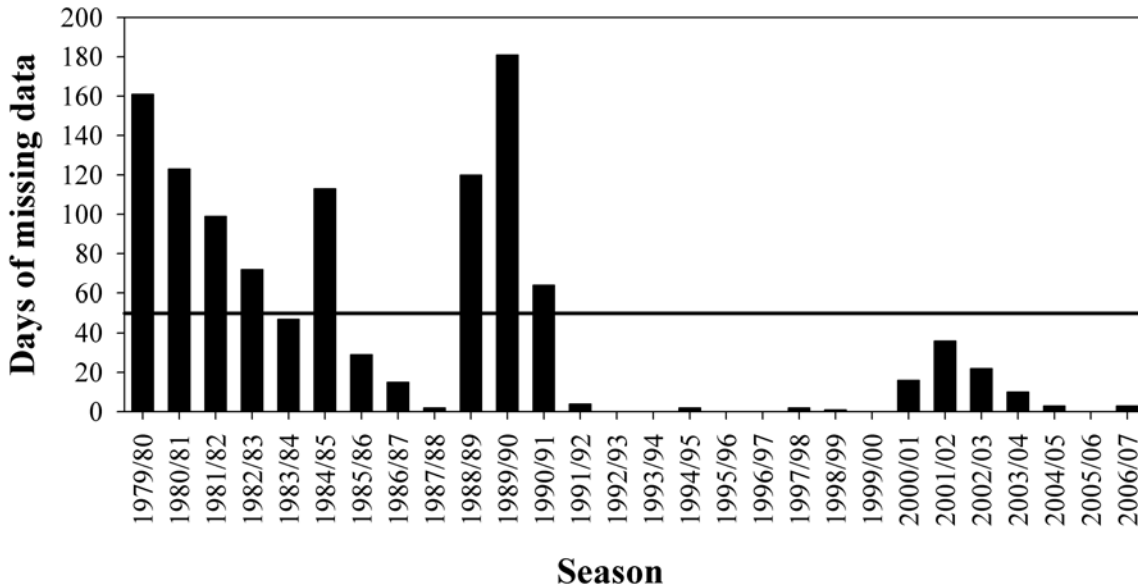


Figure 5.4. Gaps in the NCDC record of minimum daily temperatures measured at Saiq, summarized by seasons ranging from July of one year to June of the following year. The black line indicates the threshold that led to a year's exclusion from analysis of chilling hours.

### 5.3 Results

Mean annual temperatures calculated from measurements in the oases were 18.7°C for Al 'Ayn, 20.8°C for Qasha' and 24.7°C for Masayrat ar Ruwajah, with the temperature ranging from 1.9 to 33.7°C at Al 'Ayn, from 3.0 to 38.1°C at Qasha' and from 7.4 to 42.8°C at Masayrat ar Ruwajah (Fig. 5.5). At Salut, the mean annual temperature calculated from observations at the other oases was 22.0°C, with a minimum of 3.8°C and a maximum of 37.8°C.

Absolute and relative air humidity varied strongly in all three oases where measurements were taken, ranging from extremely dry conditions to saturation (Table 5.2). Between the oases, however, both mean and extreme relative air humidity were similar. In evaluating the quality of these data, it should be kept in mind that the climate loggers were installed in agricultural fields rather than above a permanent lawn area. This circumstance entails that occasionally the alfalfa (*Medicago sativa* L.) or green fodder grown in the field was cut or harvested. Such an event may at times have shifted air humidity measurements towards drier values.



Table 5.2. Absolute and relative air humidity measured at Al 'Ayn, Qasha' and Masayrat ar Ruwajah between April 2005 and April 2007.

	Al 'Ayn	Qasha'	Masayrat ar Ruwajah
<i>Absolute air humidity (<math>g\ m^{-3}</math>)</i>			
Annual mean	6.2	6.2	7.2
Annual minimum	0.2	0.0	0.0
Annual maximum	17.5	18.1	21.5
<i>Relative air humidity (%)</i>			
Annual mean	41.3	39.6	34.2
Annual minimum	2.1	4.2	2.6
Annual maximum	100.0	100.0	100.0

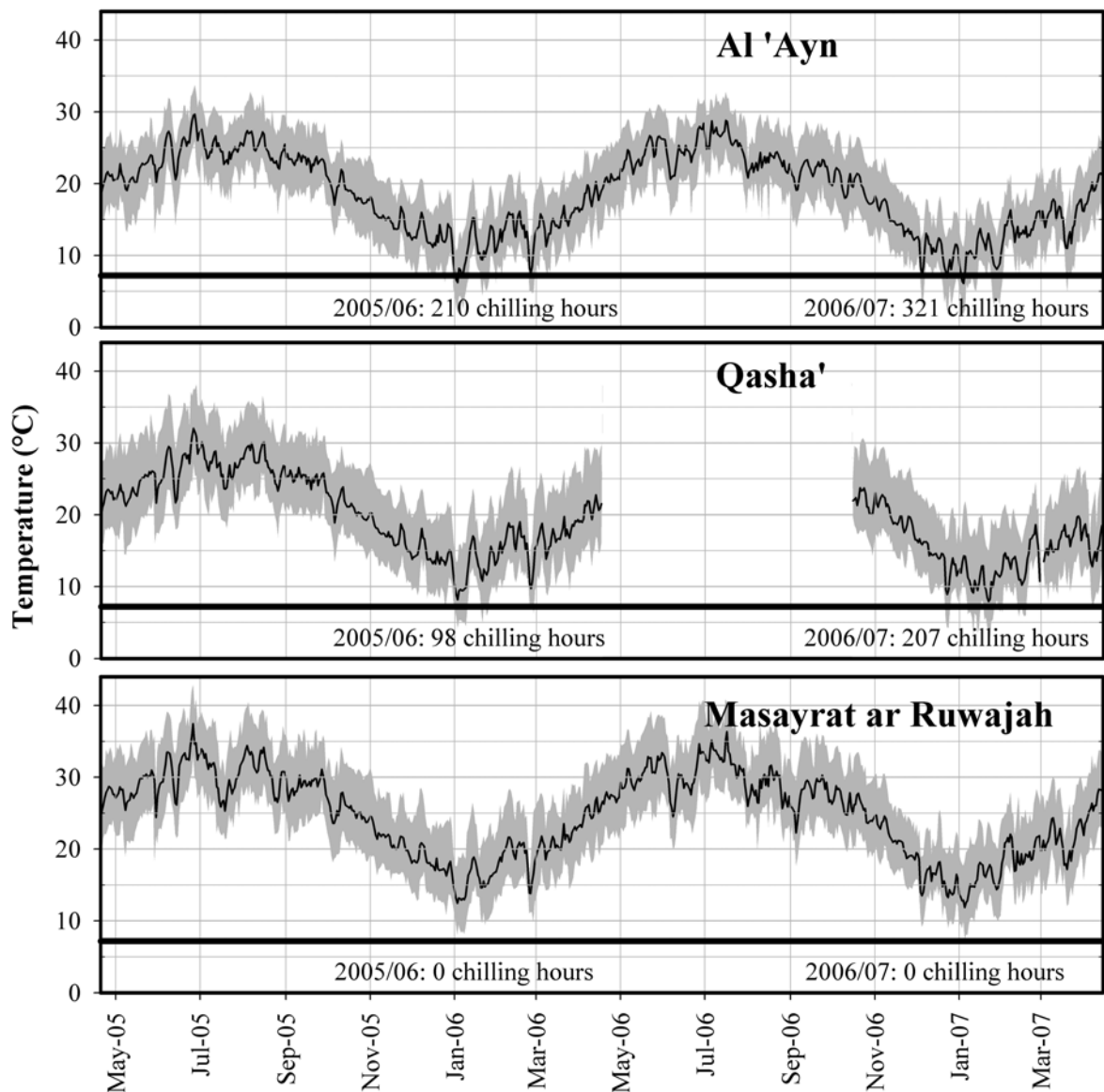


Figure 5.5. Average daily temperatures (black line) and daily temperature range (gray area) measured at the oases of Al 'Ayn, Qasha' and Masayrat ar Ruwajah in Al Jabal al Akhdar.

In the terraces around Al ‘Ayn, we found 22 species of tree and shrub crops with a total of 10,346 individual plants, the highest numbers of all oases studied. Qasha’ followed with 21 species (1358 individuals), whereas Salut (14 species, 425 individuals) and Masayrat ar Ruwajah (12 species, 1457 individuals) had substantially less species. The dominant species in the three upper oases was pomegranate, followed by rose in Al ‘Ayn and peach in Qasha’ and Salut. In Masayrat ar Ruwajah, the upper story of the vegetation was dominated by date palm, followed by banana (*Musa x paradisiaca* L.; Table 5.3; Fig. 5.7).

Shannon diversity was low at 1.33 for Al ‘Ayn, 1.53 for Qasha’, 1.44 for Salut and 1.22 for Masayrat ar Ruwajah, and Shannon evenness was 0.42 at Al ‘Ayn, 0.50 at Qasha’, 0.53 at Salut and 0.49 at Masayrat ar Ruwajah.

The mean temperature at Saiq between 1983 and 2007 was 20.1°C, while the mean daily minimum temperature was 13.4°C and the mean daily maximum temperature was 23.6°C (Table 5.4). Over the whole time span, we detected a negative trend in the mean annual temperatures, whereas mean daily minimum and maximum temperatures rose slightly. The increase of mean daily extreme temperatures was particularly pronounced during the coldest months (November to April), when more than 99% of all chill hours occurred (Table 5.4).

The number of chilling hours at the four oases calculated from the daily minimum temperatures at Saiq showed a decreasing trend over time (Fig. 5.6.). At all four oases, the highest number of estimated chilling hours accrued during the winter of 1983/84 (1047 at Al ‘Ayn, 703 at Qasha’, 353 at Salut and 44 at Masayrat ar Ruwajah), whereas the lowest numbers were estimated for the winter of 2003/04, when chilling hours dropped to 213 at Al ‘Ayn, 103 at Qasha’, 27 at Salut and 1 at Masayrat ar Ruwajah (Table 6.5). The last four winters of the record were among the warmest six winters since 1983. On average, the number of chilling hours decreased at all oases, with the largest decrease at Al ‘Ayn, where the mean annual decline amounted to 17.4 chilling hours (Table 5.5).

## 5.4 Discussion

At Masayrat ar Ruwajah, temperatures never fell below 7.2°C throughout the cropping years of 2005/06 and 2006/07. This indicates that farmers in this lowest oasis of our study cannot cultivate temperate crops or subtropical species which require chilling for fructification. The 98 chilling hours recorded at Qasha’ in 2005/06 were just below the threshold for low-chill pomegranate varieties (100 hours, Table 5.1), whereas the 207 chilling hours of 2006/07 were less critical. Only in Al ‘Ayn did the winter of 2005/06 provide an amount of chilling hours that was sufficient for pomegranates. For most other crops, however, even the 210 chilling hours recorded here are not enough for fructification. The slightly colder winter of 2006/07 (310 chilling hours), provided slightly better climatic conditions.

Table 5.3. List of all perennial crop species found in the four study oases, and their frequency relative to the total number of individuals.

English name	Botanical name	Al 'Ayn	Qasha'	Salut	Masayrat ar Ruwajah	Total
<i>Temperate species</i> (% of all tree and shrub crops of the oasis)						
Rose	<i>Rosa damascena</i> Mill.	28.21	12.37	-	-	22.72
Walnut	<i>Juglans regia</i> L.	1.01	2.28	0.47	-	1.02
Apple	<i>Malus domestica</i> Borkh.	0.52	0.59	0.47	-	0.47
Pear	<i>Pyrus communis</i> L.	0.21	0.22	-	-	0.18
Plum	<i>Prunus domestica</i> L.	0.12	0.07	-	-	0.10
<i>Subtropical species</i> (% of all tree and shrub crops of the oasis)						
Pomegranate	<i>Punica granatum</i> L.	56.97	57.14	58.35	0.34	50.96
Date	<i>Phoenix dactylifera</i> L.	0.03	0.22	2.35	65.61	7.15
Peach	<i>Prunus persica</i> L.	3.55	13.11	19.06	2.13	4.83
Lime	<i>Citrus aurantiifolia</i> (L.) Swingle	4.76	3.39	4.47	8.65	5.03
Grape	<i>Vitis vinifera</i> L.	1.02	2.21	4.94	2.06	1.38
Sufarjal	<i>Citrus limettoides</i> L.	0.45	1.47	1.65	2.88	0.85
Apricot	<i>Prunus armeniaca</i> L.	2.18	1.55	2.59	0.07	1.91
Fig	<i>Ficus carica</i> L.	0.20	0.66	2.12	1.03	0.40
Naringe	<i>Citrus aurantium</i> L.	0.09	0.29	-	-	0.10
Orange	<i>Citrus sinensis</i> (L.) Osbeck	0.01	0.29	-	-	0.04
Lemon	<i>Citrus limon</i> (L.) Burm.f.	0.08	0.15	-	-	0.07
Indian Fig (Prickly Pear)	<i>Opuntia ficus-indica</i> (L.) Mill.	0.07	-	-	-	0.05
Almond	<i>Prunus dulcis</i> (Mill.) D.A.	0.07	-	-	-	0.05
Citron	<i>Citrus medica</i> L.	0.02	-	-	-	0.01
Pigeon Pea	<i>Cajanus cajan</i> (L.) Huth	-	0.29	-	-	0.03
<i>Tropical species</i> (% of all tree and shrub crops of the oasis)						
Banana	<i>Musa x paradisiaca</i> L.	0.11	3.24	2.59	14.82	2.08
Papaya	<i>Carica papaya</i> L.	0.27	0.07	0.47	0.96	0.33
Guava	<i>Psidium guajava</i> L.	0.05	0.29	0.24	1.24	0.21
Mango	<i>Mangifera indica</i> L.	-	-	0.24	0.21	0.03
Sapodilla	<i>Manilkara zapota</i> (L.) van Royen	-	0.07	-	-	0.01

Most species found in the oases thus have chilling requirements that were not met during the winters of 2005/06 and 2006/07 (Fig. 5.8). Even at Al 'Ayn, the highest oasis in this study, chilling conditions in 2005/06 were mostly restricted to a 12-day cold spell at the beginning of January, a week at the end of January, and another four days in February. Apart from these few occasions, the winter was very mild, and fruit yields were accordingly low. Of

nine mature trees, for which apricot yields were measured, the average harvest was only 14 kg per tree, with yields at Al ‘Ayn averaging 16 kg per tree, whereas an average tree in Qasha’ only yielded 8 kg. The average harvest from eight mature peach trees measured at Qasha’ and Al ‘Ayn was only 9 kg. According to farmers’ reports, these yields are far below what they had harvested in the past, indicating that 2005/06 had a comparatively warm winter. At Qasha’ and Salut, conditions were so warm that even the pomegranate crop largely failed, whereas farmers at Al ‘Ayn and several higher settlements reported normal yields. In 2006/07, the chilling conditions at Al ‘Ayn lasted for about two months, providing much better conditions. However, the number of chilling hours was still insufficient for many fruit trees (Fig. 5.8). Yields were once again rather low in all oases, but at Al ‘Ayn this was probably caused by a hailstorm during tree blossom and by tropical cyclone Gonu that hit the area in June and uprooted many trees.

Table 5.4. Annual means of daily mean, minimum and maximum temperatures at Saig between 1983 and 2006 and average yearly changes derived from linear regressions.  $r^2$  represents the coefficient of determination.

		<b>Linear regression</b>		
		<b>Overall mean</b>	<b>Change per year</b>	<b><math>r^2</math></b>
		(°C)	(C°)	
Whole year	Mean temp.	20.1	- 0.05	0.22
	Minimum temp.	13.4	+ 0.06	0.28
	Maximum temp.	23.6	+ 0.04	0.24
Warm season (May-Oct)	Mean temp.	24.8	- 0.05	0.19
	Minimum temp.	18.2	+ 0.05	0.18
	Maximum temp.	28.2	+ 0.04	0.22
Cold season (Nov-Apr)	Mean temp.	15.3	- 0.05	0.19
	Minimum temp.	8.5	+ 0.07	0.29
	Maximum temp.	18.9	+ 0.04	0.14

Despite the discrepancy between the chilling requirements of most temperate crops and the actual chilling hours in all oases, the proportion of temperate crops in Al ‘Ayn and Qasha’ is substantial (Fig. 5.7) (Gebauer et al. 2007b). These large shares are mostly made up of rose bushes, which are generally classified as temperate shrubs and are likely to require cold temperatures as well. However, their chilling requirement cannot be very high, since Gebauer et al. (2007b) observed the same rose variety in bloom at the oasis of Balad Seet in Oman at an elevation of only 960 m a.s.l. Other than roses, there are only 193 temperate trees at Al ‘Ayn and 43 in Qasha’ (Table 3), which indicates that the reliance on temperate fruit trees is not very high.

In all oases, species diversity, as indicated by the Shannon index, was low compared to other intensively managed horticultural systems. Shannon diversity has been reported to lie between 1.6 and 3.4 for homegardens in Sulawesi, Thailand and Costa Rica (Gajaseneni and Gajaseneni 1999, Kehlenbeck and Maass 2005, Zaldivar et al. 2002), but was only between 1.2 and 1.5 in

the oases studied here. The Shannon index, however, depends strongly on the total number of species present, so that comparisons are always difficult.

Table 5.5. Estimated mean, minimum and maximum number of chilling hours at the four study oases, based on winters between 1983 and 2005 (1984/85, 1988/89, 1989/90 and 1990/91 omitted due to lack of data) and mean annual change derived from linear regression.  $r^2$  represents the coefficient of determination of this regression.

	Al ‘Ayn	Qasha’	Salut	Masayrat ar Ruwajah
Mean chilling hours	473	288	133	15
Maximum chilling hours (1983/84)	1047	703	353	44
Minimum chilling hours (2003/04)	213	103	27	1
Mean yearly change	-17.4	-12.1	-6.4	-0.8
Coefficient of determination ( $r^2$ )	0.33	0.31	0.30	0.32

Nevertheless, the low Shannon evenness values of around 50% indicate a very uneven distribution of species. In fact, over 80% of all individuals at Al ‘Ayn and Masayrat ar Ruwajah belong to only two species (pomegranate and rose at Al ‘Ayn, and date palm and banana at Masayrat ar Ruwajah). At Qasha’ and Salut, the two most frequent tree crops (pomegranate and peach) account for 68% and 75% of all individuals. The most frequent crops are thus low-risk species, which are not very susceptible to inadequate chilling. Assuming that all cultivated varieties have chilling requirements near the lower end of the range given in Table 1, the proportion of trees that are susceptible to warm winters is less than 5% in all oases (Fig. 5.8). The dominance of only a few species indicates that cultivation of these species has been successful in the past. The crop failure of pomegranate in the lower villages and peaches and apricots in all oases, however, suggests that current climatic conditions are not suitable for the cultivation of these dominant species.

An explanation for this discrepancy between what is cultivated and what the climate is suitable for is offered by the long-term trend in chilling hours in the four settlements. Apparently, minimum temperatures have risen over the past 24 years (Table 4), and the number of chilling hours has declined dramatically (Fig. 5.6). During this time span, the lower altitude limit for cultivation of all cold-loving species has gradually risen, making the climate of Salut and Qasha’ unsuitable for the most frequent fruit trees cultivated in the villages’ gardens.

The increasing trend in minimum temperatures is not restricted to the region analyzed in this study. A series of climate change workshops held in 2004 and 2005 led to an extensive analysis of climate extremes in the Middle East (Zhang et al. 2005). Their findings show that the weather station at Saiq is representative of a general trend. The workshops found that between 1970 and 2003, yearly minimum temperatures rose by 0.6°C per decade throughout the Middle East. At Saiq, the rise was with 0.7°C per decade between 1983 and 2006 very similar. This indicates that the apparent reduction of chilling

hours observed in Al Jabal al Akhdar is a more widespread phenomenon in the Middle East and even beyond.

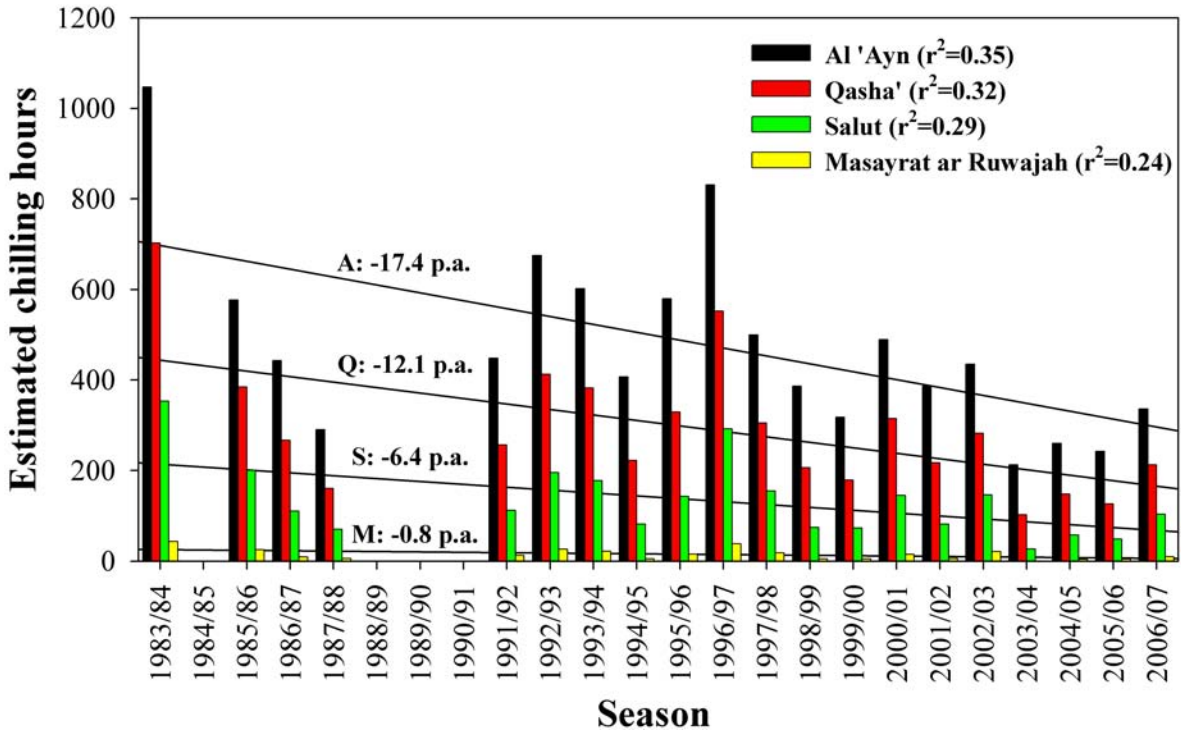


Figure 5.6. Estimated chilling hours at the oases of Al ‘Ayn (A), Qasha’ (Q), Salut (S) and Masayrat ar Ruwajah (M) during winters between 1983 and 2007 and linear regressions for each oasis. The numbers in the graph indicate the annual decrement of the regression curve and the  $r^2$  values in the legend are the coefficients of determination of the linear regressions.

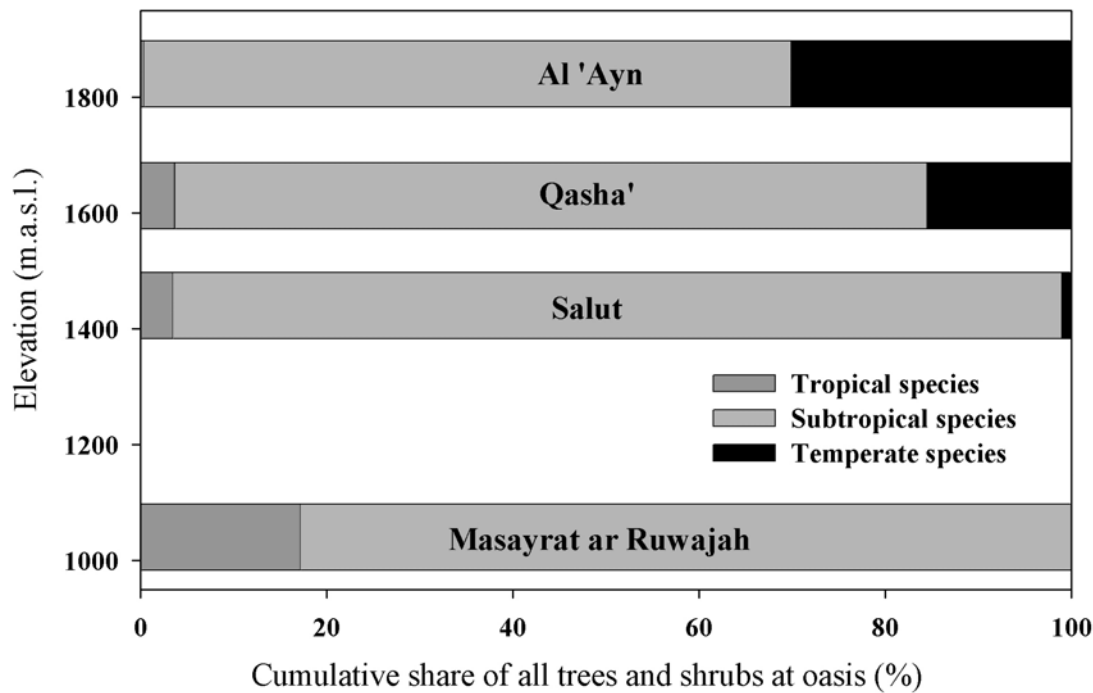


Figure 5.7. Shares of predominately temperate, subtropical and tropical species among the trees and shrubs of Al ‘Ayn, Qasha’, Salut and Masayrat ar Ruwajah.

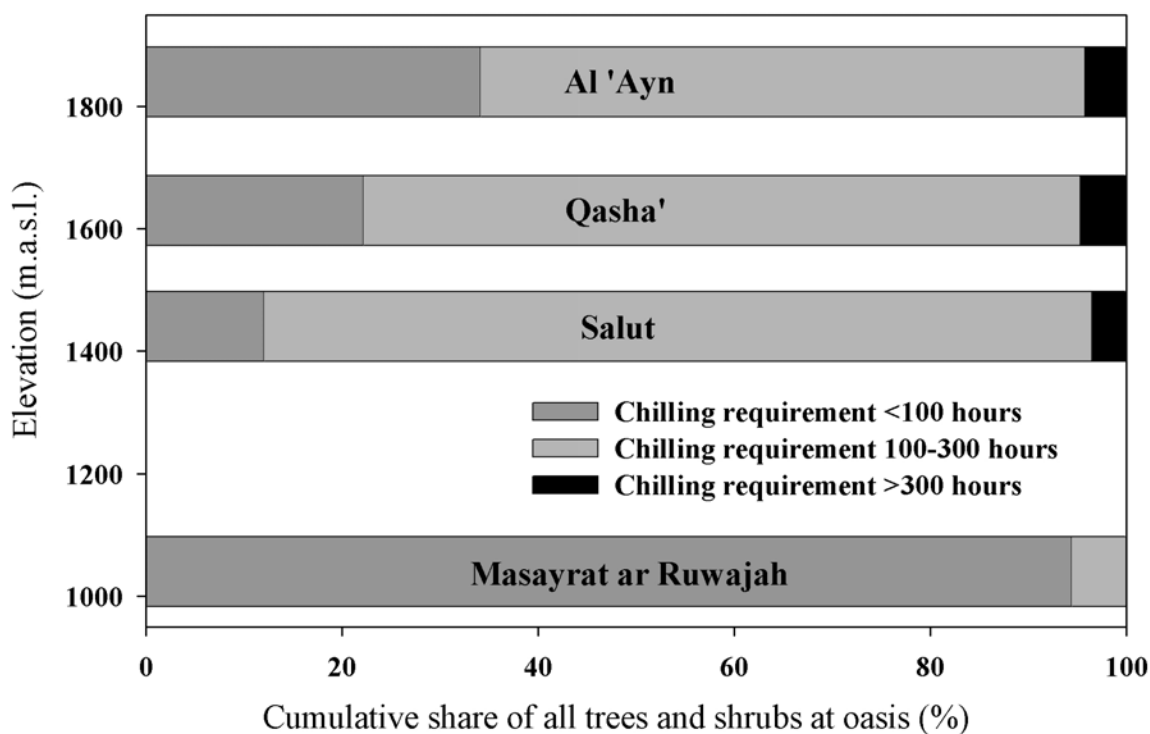


Figure 5.8. Proportion of individual trees and shrubs having chilling requirements of <100 hours, 100-300 hours and >300 hours at the four oases studied. Roses were classified in the class of lowest chilling requirement.

Even if the warming trend in the Oman Mountains does not even manifest itself in rising mean annual temperatures, it already seems to have a dramatic impact on the traditional cropping system. This illustrates how sensitive biological systems can be to slight changes in climatic conditions, if these changes happen close to a temperature threshold. The possible implications of such thresholds have not been adequately addressed by research on the impact of climate change on natural and agricultural systems. Some studies have explored the response of pathogens and other microorganisms to climate change, based on the thresholds that determine their life cycles, and attempted to predict their future ranges (Francis et al. 2003, Jenkins et al. 2006). Our study suggests that similar thresholds may also determine the future distribution of crop species and require adaptations of agricultural and horticultural production systems. While pomegranates may be expected to perform well for at least a few more years at Al 'Ayn and all oases at higher elevations, it might be advisable for farmers at Qasha' and Salut to start introducing more date palms and other insensitive species into their gardens.

## 5.5 Conclusions

Cultivation of temperate crops in the oases of Al Jabal al Akhdar represents an increasing risk for farmers, because the annual chilling hours are not always sufficient to ensure fructification. In spite of a large variety of crops, among which are some with comparatively high chilling requirements, most

cultivated individual trees and shrubs do not require many cold days during the winter.

The winter of 2005/06 was too warm for regular fructification of apricot and peach, and for all oases below 1800 m.a.s.l., even pomegranate could not fulfill its chilling requirement. The winter of 2006/07 was only slightly cooler.

The temperature niche for the cultivation of temperate crops and subtropical crops with chilling requirement is getting smaller in the Oman Mountains, and trends over the past 24 years suggest that in the long run, horticultural systems that are based on such crops might not be able to survive.

## Acknowledgments

The friendly cooperation of the farmers of Al ‘Ayn, Al ‘Aqr, Ash Sharayjah, Qasha’, Salut and Masayrat ar Ruwajah is gratefully acknowledged. We are also indebted to Dr. Maher Nagieb for carrying out fruit harvest measurements, to Sultan Qaboos University in Muscat, Oman for technical support and to the German Research Foundation (DFG) for funding (BU 1308). We also wish to express our gratitude to Dr. Herbert Dietz of the Sultanate of Oman’s Royal Court Affairs and to the Directorate General of Civil Aviation and Meteorology for granting us access to their weather records.

## References

- Blanke MM (2008). Perspectives of Fruit Research and Apple Orchard Management in Germany in a changing climate. *Acta Horticulturae* 27th International Horticultural Congress, in press.
- Cannell MGR, Grace J and Booth A (1989). Possible impacts of climatic warming on trees and forests in the United Kingdom - a review. *Forestry* 62(4), 337-364.
- Costa PM (1983). Notes on traditional hydraulics and agriculture in Oman. *World Archaeology* 14(3), 273-295.
- Erez A and Couvillon GA (1987). Characterization of the influence of moderate temperatures on rest completion in peach. *Journal of the American Society for Horticultural Science* 112(4), 677-680.
- Fischer G and Lüdders P (1995). Der Apfelnbau im Hochland Kolumbiens - Apple growing in the Colombian highlands. *Erwerbsobstbau* 37(2), 58-62.
- Fisher M (1994). Another look at the variability of desert climates, using examples from Oman. *Global Ecology and Biogeography Letters* 4(3), 79-87.
- Gajaseneni J and Gajaseneni N (1999). Ecological rationalities of the traditional homegarden system in the Chao Phraya Basin, Thailand. *Agroforestry Systems* 46(1), 3-23.
- Gebauer J, Luedeling E, Hammer K, Nagieb M and Buerkert A (2007). Mountain oases in northern Oman: An environment for evolution and in situ conservation of plant genetic resources *Genetic Resources and Crop Evolution* 54(3), 465-482.
- Ghazanfar SA (1991). Vegetation structure and phytogeography of Jabal Shams, an arid mountain in Oman. *Journal of Biogeography* 18(3), 299-309.
- Glennie K, Boeuf M, Hughes Clarke M, Moody-Stuart M, Pilaar W and Reinhardt B (1974). Geology of the Oman Mountains. *Verhandelingen Koninklijk Nederlands geologisch mijnbouwkundig Genootschap* 31, 1-423.



- Jenkins EJ, Veitch AM, Kutz SJ, Hoberg EP and Polley L (2006). Climate change and the epidemiology of protostrongylid nematodes in northern ecosystems: *Parelaphostrongylus adocoilei* and *Protostrongylus stilesi* in Dall's sheep (*Ovis d. dalli*). *Parasitology* 132, 387-401.
- Jobbagy EG and Jackson RB (2000). Global controls of forest line elevation in the northern and southern hemispheres. *Global Ecology and Biogeography* 9(3), 253-268.
- Kehlenbeck K and Maass BL (2005). Crop diversity and classification of homegardens in Central Sulawesi, Indonesia. *Agroforestry Systems* 63(1), 53-62.
- Khoshbakht K and Hammer K (2006). Savadkouh (Iran) - an evolutionary centre for fruit trees and shrubs. *Genetic Resources and Crop Evolution* 53(3), 641-651.
- Kluge J, Kessler M and Dunn RR (2006). What drives elevational patterns of diversity? A test of geometric constraints, climate and species pool effects for pteridophytes on an elevational gradient in Costa Rica. *Global Ecology and Biogeography* 15(4), 358-371.
- Koyuncu MA, Ekinici K and Gun A (2004). The effects of altitude on fruit quality and compression load for cracking of walnuts (*Juglans regia* L.). *Journal of Food Quality* 27(6), 407-417.
- Kozłowski TT and Pallardy SG (2002). Acclimation and adaptive responses of woody plants to environmental stresses. *Botanical Review* 68(2), 270-334.
- Leblanc M, Favreau G, Maley J, Nazoumou Y, Leduc C, Stagnitti F, van Oevelen PJ, Delclaux F and Lemoalle J (2006). Reconstruction of Megalake Chad using Shuttle Radar Topographic Mission data. *Palaeogeography Palaeoclimatology Palaeoecology* 239(1-2), 16-27.
- Lookingbill TR and Urban DL (2005). Gradient analysis, the next generation: towards more plant-relevant explanatory variables. *Canadian Journal of Forest Research-Revue Canadienne De Recherche Forestiere* 35(7), 1744-1753.
- Lüdders P and Wernke M (2003). Probleme des Kern- und Steinobstanbaus in tropischen Hochlagen Kolumbiens unter besonderer Berücksichtigung des Kältebedürfnisses der Bäume - Problems of pome and stone fruit trees in the highlands of Columbia with special reference to their chilling requirement. *Erwerbsobstbau* 45, 125-134.
- Luedeling E and Buerkert A (2008). Typology of mountain oases in Oman based on Landsat and SRTM imagery and geological survey data. *Remote Sensing of Environment* in press.
- Lv S, Zhou XN, Zhang Y, Liu HX, Zhu D, Yin WG, Steinmann P, Wang XH and Jia TW (2006). The effect of temperature on the development of *Angiostrongylus cantonensis* (Chen 1935) in *Pomacea canaliculata* (Lamarck 1822). *Parasitology Research* 99(5), 583-587.
- Magurran A (1988). Ecological diversity and Its measurement. Princeton University Press, Princeton, NJ, USA, 179 pp.
- Nagieb M, Siebert S, Luedeling E, Buerkert A and Häser J (2004). Settlement history of a mountain oasis in northern Oman - evidence from land-use and archaeological studies. *Die Erde* 135(1), 81-106.
- NCDC (2007). Global surface summary of the day data, version 7. National Climatic Data Center (NCDC) of the National Oceanic and Atmospheric Administration (NOAA). Accessed on 15 Apr 2007 at <http://www.ncdc.noaa.gov/oa/land.html>.
- Noel D (2007). Australasian tree crops sourcebook. Accessed on 09 July 2007 at <http://www.wanatca.org.au/atcros/LF.htm>.
- Norman WR, Shayya WH, Al-Ghafri AS and McCann IR (1998). Aflaj irrigation and on-farm water management in northern Oman. *Irrigation and Drainage Systems* 12(1), 35-48.
- Richardson EA, Seeley SD and Walker DR (1974). A model for estimating the completion of rest for Redhaven and Elberta peach trees. *HortScience* 9, 331-332.
- Schäper W (2006). Fernrohrbrille und Modellflugzeuge. *Innovation* 17, 52-57.

- Scholz F (1984). Höhensiedlungen am Jabal Akhdar - Tendenz und Probleme der Entwicklung einer peripheren Region im Oman-Gebirge. *Zeitschrift für Wirtschaftsgeographie* 28(1), 16-30.
- Seguin B (2003). Adaptation of agricultural production systems to climatic change. *Comptes Rendus Geoscience* 335(6-7), 569-575.
- Shaltout AD and Unrath CR (1983). Rest completion prediction model for Starkrimson Delicious apples. *Journal of the American Society for Horticultural Science* 108(6), 957-961.
- Vetaas OR (2002). Realized and potential climate niches: a comparison of four Rhododendron tree species. *Journal of Biogeography* 29(4), 545-554.
- Watkins JE, Cardelus C, Colwell RK and Moran RC (2006). Species richness and distribution of ferns along an elevational gradient in Costa Rica. *American Journal of Botany* 93(1), 73-83.
- Zaldivar ME, Rocha OJ, Castro E and Barrantes R (2002). Species diversity of edible plants grown in homegardens of Chibchan Amerindians from Costa Rica. *Human Ecology* 30(3), 301-316.
- Zhang XB, Aguilar E, Sensoy S, Melkonyan H, Tagiyeva U, Ahmed N, Kotaladze N, Rahimzadeh F, Taghipour A, Hantosh TH, Albert P, Semawi M, Ali MK, Al-Shabibi MHS, Al-Oulan Z, Zatar T, Khelet IA, Hamoud S, Sagir R, Demircan M, Eken M, Adiguzel M, Alexander L, Peterson TC and Wallis T (2005). Trends in Middle East climate extreme indices from 1950 to 2003. *Journal of Geophysical Research-Atmospheres* 110(D22), D22104.

**Chapter 6***submitted to Plant and Soil***Effects of land use changes on the hydrological sustainability of mountain oases in northern Oman****Eike Luedeling<sup>a</sup> and Andreas Buerkert<sup>a</sup>**

<sup>a</sup> *Department of Organic Plant Production and Agroecosystems Research in the Tropics and Subtropics, University of Kassel, Steinstr. 19, D-37213 Witzenhausen, Germany*

---

**Abstract**

While traditional oases in hyperarid Oman have been practicing apparently sustainable agriculture for many centuries, the hydrological sustainability of their production systems might depend on preserving traditional land use patterns. We hypothesized that recent land use changes are having detrimental effects on oasis agriculture and tested this hypothesis in five oases in the high-mountain region of Al Jabal al Akhdar, by comparing the agricultural water use patterns of Al ‘Aqr, Al ‘Ayn, Ash Sharayjah, Qasha’ and Masayrat ar Ruwajah in 1978 and 2005.

Current land use was assessed by mapping agricultural crops in April and September 2005, and water demand was estimated using the Penman-Monteith equation to model crop evapotranspiration. As input variables, we measured temperatures at three elevations. From measured solar radiation and wind speed, we modeled these parameters for the entire study region. We classified each oasis into five land use types and calculated mean water requirements per area for each type based on modeled water demand in 2005. From these values, we estimated historical water demand based on classified aerial photographs from 1978. We quantified available water by measuring the flow of all springs in the area.

Between 1978 and 2005, combined annual water demand of the studied oases rose from 218,800 m<sup>3</sup> to 256,377 m<sup>3</sup>, with much higher demand in summer than in winter. Since 1978, land use changes have led to an expansion of deciduous orchards at the expense of field crops at all oases except Masayrat ar Ruwajah. Since, in contrast to annual fields, these orchards must be irrigated throughout the summer, this change raised the water demand in the critical summer months, increasing vulnerability to drought. Summer water demand in 2005 was larger than mean water supply in Al ‘Aqr and Qasha’, and larger than observed minimum spring flow in all oases. Water supply might already be affected by water extracted for use by a new town in the vicinity.

Only Masayrat ar Ruwajah maintained enough area under field crops in 2005 to follow the traditional strategy of compensating for low spring flows by reducing the field crop area during the summer.

---

## 6.1 Introduction

The climate of northern Oman is hot and hyperarid. Mean annual temperatures range between 18°C in the high mountains and 28°C in the lowlands (Fisher 1994), with maximum values frequently exceeding 40°C in the summer (Dorvlo and Ampratwum 1998). Rainfall is very scarce and erratic, with mean annual precipitation varying between 39 and 312 mm among stations in Oman, and coefficients of variation of the annual rainfall between 48 and 162% (Fisher 1994).

Today most agricultural areas in the country, which total less than 0.3% of the land area (FAO 2007), are irrigated with groundwater pumped up to the surface of the coastal plain. Traditional agricultural systems, however, did not have that option and were thus confined to specific hydrological settings, where water accumulated and was dispensed over longer time spans (Luedeling and Buerkert 2008a). Where water surfaced naturally or could be harvested by carving tunnels into storage rock formations, farmers collected it and directed it to the cropping areas through a system of irrigation channels, called aflaj in Arabic (Sing.: falaj) (Costa 1983). On irrigated terraced fields (Luedeling et al. 2005b), farmers cultivate date palms (*Phoenix dactylifera* L.) and other tropical and subtropical crops, along with vegetables and fodder for the goats, sheep, camels and cattle that are traditionally kept in the oases.

Several studies have shown that traditional oasis agriculture in Oman is very water-efficient. Estimates of its water use efficiency range between 60% and 98%, with a mean of 79% for several plots at Falaj Hageer in Wadi Bani Kharus (Norman et al. 1998b), while Siebert et al. (2007) computed a water use efficiency of 75% for the oasis of Balad Seet in Wadi Bani Awf.

Given the large variation in potential evapotranspiration over the course of a year (Siebert et al. 2007), such high efficiencies cannot be achieved without adaptations to the changes of the seasons. While farmers at Balad Seet have to irrigate their date palm orchards throughout the year, they compensate for the higher water requirements of these perennials during the summer by reducing the area under field crops (Siebert et al. 2007). Such adaptations can be observed in all traditional settlements, except where water is so abundant that there is no shortage during the summer. An example of such a setting with ample year-round water supply is the line of oases along narrow Wadi Tiwi (Korn et al. 2004a), where space rather than water is the limiting factor for crop production. While typically most of the oasis area is covered by perennial orchards, there is almost always a sizeable proportion under field crops, which can be adjusted from year to year as a response to falaj flow.

Many of the most remarkable traditional settlements lie in the mountainous interior of the country. The topography of northern Oman is characterized by the

range of the Oman Mountains, which stretches in a long arc from the Musandam Peninsula in the north to the Arabian Sea in the south. Its highest peak, Jabal Shams, which reaches an elevation of almost 3000 m above sea level, is the highest point of an extensive high plain made up of limestones of Late Permian to Middle Cretaceous age (Glennie et al. 1974). These limestones often contain large aquifers, and where they overlay impermeable formations, they often give rise to permanent springs, which feed the terraced fields of small mountain oases.

Five such oases in a single watershed in Al Jabal al Akhdar, the highest agricultural region of Oman are the subject of this study (Fig. 6.1). Other than those of the lowland oases, farmers in these settlements, which lie at elevations of up to 2000 m a.s.l., do not rely on date production for their sustenance, but grow crops that are more appropriate for the climate at this altitude (Gebauer et al. 2007a). Here, farmers successfully cultivate pomegranates (*Punica granatum* L.), apricots (*Prunus armeniaca* L.), peaches (*Prunus persica* L.), roses (*Rosa damascena* L.) for the production of rose water and other temperate and subtropical fruits. Most of the fruits of these oases are not grown in the lowlands, because they cannot fulfill their winter chilling requirement (Luedeling et al. 2008b). For field crops, farmers grow garlic (*Allium sativum* L.) and cereals, mainly barley (*Hordeum vulgare* L.), oats (*Avena sativa* L.) and maize (*Zea mays* L.), as well as some vegetables and animal fodder. How long the oases of Al Jabal al Akhdar have existed, is unknown (Melamid 1992), but oral accounts of inhabitants referring to the time of Portuguese occupation make it likely that these villages have been inhabited at least since the 16<sup>th</sup> century, but probably much longer.

For most of their existence, the high-mountain oases remained mostly undisturbed by events in the rest of the country, because they could only be reached via tiresome hikes along steep footpaths or donkey trails. High transaction costs thus lay on all interactions with the outside world, putting constraints on the farmers' ability to trade food and other goods with outsiders. A large proportion of the agricultural area was thus dedicated to subsistence food and fodder production. All marketable products, such as pomegranates and garlic had to pass through the economic bottleneck of the donkey transport, placing a natural limitation on the area devoted to market-oriented production. These conditions persisted through the centuries, remaining largely unchanged until the beginning of the reign of Sultan Qaboos bin Said in 1970.

One of the priorities of the new government has been to use oil revenues for developing the country's infrastructure and for modernizing its society. Al Jabal al Akhdar was one of the priority regions for development, given its role in the so-called Jabal War of the 1950s (Scholz 1984). Since the 1970s, several new developments have impacted the oases, starting a transformation process that can be observed to some degree in all oases of Oman.

The first dramatic change for the mountain villages was the building of a military camp and the required access road in 1959 (Scholz 1984). The camp provided off-farm employment for villagers, and the road connected the settlements to markets in the lowlands, which could now be reached within a

few hours' drive rather than after a long day of hiking through the mountains. These developments changed the economic realities of the oases, leading to a decrease in cereal production (Abercrombie 1981, Scholz 1984), which was replaced by importing grains from the lowlands, and to an expansion of the area planted to fruit trees, whose harvested fresh products would not have endured the long transport down the mountains on donkey-back.

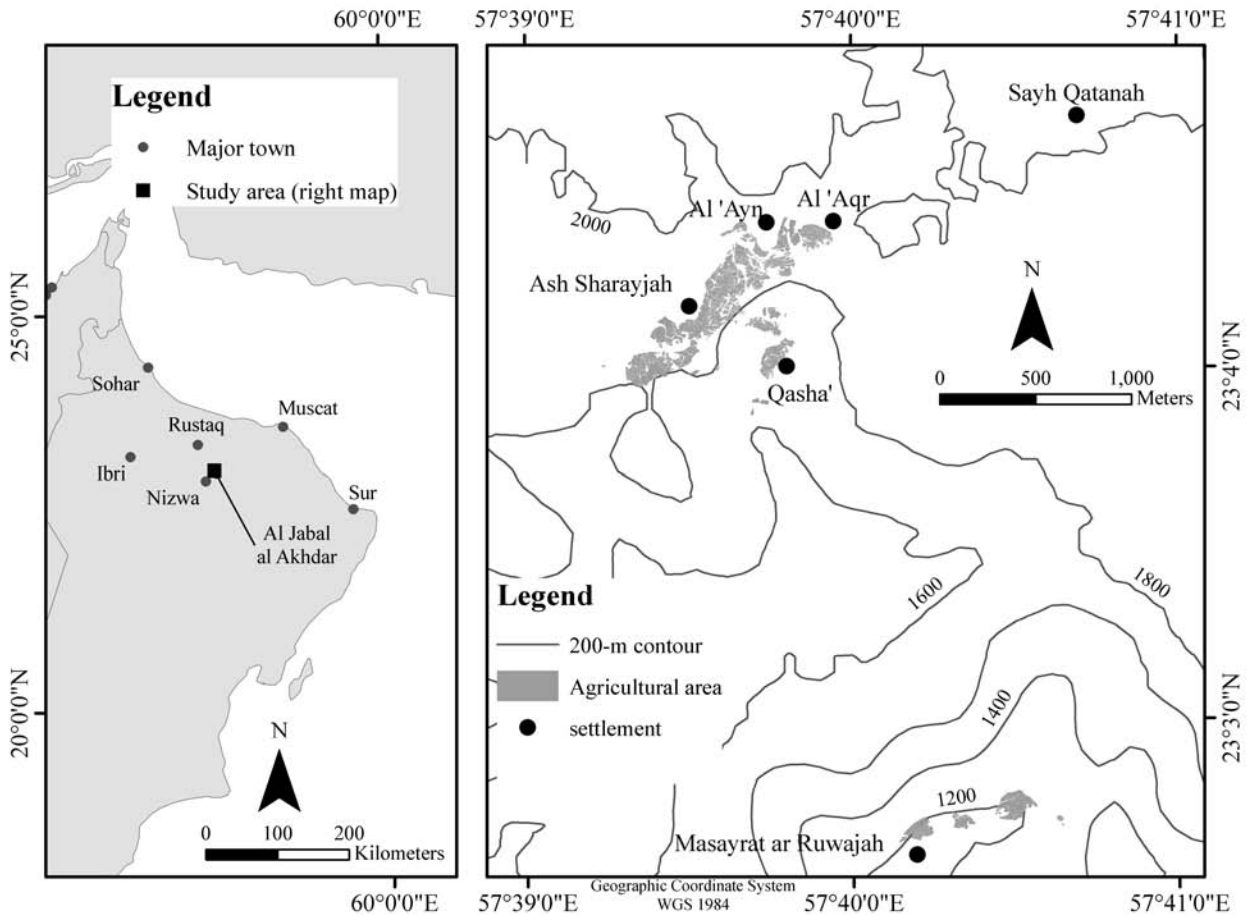


Figure 6.1. Overview of the study area (right map) and its location within Oman.

Another manifestation of the transformation process that is still in progress was the development of the town of Sayh Qatanah on the Sayq Plateau, only a few kilometers from the oases (Fig. 6.1). The water demand of this town is met by boreholes that were drilled into the same aquifer that supplies the irrigation water to the oases. To what degree the new settlement actually competes with the agricultural oases for water has never been discussed, but the town certainly brought the modern world closer to the inhabitants of the oases, eroding the agricultural lifestyle of the oasis farmers. The ongoing rapid expansion of tourism in the area is likely to accelerate this process.

As a more direct influence on the agricultural systems, the opening of an agricultural extension center in the new town, as well as the establishment of a new farm on the plateau, which produces temperate fruits for the Sultan's Court, influenced oasis farmers, putting more and more emphasis on fruit production. Lastly, an epidemic of Witches' Broom of Lime, a phytoplasma disease (Garnier

et al. 1991), almost eradicated lime trees (*Citrus aurantiifolia* (L.) Swingle) at lower elevations of Oman (Khan and Grosser 2004). While the high-altitude settlements on Al Jabal al Akhdar were mostly spared from this disease, mid-altitude oases were badly affected.

The objective of this study was to investigate, to what degree changes in land use have impacted the hydrological sustainability of the oases of Al Jabal al Akhdar. The seemingly fine balance in Omani oases between orchards and field crops, with the orchard area apparently correlating with the long-term minimum water supply that can be relied upon, leads to our hypothesis that the recent and on-going land use changes put the hydrological sustainability of the traditional land use system at risk. Recently, many farmers of the villages in this area have complained about water shortages, mostly putting the blame on insufficient rainfall. While reliable rainfall data for the past few years is lacking, several major rainstorms in recent months and measurements of high subsequent spring flows make it unlikely that lack of precipitation is the only major factor putting the oases' water balance under pressure. Rainfall records given by Fisher (1994) also indicate that periods of at least two subsequent years of annual rainfall of well under 100 mm, a third of the long-term average, are not uncommon in this region, and there is no evidence that oasis systems suffered excessively during such periods. We therefore hypothesize that above all else, land use changes in the oases have led to increased agricultural water demand and to a less favorable seasonal distribution of water use.

## 6.2 Materials and Methods

### 6.2.1. Study sites

The study was conducted in five mountain oases in Al Jabal al Akhdar, the highest agricultural area in the Sultanate of Oman (Luedeling et al. 2008b, Scholz 1984). Three of the oases, the villages of Al 'Aqr (57°39'58"E, 23°04'22"N, 1950 m a.s.l.), Al 'Ayn (57°39'44"E, 23°04'22"N, 1900 m a.s.l.) and Ash Sharayjah (57°39'30"E, 23°04'10"N, 1900 m a.s.l.) lie at the top of a large eroded basin at the edge of the Sayq Plateau, a large dissected plain at an altitude above about 1950 m a.s.l. (Fig. 6.1). The ground surface of the plateau consists of Late Permian to Middle Cretaceous limestones of the Hajar Supergroup, and all important springs of the area emerge from the unconform geologic boundary at the bottom of the lowest formation in this unit (Luedeling and Buerkert 2008a). The agricultural areas of the three highest oases of our study are fed by two springs which emerge from this setting. The terraced fields lie directly underneath the level of the springs, along the slope of the eroded basin. The terraced area of Ash Sharayjah amounts to 13.5 ha, Al 'Aqr has 1.7 ha and the farmers of Al 'Ayn cultivate 1.4 ha.

Below this set of oases lies the settlement of Qasha' (57°39'50"E, 23°04'00"N, 1640 m a.s.l.). Qasha's 2.1 ha of terraced fields obtain their water from one of the springs at Al 'Ayn, from where the water flows through a steep

channel down to the oasis. One smaller spring in the valley adds to Qasha's water supply.

The lowest oasis, Masayrat ar Ruwajah ( $57^{\circ}40'13''\text{E}$ ,  $23^{\circ}02'37''\text{N}$ , 1030 m a.s.l.), lies about 900 m below the plateau in a deeply incised wadi. Its agriculture is characterized by date palms and other tropical and subtropical crops, corresponding closely to the farming system described by Nagieb et al. (2004b) for the oasis of Balad Seet at the upper end of Wadi Bani Awf. The oasis' water supply is ensured by one spring emerging from a similar setting as in the upper oases. From the inaccessible spring site, the water falls several hundred meters into a dam, from where it is conducted to the fields through a falaj of more than 2 km length.

### *6.2.2. Assessment of current and historic land use*

To determine current land use, we took aerial images of the oasis area using a digital camera mounted on a model plane (Buerkert et al. 1996, Schäper 2006). Photographs were taken from flight altitudes ranging from several hundred meters to 1.5 km, providing a complete coverage of the entire oasis area, as well as sufficient detail to map land use on the ground. For georeferencing these photographs, DGPS (Differential Global Positioning System) ground-truthing information was collected using two Trimble Pathfinder Pro XRS receivers (Trimble Navigation Ltd., Sunnyvale CA, USA) as field rover and base station. The photographs were then rectified using ERDAS Imagine 8.5 (Leica Geosystems GIS & Mapping LLC., Norcross, GA, USA).

Based on the maps obtained through this process, a detailed field survey was carried out, during which all trees of the oases were counted and classified by species (Gebauer et al. 2007a). Areas covered by field crops were also registered on two occasions, in April and September of 2006, to account for different cropping patterns during the summer and winter season.

In addition to this detailed survey, we classified vegetation of each terrace based on the appearance of the terrace on the aerial photograph. Since for most tree and field crops, the crop species could not be determined on the images, all terraces were assigned one of five classes that could be visually distinguished with sufficient certainty. The resulting land use classes were 'rose gardens', 'date palm orchards', 'other orchards', 'field crops' and 'bare ground'.

Historic aerial images of all oases except Masayrat ar Ruwajah were obtained from an archive of such images set up by Prof. Fred Scholz (Free University of Berlin, Germany), who studied the development of Oman and its oases over several decades. All images were taken in 1978 and showed all upper oases in sufficient detail for coarse classification. For Masayrat ar Ruwajah, no such aerial image was available, but since the oasis lies in a deep valley, its whole extent was captured by a panoramic photograph taken by Prof. Scholz during an expedition to the area in 1976. Several photographs from the same and one subsequent expedition, as well as two color plates from a 1981 issue of National Geographic, which featured an article about Oman (Abercrombie 1981), helped



in the assessment of historic land use. As described for current land use, we classified vegetation in the oases into the five classes mentioned above.

### 6.2.3. Evapotranspiration modeling

For modeling evapotranspiration ( $ET$ ), we used the Penman-Monteith equation (Francis et al. 2003), in the standardized version of the American Society of Civil Engineers (ASCE 2005). This equation uses information on geographic location, climate and land use to estimate crop evapotranspiration ( $ET_c$ ). In the version of the FAO (Francis et al. 2003), the equation consists of a reference evapotranspiration  $ET_0$ , depending solely on geographic and climatic parameters, which is multiplied by a crop-specific coefficient  $k_c$ . Instead of the classic  $ET_0$ , we used the reference evapotranspiration ( $ET_{sz}$ ) from ASCE's Standardized Reference Evapotranspiration Equation, for which the basic equation, as recommended by ASCE (2005) is:

$$ET_{sz} = \frac{0.408 \cdot \Delta \cdot (R_n - G) + \gamma \cdot \frac{C_n}{T + 273} \cdot u_2 \cdot (e_s - e_a)}{\Delta + \gamma \cdot (1 + C_d \cdot u_2)}, \text{ with}$$

$R_n$  = calculated net radiation at the crop surface ( $\text{MJ m}^{-2} \text{d}^{-1}$ ),

$G$  = soil heat flux density at the soil surface ( $\text{MJ m}^{-2} \text{d}^{-1}$ ),

$T$  = mean daily temperature at 1.5 to 2.5 m height ( $^{\circ}\text{C}$ ),

$u_2$  = mean daily wind speed at 2 m height ( $\text{m s}^{-1}$ ),

$e_s$  = saturation vapor pressure at 1.5 to 2.5 m height (kPa),

$e_a$  = mean actual vapor pressure at 1.5 to 2.5 m height (kPa),

$\Delta$  = slope of the saturation vapor pressure-temperature curve ( $\text{kPa } ^{\circ}\text{C}^{-1}$ ),

$\gamma$  = psychrometric constant ( $\text{kPa } ^{\circ}\text{C}^{-1}$ ),

$C_n$  = numerator constant ( $\text{K mm s}^3 \text{Mg}^{-1} \text{d}^{-1}$ ),

$C_d$  = denominator constant ( $\text{s m}^{-1}$ ).

Most of the parameters required by the equation are difficult to measure directly in the field, but following ASCE (2005), they can be calculated from variables that can easily be assessed.  $R_n$  was calculated as the difference between net short-wave radiation ( $R_s$ ) and net outgoing long-wave radiation ( $R_{nl}$ ), both of which could be derived from a range of equations based on three-dimensional site coordinates (latitude  $\varphi$ , longitude  $\delta$  and elevation  $z$ ), measured temperatures (minimum temperature  $T_{min}$  and maximum temperature  $T_{max}$ ), and time (day  $D$ , month  $M$  and year  $Y$ ):

$$R_n(R_s, T_{max}, T_{min}, \varphi, \delta, z, D, M, Y) = R_{ns}(R_s, \alpha) - R_{nl}(T_{max}, T_{min}, e_a, R_s, z, G_{sc}, \varphi, \delta, D, M, Y).$$

The equation also contains constants for the solar constant  $G_{sc}$ , and the albedo  $\alpha$ , which are set to  $4.92 \text{ MJ m}^{-2} \text{h}^{-1}$  and 0.23 in the standardized calculation of  $ET_{sz}$ .  $R_{ns}$  and  $R_{nl}$  were calculated as described by ASCE (2005).

For monthly calculation intervals, the soil heat flux density  $G$  is not negligible and was computed as

$G(T_{month-1}, T_{month+1}) = 0.07 \cdot (T_{month+1} - T_{month-1})$  , with  $T_{month-1}$  being the mean temperature of the past month and  $T_{month+1}$  the mean temperature of the following month.

Rather than computing mean daily temperatures  $T$  as the arithmetic mean of all measured temperatures, we follow the recommendations by FAO (Francis et al. 2003) and ASCE (2005), calculating  $T$  as

$$T(T_{min}, T_{max}) = \frac{T_{min} + T_{max}}{2}$$

Saturation vapor pressure  $e_s$  was derived from measured temperatures as

$$e_s(T_{min}, T_{max}) = 0.5 \cdot (0.6108 \cdot e^{\frac{17.27 \cdot T_{max}}{T_{max} + 237.3}} + 0.6108 \cdot e^{\frac{17.27 \cdot T_{min}}{T_{min} + 237.3}}).$$

Our estimate of mean actual vapor pressure  $e_a$  is based on an estimate of the dew point temperature  $T_{dew}$ , for which the daily minimum temperature is reduced by 2°C. Because of the non-standard conditions, with largely barren landscape around our study sites, measured dew points or relative humidity had to be discarded and the simplified calculation be applied instead (ASCE 2005, Francis et al. 2003). Mean actual vapor pressure was thus calculated as

$$e_a(T_{min}) = 0.6108 \cdot e^{\frac{17.27 \cdot (T_{min} - 2)}{T_{min} - 2 - 237.3}}.$$

The slope of the saturation vapor pressure-temperature curve  $\Delta$  was calculated as

$$\Delta(T) = \frac{2503 \cdot e^{\frac{17.27 \cdot T}{T + 237.3}}}{(T + 237.3)^2}.$$

For estimating the psychrometric constant  $\gamma$ , we used the following equation:

$$\gamma(z) = 0.000665 \cdot 101.3 \cdot \left(\frac{293 - 0.0065 \cdot z}{293}\right)^{5.26}, \text{ with } z = \text{site elevation.}$$

From the two reference vegetation types given by ASCE (2005), we chose the tall vegetation type, because vegetation in the oases of Oman resembles much more closely alfalfa than clipped grass in terms of crop height and vigor. Accordingly, the numerator constant  $C_n$  was set to 1600 and the denominator constant  $C_d$  to 0.38.

After all of these substitutions the standardized reference evapotranspiration was calculated by a function of twelve variables.

$$ET_{sz} = ET_{sz}(\varphi, \delta, z, D, M, Y, T_{min}, T_{max}, T_{month-1}, T_{month+1}, R_s, u_2)$$

Thus, only four climatic variables,  $T_{min}$ ,  $T_{max}$ ,  $R_s$  and  $u_2$ , remained to be determined in the field, with  $T_{month-1}$  and  $T_{month+1}$  being derived from these measurements.

### Crop coefficients $k_c$

Crop coefficients were assigned to each crop according to the appropriate table of Allen et al. (2003). For the lengths of crop development stages, we also referred to this report, but adapted the growing periods to local conditions as observed in the field. Where crop coefficients for a crop were unavailable, we used  $k_c$  values for the crops in the FAO list, for which growth habits

corresponded most closely to the crops we encountered in the field. For pomegranates, this required using the growth stages of deciduous orchards and the crop coefficients of the ‘Apricot, Peaches, Stone Fruit’ category from the FAO table. For roses, we used the same crop coefficient, but accounted for the shorter period of cultivation by using only half the stage length recommended for deciduous orchards. For roses, the duration of water use was thus reduced from 240 days to 120 days, which corresponds well to our field observations, according to which roses are mainly irrigated between January and April. Between May and August/September, roses receive about one irrigation per month to sustain their vegetative growth. We approximated this irrigation regime by setting  $k_c$  to 0.3 for June to August and 0.15 for September.

We determined the start and end month of the growing season for each crop by interviewing farmers and observing cultivation patterns in the field. To account for the temporal variation in field cultivation among farmers, we used three different starting dates for each crop. Starting dates were set to the estimated average planting date, and dates for early and late planters set to two weeks before and after this date. For fodder crops, which are replanted after harvest, each cultivation interval started five days after the harvest of the previous crop.

As recommended by Allen et al. (2003), crop coefficients were adjusted to account for crop height and deviations of wind speed and relative humidity from the standard values of  $2 \text{ m s}^{-1}$  and 45 %. We consequently adjusted  $k_{c\text{ end}}$  and  $k_{c\text{ mid}}$  as:

$$k_c = k_c(\text{table}) + [0.04 \cdot (u_2 - 2) - 0.004 \cdot (RH_{\min} - 45)] \cdot \left(\frac{h}{3}\right)^3,$$

with  $u_2$  being the mean wind speed of the site,  $RH_{\min}$  an estimate of the mean daily minimum of relative humidity and  $h$  the approximate crop height.

Mean wind speeds for Al ‘Ayn, Al ‘Aqr, Ash Sharayjah and Qasha’ were derived from the wind speed grid described below, from which we calculated the mean wind speed for the entire area of each oasis. Measurements of relative humidity were taken, but yielded monthly minima that often were below 10% and monthly means of between 20 and 70%. Since these data are lower than the range of  $RH_{\min}$  allowed as input for the  $k_c$  adjustment equation, we decided to substitute our measurements by setting  $RH_{\min}$  to 20%, corresponding to conditions expected in such an arid area (Francis et al. 2003). Crop height was set to 1 m for field crops, 2 m for roses, 10 m for date palms and 5 m for all other tree crops. Adjustments added to the  $k_c$  values for each oasis and crop type are summarized in Table 6.1.

For all months between December and May, we assigned crop coefficients according to the crop identified during the April survey, and for the remaining months, we used the coefficients corresponding to the crops encountered in September. Crop coefficients were calculated for every day of the year, and averaged for each combination of month, crop and oasis.

#### 6.2.4. Measurement of climatic parameters

Since modeling evapotranspiration requires information about the insolation of a site, we measured solar radiation using a small weather station (Weather Station III, O. Feger, Traunstein, Germany). The station's pyranometer was placed at a well exposed location on the roof of the Agricultural Extension Service station in the town of Sayh Qatanah (57°40'36"E, 23°04'51"N, 2009 m a.s.l.). Data was recorded at 10-min intervals for a period of one year between January and December of 2006.

Table 6.1. Adjustments to the  $k_c$  values for crops in Al 'Aqr, Al 'Ayn, Ash Sharayjah, Qasha' and Masayrat ar Ruwajah, Oman, calculated from crop height, mean wind speed and the estimated mean minimum of relative humidity.

	Mean wind speed (m s <sup>-1</sup> )	Estimated RH <sub>min</sub> (%)	Adjustments to $k_c$ (crop height)			
			Field crops (1 m)	Roses (2 m)	Trees (5 m)	Date palms (10 m)
Al 'Aqr	0.59	20	0.03	0.04	0.05	-
Al 'Ayn	0.71	20	0.03	0.04	0.06	-
Ash Sharayjah	0.72	20	0.04	0.04	0.06	-
Qasha'	0.75	20	0.04	0.04	0.06	-
Masayrat ar Ruwajah	0.68	20	0.03	-	0.06	0.07

For determining minimum, mean and maximum temperatures, we used HOBO Pro data loggers (Onset Computer Corp., Pocasset, MA, USA), which were installed in the gardens of Al 'Ayn (57°39'48"E, 23°04'21"N, 1900 m a.s.l.), Qasha' (57°39'46"E, 23°04'02"N, 1640 m a.s.l.) and Masayrat ar Ruwajah (57°40'13"E, 23°02'40"N, 1030 m a.s.l.). Loggers were placed in standard wooden cases designed for weather stations and positioned 1.5 m above terraces cropped with alfalfa (Al 'Ayn and Masayrat ar Ruwajah) or annual fodder grasses (Qasha'). Temperatures were recorded at half-hourly intervals between February 2005 and April 2007 at Al 'Ayn, between March 2005 and May 2007 at Masayrat ar Ruwajah and between April 2005 and April 2007 at Qasha'. Because the logger at Qasha' disappeared between April and September 2006, data for this time span could not be recorded for this oasis. We therefore chose to consider temperatures between April 2005 and March 2006 as measurements for one year. The measurement periods for radiation and temperature thus do not completely match, but due to the homogeneous clear sky conditions that prevail almost throughout the entire year, we consider the monthly averages of our radiation measurements representative of the period, during which temperature was recorded.

Wind speed measurements were taken between April and June of 2007 at a well exposed location in the gardens of Ash Sharayjah (57°39'32"E, 23°04'06"N, 1853 m a.s.l.) using the anemometer of a WatchDog 2700 Weather Station (Spectrum Technologies Inc., Plainfield, IL, USA). Data recorded on June 5<sup>th</sup> and June 6<sup>th</sup> were discarded, because they were affected by the tropical

cyclone Gonu, which led to wind speeds that were far above what would be measured during a normal year.

### 6.2.5. Wind speed modeling

To estimate site-specific wind speeds, we used an adapted version of the diagnostic windfield model NUATMOS 5 (Ross et al. 1988), which Bachmann (1998) had adapted for use in combination with the GIS package ARC/INFO (ESRI Inc., Redlands, CA, USA). Since an ARC/INFO license was not available, we modified the model's FORTRAN code to work as a stand-alone application. We also adapted the model to work with larger grids than were allowed in the original version, which appears to have been programmed for computers with much lower processing capacity than today's machines.

As inputs, the NUATMOS model requires a digital elevation model (DEM) and observations of wind speed and wind direction from the area, for which winds are to be modeled. As outputs it produces one grid of wind speeds and another one of wind directions. Bachmann (1998) modified the source code, so that his version of the model works with ASCII grids, which can easily be imported into and created by ArcGIS.

We used a DEM by Luedeling et al. (2007c), who filled gaps in the elevation model obtained by the Shuttle Radar Topography Mission (SRTM) using topographic information extracted from Russian military maps. This model was improved using a local high resolution dataset, from which altitude lines were digitized and interpolated to form a 10-m DEM. This model was then merged, using a TIN-based delta surface approach (Luedeling et al. 2007c), with the SRTM-based model, which had been resampled from its original resolution of 81 m to 10 m. Since high-resolution elevation information had only been mapped for part of our study area, the level of topographic detail in the model varies and is substantially lower for the area around Masayrat ar Ruwajah and Al 'Aqr.

Since the NUATMOS model only allows calculations of instantaneous windfields rather than average wind speeds over longer time spans, we followed the approach by Bowling and Lettenmaier (1997) and calculated distinct windfields for the main wind patterns encountered in our study area. To determine these patterns, we used SPSS 14.0 (SPSS Inc., Chicago, IL, USA) to perform a two-way cluster analysis on wind speeds and wind directions observed by our anemometer. Using wind direction and wind speed as inputs for this analysis is problematic, because of the difficulty of dealing with the wind direction. Wind direction is given in degrees on a 0 to 360 scale, with directions on the low and high end of this scale being northerly directions. While such directions are very similar, they are certain to be separated by a cluster analysis. Therefore, we converted wind directions and speeds into the wind's easterly ( $v_E$ ) and northerly ( $v_N$ ) components by applying the following transformations:

$v_E = v_{wind} \cdot \sin \beta$  and  $v_N = v_{wind} \cdot \cos \beta$ , with  $v_{wind}$  being the wind speed and  $\beta$  the wind direction in degrees.

The number of clusters is automatically determined by the software, delivering the main wind situations encountered in the area. After running the NUATMOS model for each of these settings, we calculated an average wind speed, weighted by the frequency, at which the different wind patterns occurred. One anomaly in the calculated windfield consisted of a sudden peak of wind speeds that were about ten times higher than anywhere else in the study area and partly overlapped with the oasis of Masayrat ar Ruwajah. This area was cut out of the grid and replaced by interpolated values. The cause of this anomaly, which covered about 6 ha, with 1 ha overlapping with the oasis, seemed to be the presence of a very steep slope adjacent to the oasis.

#### 6.2.6. Modeling of solar radiation

Solar radiation was modeled for monthly intervals using the standard tool provided by the Spatial Analyst extension for ArcGIS 9.2 (ESRI Inc., Redlands, CA, USA). The model requires inputs of latitude, sky size, diffuse proportion of the radiation, transmittivity of the atmosphere and a digital elevation model. Furthermore, it requires information on whether or not to incorporate the effects of slope and slope bearing (aspect) on insolation. We modeled radiation based on the elevation model described above using the default settings for the simulation. Since all agricultural production in our study region happens on terraced fields, which have been well leveled for the flood irrigation typically practiced in the oases, we did not differentiate between different slopes or aspects. Variation of radiation is thus mostly due to different levels of shading caused by the surrounding topography.

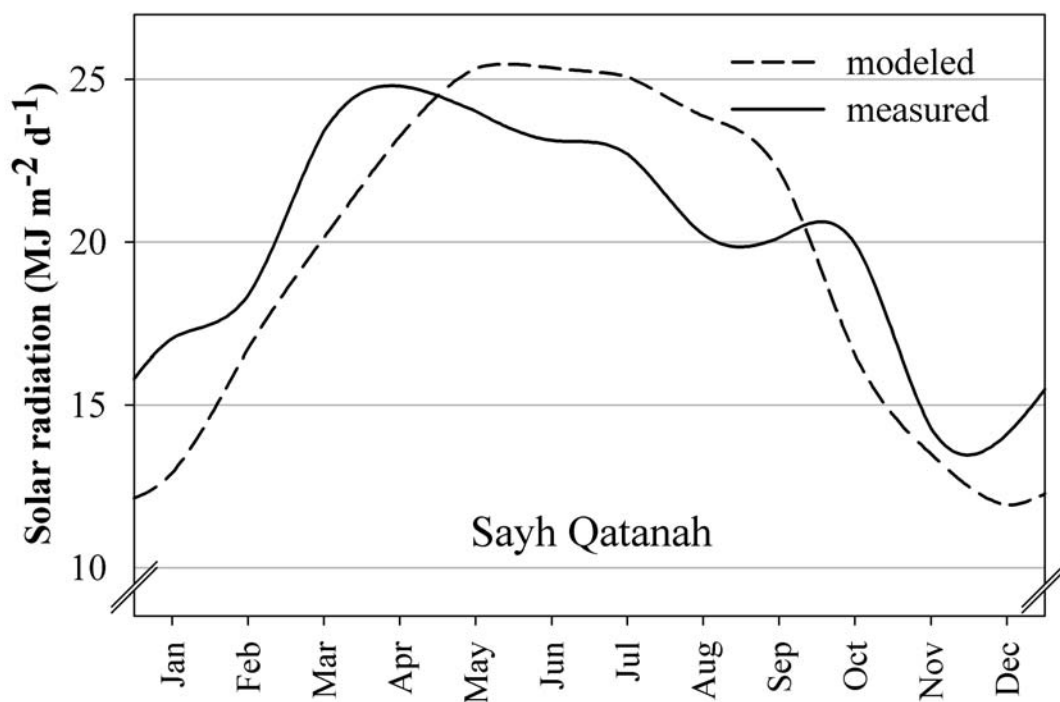


Figure 6.2. Measured and modeled radiation for the town of Sayh Qatanah, Oman, between January and December of 2006.

Rather than modifying the radiation settings in the ArcGIS tool, we adapted the modeled radiation to local conditions using our own measurements of radiation. To this end, we divided the modeled radiation grid by the radiation calculated for the measurement site. This normalized radiation grid was then multiplied by the radiation measured at the site. For some months, measured radiation was higher than modeled radiation (Fig. 6.2). In these cases, we used only the modeled radiation as input for the Penman-Monteith equation, since higher values would be difficult to explain and are probably caused by reflections from the area surrounding the pyranometer rather than by elevated solar radiation. The output of these calculations was a set of twelve grids containing the site-specific monthly radiation for the entire study area at a resolution of 10 m.

#### 6.2.7. *Water availability*

Spring flow of all oases was estimated using the methodology described in detail by Luedeling et al. (2008a). For the spring feeding the gardens of Al ‘Aqr, Al ‘Ayn and Qasha’, as well as for the separate spring at Qasha’, measurements were based on a volumetric method, in which we determined the time it took to fill containers of known volume, whereas the flow of the aflaj of Masayrat ar Ruwajah and Ash Sharayjah could only be determined by measuring the speed of a floating device on the water surface and multiplying this speed by the diameter of the channel. We estimated the average and minimum falaj flow based on monthly measurements carried out between December of 2006 and August of 2007. The highest flow of each falaj was discarded, because this flow measurement was taken directly after heavy rainfall, so that the flow did not represent normal conditions.

Despite the extreme aridity of our study region, occasional heavy rainfalls occur. These are, however, so erratic that direct assessment during the short period of our study would hardly be representative of average conditions. We therefore used a 12-year average calculated by Fisher (1994), who reported mean annual precipitation in this region to be 312 mm. In addition to the spring flow, this water is also available for crop production. We accounted for this source by adding the mean monthly rainfall as derived from this average on top of the average spring flow of the oases for estimating water availability during an average year. Even though the climate diagram presented by Fisher (1994) shows two pronounced rainfall peaks in February and August, we chose to assume an even distribution, because the detailed rainfall records presented in the same study indicate that these peaks are owed to very few exceptionally humid months within the observation period of twelve years. As reference area for estimating the amount of water derived from rainfall, we used at each site the entire oasis area, excluding all areas classified as bare soil. To estimate the minimum water supply of the oases, we extracted the minimum flow from the spring flow dataset and calculated available water based on this flow rate. To this estimate, we did not add any rainfall, because long dry-spells of several

months are frequent and, because of the coupling of rainfall with aquifer recharge, not unlikely to coincide with low spring flows.

### 6.2.8. Implementation of the models

We used ArcGIS 9.2 ModelBuilder (ESRI Inc., Redlands, CA, USA) to calculate a 10-m grid of  $ET_{sz}$  for the study area. This allowed the combination of radiation and wind speed data, which are raster datasets, with the numerical modeling required to calculate all other elements of the Penman-Monteith equation. To account for different temperatures measured at different elevations, we ran each calculation separately for each elevation level. For the upper oases, Al ‘Aqr, Al ‘Ayn and Ash Sharayjah, we used the  $ET_{sz}$  calculated from the temperatures measured at Al ‘Ayn, whereas for Qasha’ and Masayrat ar Ruwajah, we calculated  $ET_{sz}$  based on temperatures measured in the oases themselves.

For each agricultural terrace, we extracted the average  $ET_{sz}$  from the resulting raster. Crop coefficients were then transferred into the data table belonging to each terrace, as separate entries for trees and field crops and for each month of the year. For all terraces that had more than one tree or shrub species, we calculated a weighted average of all individual  $k_c$  values, weighting each contributing  $k_c$  by the proportion of the corresponding species among all trees. Subsequently, multiplying the modeled  $ET_{sz}$  for each month with the corresponding crop coefficients yielded  $ET_c$ , the crop evapotranspiration per crop type and terrace.

Since not the entire terrace was cropped in all cases, we estimated the proportion of each terrace that was covered by field crops. The product of this proportion and the area of the terrace was accepted as cropped area. For trees, only the numbers were assessed in the field, which had to be converted to areas for use with the Penman-Monteith equation. Therefore, we calculated the crop density per terrace of roses, date palms and other trees and analyzed the density distribution, comparing it with our aerial photographs, to define the density threshold that corresponded to full cover. We set the threshold values for full cover to 400 roses ha<sup>-1</sup>, 100 date palms ha<sup>-1</sup> and 200 other trees ha<sup>-1</sup>. For terraces with densities of roses, date palms and trees below these thresholds, we calculated the area covered by the respective perennials as the product of the number of specimens and the average area per tree according to the threshold density, which was 25 m<sup>2</sup> for roses, 100 m<sup>2</sup> for date palms and 50 m<sup>2</sup> for other trees. All other area was interpreted as bare. This assumption is realistic, because all terraces are divided into so-called jalbas, small irrigation plots that are separated from the rest of the terrace by low ditches. Jalbas that currently have no vegetation are not irrigated and thus do not contribute to evapotranspiration.

The product of the effectively cultivated area and  $ET_c$  is the daily volume of water per terrace that evaporates from the soil or is transpired by the plants.



Multiplying this value by the number of days in the respective month yielded the monthly evapotranspiration.

### 6.2.9. Historic water use

To determine historic water use patterns, we calculated the average water consumption per month and ha of each land use type assigned to the 2005 vegetation based on our aerial photographs. For most land use types, whose species composition is assumed to have changed only little over time, this mean water consumption was used to calculate historic water use by multiplying it with the area assigned to the land use type as interpreted from the historic photographs.

Adjustments were necessary for the land use type of field crops in the upper oases, for which historic sources (Abercrombie 1981, Scholz 1984) indicate the presence of large areas of onion and garlic, along with some cereals, mostly wheat. We implemented this adjustment by assuming a full cover of 80% garlic and 20% wheat covering 80% of the area of these terraces. Subsequently, we calculated water use on the terraces as described above, and calculated the average water consumption per month and area. For the mean historic water consumption of the land use type ‘field crops’, we then calculated a weighted average of current and assumed historic water consumption, assigning a weight of 0.2 to the consumption derived from the modern analysis and 0.8 to the water use pattern modeled for exclusive cultivation of garlic and wheat. Multiplying this average with the area under field crops in 1978 yielded the historic water consumption by field crops.

Similarly, the land use type of non-date trees, which no longer exists in Masayrat ar Ruwajah, had to be defined for the historic analysis. Based on our aerial photographs, we assumed that this land use type was composed almost exclusively of lime trees, which, according to information obtained from local farmers, was partly intercropped with fodder grasses. In an analysis similar to the one for the field crops of the upper oases, we assumed a vegetative cover of 80% lime and 10% fodder crops, composed of a combination of maize and barley. We assumed the remaining 10% of the area to be bare soil. We followed the above procedure to calculate the oasis’ water consumption per area. Multiplication by the historic tree area at Masayrat ar Ruwajah yielded the water consumption by these trees in 1978.

For both 1978 and 2005, we estimated irrigation water use efficiency according to Norman et al. (1998b) as:

$$IWUE = \frac{ET_a - P_e - \Delta S}{I_s}, \text{ where } ET_a \text{ is the actual evapotranspiration, } P_e \text{ the}$$

effective precipitation and  $\Delta S$  the change in root zone moisture. We follow the reasoning by Siebert et al. (2007), that on terraced fields all rainfall is effective and that changes in root zone moisture are negligible.

## 6.3 Results

### 6.3.1. Current and historic land use

The main field crops in the oases (Table 6.2) were maize, barley, oats, garlic, alfalfa (*Medicago sativa* L.), sweet potato (*Ipomoea batatas* (L.) Lam.), sorghum (*Sorghum bicolor* (L.) Moench) and potato (*Solanum tuberosum* L.). On areas of less than 100 m<sup>2</sup>, we also encountered guinea grass (*Panicum maximum* Jacq.), egg plant (*Solanum melongena* L.), radish (*Raphanus sativus* L.), cucurbits (*Cucurbita pepo* L.), hyacinth bean (*Lablab purpureus* (L.) Sweet), cabbage (*Brassica oleracea* L.), lettuce (*Lactuca sativa* L.), chili (*Capsicum frutescens* L.), parsley (*Petroselinum crispum* (Mill.) Nym.), carrot (*Daucus carota* L.), tomato (*Lycopersicon esculentum* Mill.), faba bean (*Vicia faba* L.) and wheat (*Triticum aestivum* L.) (Table 6.2).

Table 6.2. Crop species composition encountered in the oases of Al ‘Aqr, Al ‘Ayn, Ash Sharayjah, Qasha’ and Masayrat ar Ruwajah, Oman, during surveys in April (trees and field crops) and September (field crops only).

Species	Al ‘Aqr		Al ‘Ayn		Ash Sharayjah		Qasha’		Masayrat ar Ruwajah	
	<i>Field crops (area in m<sup>2</sup>; April survey September survey)</i>									
Alfalfa	106 /	79	1029 /	854	148 /	129	- /	-	703 /	579
Barley/oats	3173 /	38	1322 /	10	4511 /	165	280 /	-	1528 /	-
Garlic	634 /	-	988 /	-	7422 /	18	310 /	-	230 /	-
Maize	749 /	2718	1515 /	2787	2897 /	7301	1740 /	1623	3945 /	5171
Potato	- /	-	- /	65	20 /	350	- /	38	- /	-
Sorghum	9 /	-	19 /	-	75 /	70	- /	-	336 /	291
Sweet potato	- /	-	- /	9	38 /	58	122 /	264	65 /	409
Others	18 /	14	13 /	14	76 /	-	10 /	42	- /	107
<i>Trees and shrubs (frequency)</i>										
Apricot	11		34		181		21		1	
Banana	0		0		11		44		216	
Citrus	41		37		481		76		168	
Date	0		0		3		3		956	
Fig	7		2		12		9		15	
Grape	15		8		83		30		30	
Tropical fruits	0		27		6		6		35	
Peach	57		45		265		178		30	
Pear, plum, apple	36		8		44		12		1	
Pomegranate	817		265		4812		776		5	
Rose	295		635		1989		168		0	
Walnut	8		11		86		31		0	
Others	0		0		9		4		0	

The most frequent tree or shrub crops in the oases (Table 6.2) were pomegranate, rose, date palm (*Phoenix dactylifera* L.), lime and peach. In smaller numbers, bananas (*Musa x paradisiaca* L.), apricots, grapes (*Vitis vinifera* L.), walnuts (*Juglans regia* L.), pears (*Pyrus communis* L.), plums

(*Prunus domestica* L.), apples (*Malus domestica* Borkh.), papayas (*Carica papaya* L.), guavas (*Psidium guajava* L.) and figs (*Ficus carica* L.) were present.

The percentage of the area that was covered by field crops in 1978 ranged from 9% at Masayrat ar Ruwajah to 42% at Al ‘Ayn and Qasha’ (Fig. 6.3, Table 6.3). Rose gardens made up between 0% of the area at Masayrat ar Ruwajah and Al ‘Aqr and 18% at Al ‘Ayn. The proportion of the area covered by trees was highest at 74% at Al ‘Aqr and lowest at 25% at Qasha’. Palm groves were only present at Masayrat ar Ruwajah, where they covered 40% of the area. Areas of bare soil covered 31% at Qasha’, 10% at Ash Sharayjah and below 10% at the other oases. At Masayrat ar Ruwajah, no bare areas were found.

In some respects, land use in 2005 differed substantially from land use in 1978. At Al ‘Aqr, rose gardens expanded from 0% to 15% of the area, with much of what was previously under field crops (decline from 23% to 6%) being converted to rose plantations. At Al ‘Ayn, a similar increase in the rose area occurred, from 18 to 31% of the area. Here, the additional area was mainly gained from a reduction in orchard size from 34 to 24% of the area. Some of this decline was due to the building of a new road on the area of a former orchard. At Ash Sharayjah, much of the former field crop area had been abandoned, leading to a decline in field crop area from 29 to 9% and an increase in bare area from 10 to 27%.

The greatest land use changes happened at Qasha’ and Masayrat ar Ruwajah. At Qasha’, the area under temperate and subtropical orchards was expanded from 25% to 61% of the area, at the expense of field crops (42 to 5%) and bare ground (31 to 24%). Masayrat ar Ruwajah lost virtually all of its area under non-palm orchards, which had covered half of the oasis area before. The area previously under this land use type was converted to palm groves (40 to 60%), field crops (9 to 32%) and bare ground (0 to 8%).

### 6.3.2. Climatic parameters

#### Temperature

Measured temperatures reflected the different elevations of the sites (Fig. 6.4). At Al ‘Ayn, mean monthly minimum temperatures ( $T_{min}$ ) ranged from 6.6°C in January to 22.0°C in July, whereas mean monthly maximum temperatures ( $T_{max}$ ) were between 15.1 and 30.4°C. At Qasha’,  $T_{min}$  ranged between 8.0 and 22.4°C, while  $T_{max}$  was between 18.4 and 33.3°C. Masayrat ar Ruwajah was the warmest site, with  $T_{min}$  between 11.0 and 26.4°C and  $T_{max}$  between 24.1 and 37.6°C. The absolute minimum temperature in this study was measured at Al ‘Ayn with 1.9°C, while the absolute maximum was 42.8°C at Masayrat ar Ruwajah. Mean temperatures were slightly higher than the arithmetic mean of  $T_{min}$  and  $T_{max}$ , which is recommended for modeling  $ET_{sz}$  (ASCE 2005, Francis et al. 2003), on average by 0.13°C at Al ‘Ayn, 0.64°C at Qasha’ and 0.37°C at Masayrat ar Ruwajah.

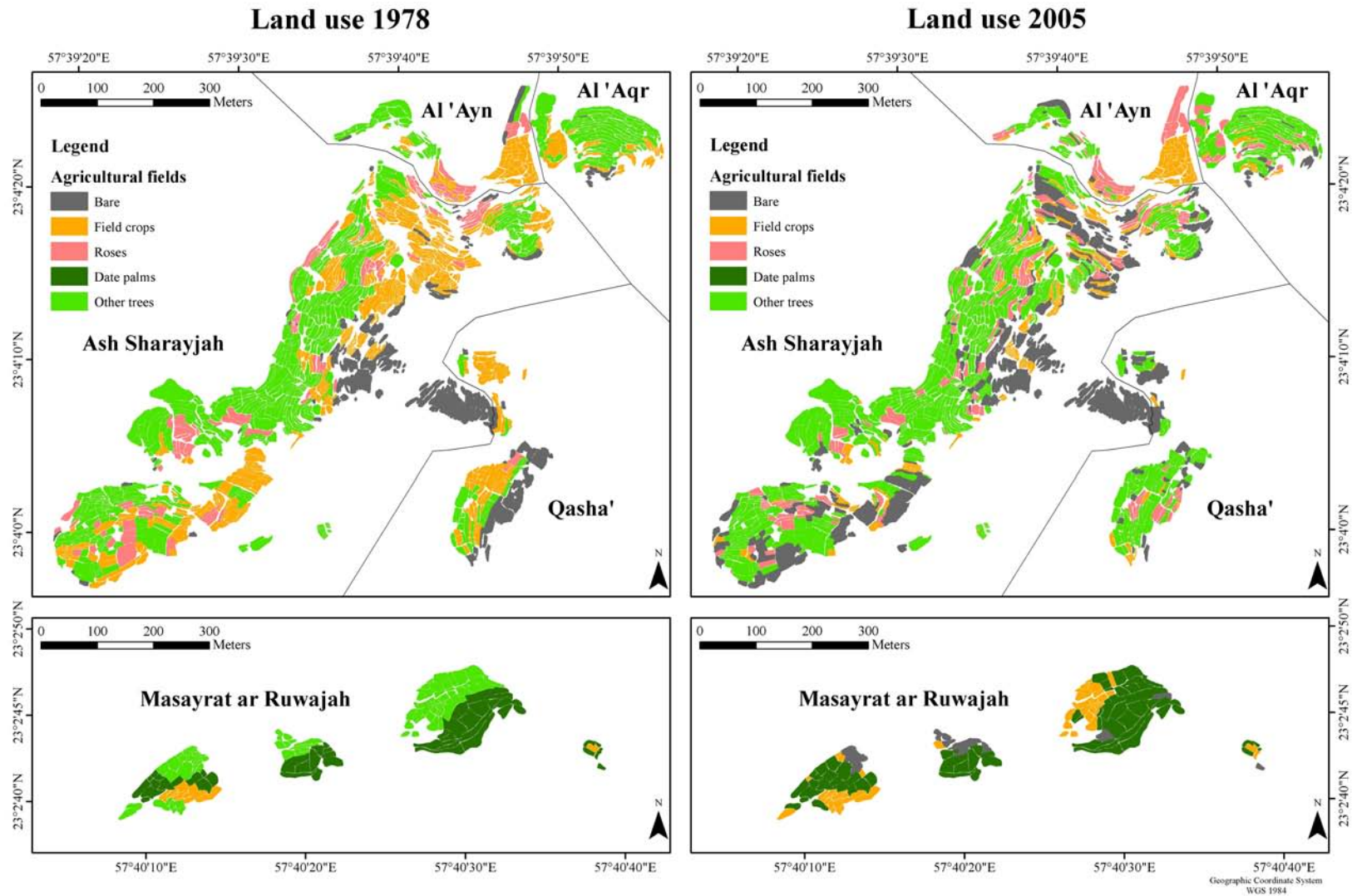


Figure 6.3. Land use in the oases of Al 'Aqr, Al 'Ayn, Ash Sharayjah, Qasha' and Masayrat ar Ruwajah, Oman, as mapped from aerial photographs.

Table 6.3. Area covered by rose gardens, date palm orchards, other orchards, field crops and bare ground in the oases of Al ‘Aqr, Al ‘Ayn, Ash Sharayjah, Qasha’ and Masayrat ar Ruwajah as mapped from aerial photographs, and water consumption per area based on water use calculated from modeled evapotranspiration.

	Name of oasis	Roses	Date palm orchards	Other orchards	Field crops	Bare
Area 1978 (1000 m <sup>2</sup> )	Al ‘Aqr	-	-	12.6	3.8	0.6
	Al ‘Ayn	2.7	-	5.2	6.5	1.0
	Ash Sharayjah	16.2	-	68.1	40.8	14.5
	Qasha’	0.4	-	5.4	9.0	6.7
	Masayrat ar Ruwajah	-	18.2	23.1	4.2	-
Area 2005 (1000 m <sup>2</sup> )	Al ‘Aqr	2.6	-	12.4	1.0	1.0
	Al ‘Ayn	4.8	-	3.7	5.9	0.9
	Ash Sharayjah	14.9	-	75.3	12.3	37.1
	Qasha’	2.0	-	13.3	1.2	5.2
	Masayrat ar Ruwajah	-	27.4	-	14.6	3.4
Water consumption per ha and year (1000 m <sup>3</sup> )	Al ‘Aqr	14.4	-	13.7	9.9	1.5
	Al ‘Ayn	11.3	-	12.0	9.5	0
	Ash Sharayjah	11.1	-	11.6	6.1	1.1
	Qasha’	10.2	-	12.2	7.4	0.7
	Masayrat ar Ruwajah	-	22.5	12.0	12.4	12.7

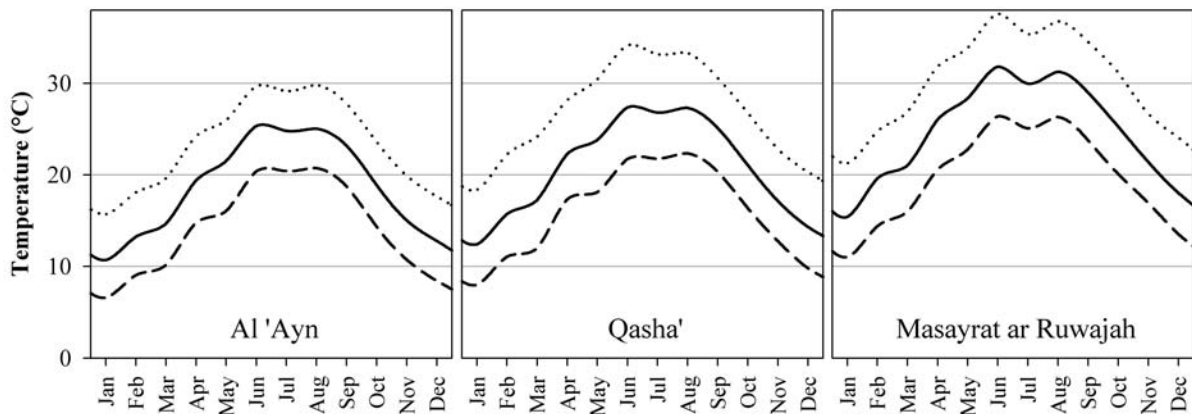


Figure 6.4. Mean daily minimum (dashed), mean (solid) and maximum (dotted) temperatures recorded at Al ‘Ayn, Qasha’ and Masayrat ar Ruwajah, Oman, between April 2005 and March 2006. For better illustration of the course of the year, monthly values for January to March 2006 are displayed before April to December of 2005.

### Measured and modeled radiation

Measured solar radiation at Sayh Qatanah ranged between  $14.1 \text{ MJ m}^{-2} \text{ d}^{-1}$  in November and  $24.8 \text{ MJ m}^{-2} \text{ d}^{-1}$  in April, whereas modeled radiation had a slightly greater range between  $11.9 \text{ MJ m}^{-2} \text{ d}^{-1}$  in December and  $25.4 \text{ MJ m}^{-2} \text{ d}^{-1}$  in July (Fig. 6.2). Because of the shading effect of the surrounding mountains,

modeled radiation slightly deviated from the distribution expected for a flat landscape. For all months between September and April, measured radiation was above modeled radiation. As described above, we therefore used the modeled instead of the measured radiation as input for estimating  $ET_{sz}$ .

### Measured and modeled wind speed

Wind measurements at Ash Sharayjah were only available for a time span of about six weeks between early May and mid June due to the weather extremes described above. Based on the half-hourly measurements taken during this time, the cluster analysis detected three major wind patterns, with very low wind ( $0.27 \text{ m s}^{-1}$ ) from the north-east occurring 69% of the time, slightly stronger winds ( $0.80 \text{ m s}^{-1}$ ) from the south blowing 4% of the time, and moderate southerly winds ( $2.36 \text{ m s}^{-1}$ ) occurring 27% of the time.

The weighted average of the respective runs of the NUATMOS model amounted to mean wind speeds for the oases of between  $0.59$  and  $0.75 \text{ m s}^{-1}$  (Table 6.1).

### 6.3.3. Water availability

The flow rate of the four main springs of our study area was quite variable over time. The spring supplying the gardens of Ash Sharayjah delivered between  $15$  and  $52 \text{ m}^3 \text{ h}^{-1}$ , the spring flow of Masayrat ar Ruwajah was between  $10$  and  $34 \text{ m}^3 \text{ h}^{-1}$ , the flow of the spring delivering the irrigation water of Al ‘Aqr, Al ‘Ayn and the larger proportion of Qasha’s water supply ranged between  $6$  and  $13 \text{ m}^3 \text{ h}^{-1}$  and the small separate spring of Qasha’ varied between  $0.2$  and  $4 \text{ m}^3 \text{ h}^{-1}$ . After excluding the highest flow rate of each spring, which occurred just after a major rainstorm, and distributing the water from the spring at Al ‘Ayn according to the oases’ traditional water rights, the average flow to the oases was thus  $89 \text{ m}^3 \text{ d}^{-1}$  to Al ‘Aqr,  $96 \text{ m}^3 \text{ d}^{-1}$  to Al ‘Ayn,  $88 \text{ m}^3 \text{ d}^{-1}$  to Qasha,  $607 \text{ m}^3 \text{ d}^{-1}$  to Ash Sharayjah and  $447 \text{ m}^3 \text{ d}^{-1}$  to Masayrat ar Ruwajah.

Adding mean rainfall (Fisher 1994) to these mean values resulted in an average daily water supply of  $103 \text{ m}^3$  at Al ‘Aqr,  $108 \text{ m}^3$  at Al ‘Ayn,  $694 \text{ m}^3$  at Ash Sharayjah,  $102 \text{ m}^3$  at Qasha’ and  $482 \text{ m}^3$  at Masayrat ar Ruwajah.

For the minimum flow rates of all springs, the water supply of Al ‘Aqr amounted to  $53 \text{ m}^3 \text{ d}^{-1}$ , Al ‘Ayn received  $57 \text{ m}^3 \text{ d}^{-1}$ , Qasha  $42 \text{ m}^3 \text{ d}^{-1}$ , Ash Sharayjah  $404 \text{ m}^3 \text{ d}^{-1}$  and the spring of Masayrat ar Ruwajah delivered  $231 \text{ m}^3 \text{ d}^{-1}$ .

### 6.3.4. Evapotranspiration modeling

Reference evapotranspiration varied between  $1.9$  and  $7.2 \text{ mm d}^{-1}$  (Fig. 6.5). In spite of the elevation gradient, which led to different levels of radiation and temperature, mean monthly  $ET_{sz}$  was surprisingly similar between the oases, indicating that shading by the surrounding mountains largely offset the influence of higher temperatures on  $ET_{sz}$  at Masayrat ar Ruwajah. Mean daily  $ET_{sz}$  was

lowest at Al ‘Aqr and Ash Sharayjah with  $4.43 \text{ mm d}^{-1}$  and highest at Masayrat ar Ruwajah with  $4.50 \text{ mm d}^{-1}$ . Variation of  $ET_{sz}$  within one oasis was highest in Ash Sharayjah, reflecting the different levels of shading by surrounding mountains in this large oasis. At Masayrat ar Ruwajah, where all fields lie at the bottom of a valley in very similar topographic settings, modeled  $ET_{sz}$  is very similar between all parts of the oasis.

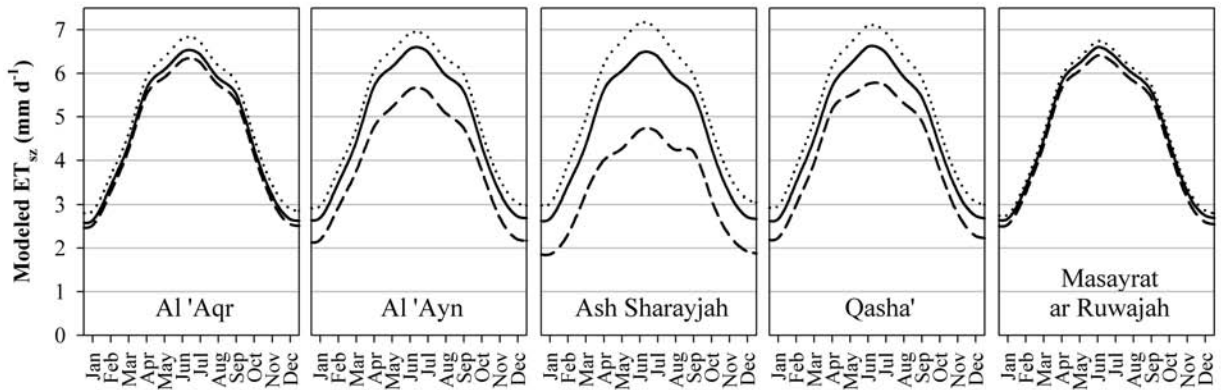


Figure 6.5. Minimum (dashed), mean (solid) and maximum (dotted) modeled reference evapotranspiration ( $ET_{sz}$ ) for the fields of Al ‘Aqr, Al ‘Ayn, Ash Sharayjah, Qasha’ and Masayrat ar Ruwajah, Oman, throughout the year of 2006.

### 6.3.5. Current and historic water demand

Based on our estimates, the total water requirement of all oases increased from  $218,800 \text{ m}^3$  in 1978 to  $256,377 \text{ m}^3$  in 2005. In both investigated periods, water use followed a strong seasonal pattern. In 1978, overall demand by all oases amounted to  $27,903 \text{ m}^3$  in June, the month of the highest solar radiation, and only  $6218 \text{ m}^3$  in December, when solar radiation was lowest (Fig. 6.6).

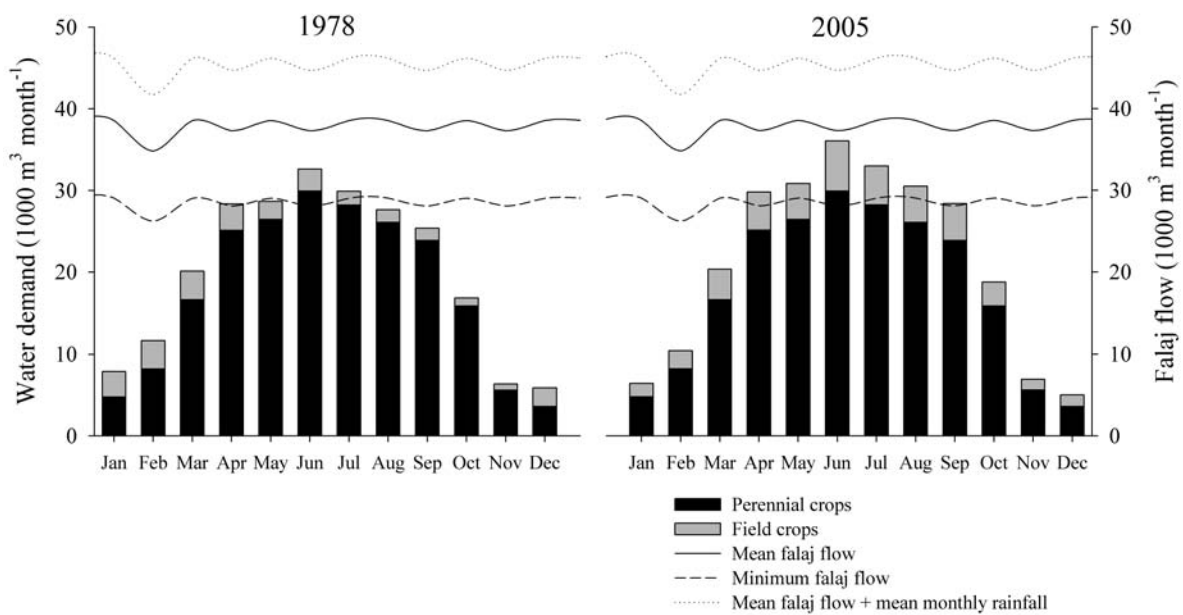


Figure 6.6. Monthly water demand of the oases of Al ‘Aqr, Al ‘Ayn, Ash Sharayjah, Qasha’ and Masayrat ar Ruwajah modeled for 1978 and 2005.

In 2005, the water demand in June was at 36,037 m<sup>3</sup> substantially higher than in 1978, while water use in December was much lower at 5020 m<sup>3</sup>. The proportion of the water consumed by field crops was equally variable throughout the year, ranging from 39% in winter to 6% in summer in 1978, and from 35% in winter to 14% in summer in 2005.

Among the oases, water demand patterns were slightly different. Masayrat ar Ruwajah, which lies at much lower altitude than all other settlements, has a temperature regime that is more suitable for year-round cultivation than at the other places. Since the palm trees grown here are irrigated throughout the year, the winter depression in water requirement is less pronounced than in the higher oases (Fig. 6.7). The disappearance of lime trees and the conversion of much of the orchard area to fodder production have raised the proportion of the water that is consumed by field crops.

Of the upper oases, water demand by field crops was highest at Al ‘Ayn, where they covered 49% of the area in 1978 and 45% in 2005. Here, the proportion of the irrigation water that is consumed by vegetables and fodder crops never dropped below 25% in the summer of 2005, and was thus higher than in 1978, when field crops accounted for only 12% of water use in August. The biggest change at Al ‘Aqr and Ash Sharayjah was an increase in the amount of water consumed by trees in all months of 2005 compared to 1978. Accordingly, water use by field crops decreased.

At Qasha’, the orchard area expanded by 162%, causing a 166% rise in water consumption by perennial trees and shrubs. This oasis experienced the strongest increase in overall water requirements, which rose by 93%, compared to 36% at Al ‘Ayn, 18% at Al ‘Aqr, 15% at Masayrat ar Ruwajah and 9% at Ash Sharayjah.

Irrigation water use efficiency in 1978 (Table 6.4) was lowest at Qasha’ (0.17) and highest at Al ‘Aqr (0.42). By 2005, overall water use efficiency had increased in all oases. The least efficient oasis was now Al ‘Ayn at 0.31, while Al ‘Aqr was still the most efficient, with an irrigation water use efficiency of 0.52.

Table 6.4. Irrigation water use efficiencies (IWUE) of Al ‘Aqr, Al ‘Ayn, Ash Sharayjah, Qasha’ and Masayrat ar Ruwajah in Al Jabal al Akhdar, Oman, in 1978 and 2005.

<b>Name of oasis</b>	<b>IWUE 1978</b>	<b>IWUE 2005</b>
Al ‘Aqr	0.42	0.52
Al ‘Ayn	0.20	0.31
Ash Sharayjah	0.30	0.38
Qasha’	0.17	0.45
Masayrat ar Ruwajah	0.36	0.44
Total	0.31	0.41



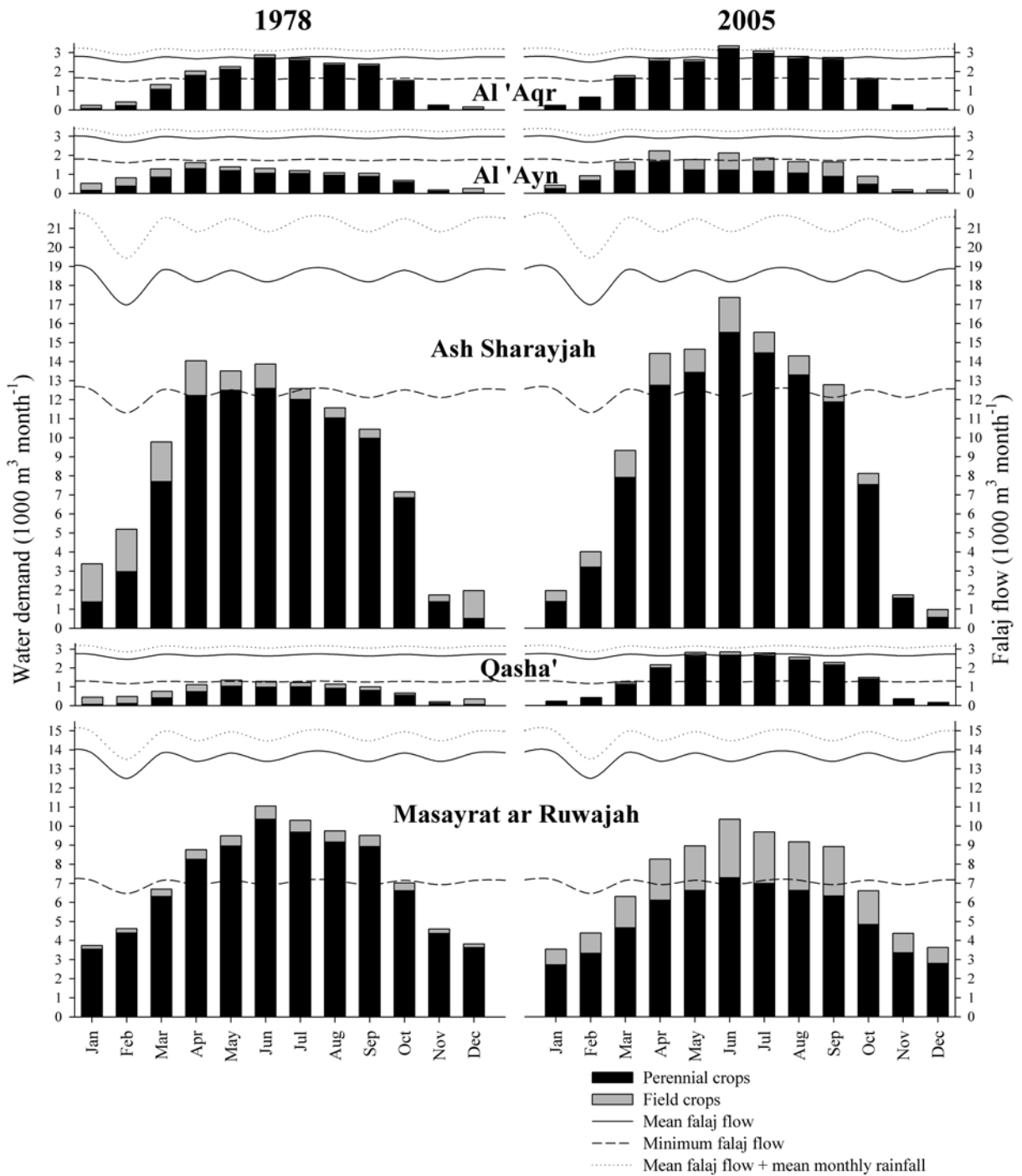


Figure 6.7. Modeled monthly water demand in 1978 and 2005 at the oases of Al 'Aqr, Al 'Ayn, Ash Sharayjah, Qasha' and Masayrat ar Ruwajah, Oman, and available water based on calculations of minimum falaj flow, mean falaj flow and mean falaj flow plus mean monthly rainfall, based on falaj flow measurement between December 2006 and August 2007.

### 6.4 Discussion

Considering the annual total supply and demand, all oases have sufficient water, with the ratio of available to needed water ranging from 2.0 at Al 'Aqr to 3.7 at Qasha' in 1978, and between 1.7 at Al 'Aqr and 2.2 at Al 'Ayn in 2005. The resulting irrigation water use efficiencies of between 0.17 and 0.52 were thus relatively low compared to those found by Norman et al. (1998b) and

Siebert et al. (2007), which ranged between 0.60 and 0.98. In the arid climate of Oman and in cropping systems that rely to a high degree on perennial crops that need a certain amount of water to stay alive during all seasons, considerations about the annual total water supply and demand are not very meaningful. Because of the higher temperature and radiation levels in the summer, water use by such perennials is much higher in the summer than in the winter, whereas available irrigation water remains more or less the same. Farmers in the oases of Al Jabal al Akhdar have no way of storing the winter's water surplus for use in the summer months. Consequently, considerations about the sufficiency of the incoming water should focus on the time of year, when water shortage is most likely to occur. While, for instance, water supply at Ash Sharayjah was 13 times higher than the demand in January of 2005, it exceeded the crop requirements by only 20% in June of the same year. Based on average flow conditions and mean rainfall, water excess in June was 53% at Al 'Ayn, 40% at Masayrat ar Ruwajah and 8% at Qasha', while Al 'Aqr had a water deficit of 8%. Irrigation water use efficiency in June thus ranged between 72 and 102%, values which typically indicate a high risk of water shortage. Since spring flow could only be measured close to the springs, inevitable losses during conveyance of water to the fields have not been taken into account and are likely to further aggravate the water deficit. Leaching of water below the root zone, in contrast, should not lead to major water losses during the summer, since it only appears to occur after large irrigation or rainfall events, which provide excessive amounts of water (Luedeling et al. 2005b). While major rainfalls can occur at all times of year, excessive summer irrigation is unlikely.

Based on water supply and demand computed from minimum falaj flow and crop water requirements, the oases of Al Jabal al Akhdar seem very vulnerable to drought years. When the amount of incoming water corresponds to the minimum spring flow during our study period, the oases would be water-deficient between March to April and July to September, with the amount of lacking water reaching a peak of 56% of the crop requirement at Qasha'. In such years, farmers at Masayrat ar Ruwajah could respond by leaving most of their field crop area uncultivated throughout the summer, which would almost eliminate their water deficit. At Ash Sharayjah and Al 'Ayn, similar adaptations would be possible, but alleviate the water shortage to a lesser degree, because the proportion of the area that is cropped with field crops is much smaller than at Masayrat ar Ruwajah. At Qasha' and Al 'Aqr, farmers have almost no way of adapting to water shortage by not cultivating annual fields. The area under field crops is so small, that such measures would have no significant effect on the water shortage.

In principle, storage of excess water during the winter in reservoirs and gradual release during the summer months would provide a possibility to alleviate the risk of water shortages. At Masayrat ar Ruwajah, such an irrigation dam has already been constructed. At the other locations, however, this type of

construction is precluded by the elevation of the springs, which is directly above the level of the terraces, and by unsuitable terrain.

Between 1978 and 2005, the ability of farmers at most oases to adapt to the seasonal variation in crop water requirement decreased. While at Masayrat ar Ruwajah, the abandonment of large-scale lime production has actually increased the farmers' flexibility in distributing water use over the year, the expansion of the orchard area at all other oases had less favorable effects. In years of drought, and at Qasha' and Al 'Aqr even in years of average spring flow and mean rainfall, farmers face seasonal water shortages in summer. During the hottest months of the year, the water supply is then not sufficient to attribute an optimal amount to all perennial fruits and shrubs. Especially the conversion of many annual fields at Qasha' to fruit orchards increased the minimum monthly water need in this oasis to a level that can hardly be met by the flow of the springs during the summer. All oases except Masayrat ar Ruwajah have thus increased their vulnerability to the interannual variation of water supply that is a defining characteristic of Omani oasis agriculture (Luedeling et al. 2008a, Siebert et al. 2005).

In considering water use efficiency for a whole oasis, however, it should be taken into account that water is not equally distributed within the oases. The number of households that receive a certain proportion of the overall water according to traditional water rights (Abdel-Rahman and Omezzine 1996) ranges between 11 at Qasha' and about 25 at Ash Sharayjah. While some of these households, especially those with substantial off-farm income, might cultivate an area that is smaller than in the past, and thus require less than their allotted share of water, others might face severe seasonal water shortage. Some households that have left the oases over the past few decades might even not use their share of water at all. Water rights are therefore traded among farmers (Abdel-Rahman and Omezzine 1996), but farmer interviews revealed that some farmers remained short of water.

There is evidence that the human energy expended for maintaining the irrigation infrastructure decreased substantially between 1978 and 2005. As already described in 1984 (Scholz 1984), migration to the cities and towns of the lowlands, especially by the younger generation, as well as off-farm employment have decreased available farm labor and elevated the risk of labor shortages. Consequently, the average age of the household heads, who are often the only people permanently employed in agriculture, is fairly high today. According to a survey conducted in 2006, 80% out of 41 interviewed farmers in Masayrat ar Ruwajah, Qasha' and Ash Sharayjah were over 50 years of age, with 68% over 60 (Dickhoefer, unpublished data). So far, the lack of maintenance, along with damage inflicted to the terrace systems during the Jabal War (Scholz 1984), has mainly led to the decay of many terraces formerly cropped with field crops. While this damage to the agricultural infrastructure reduces the ability to make use of the excess water in winter, it does not put the perennial crops at risk. However, as soon as the irrigation infrastructure is affected by lack of maintenance, water shortages will increase.

With the current distribution of annual water use, oases in Al Jabal al Akhdar do not show a particular adaptation of cropped area to the seasonal variation of crop water requirements. A large number of abandoned terraces at Ash Sharayjah still gives testimony of a much better functioning of this mechanism in the past. We assume that after the destructions of the war, the economic incentive of producing field crops was no longer strong enough to warrant rebuilding the terraces. Besides, since these terraces are often far from the main village and require both long walks to and from the fields and the maintenance of long irrigation channels, labor shortages might have precluded continued use of these land resources. Today, the abandoned terraces increasingly fall into disrepair, making a return to cultivation unlikely. Even though we have no evidence on how the agricultural areas were used before the 1950s, we assume that the area under annual crops was much greater than today, ensuring sufficient food production for the then much greater number of inhabitants of the oases.

In the future, it is likely that the water supply of the oases might recede due to the competition by urban water use in the new town of Sayh Qatanah. While the town did not exist at all in 1978, the infrastructure has since then grown to 297 buildings, many with irrigated gardens around them, and according to the development plan for the town, the number of houses is projected to rise to 920 within the next few years. In addition to the developments envisioned by this plan, additional housing areas are being built closer to the villages of Al ‘Ayn and Ash Sharayjah, and new tourism facilities are expected to arise close to an already existing hotel on the plateau. All of these will extract water, and it is likely that, in the long run, they will compete for water with agricultural production. To what extent this competition has already affected the oases’ water supply is unclear, but it is likely that the boreholes supplying Sayh Qatanah have already led to decreasing spring flows in springs that are fed by the same aquifer. According to statistics of the Waterworks on Al Jabal al Akhdar (Ministry of Housing, Electricity and Water, Sultanate of Oman), water extraction from the main well of Sayh Qatanah amounted to 234,410 m<sup>3</sup> in 2004 and 244,360 m<sup>3</sup> in 2005. It thus already equals the water demand of all oases combined, and is likely to substantially exceed it in the future. While the new town is likely to generate employment for the inhabitants of the oases, which might prevent many from leaving the area, it might on the other hand put pressure on the complex hydrological sustainability of traditional oasis agriculture.

## **6.5 Conclusions**

The seasonal distribution of water demand is more unequal in the high-mountain oases of Al Jabal al Akhdar than reported in comparable studies of oases at lower altitudes, and recent land use changes have aggravated this imbalance. It is likely that, in addition to increased water demand, water supply has also decreased and is likely to further decrease in the future, because of

recent expansions of urban developments in the vicinity of the oases, which compete with agriculture for water. Overall, the hydrological sustainability of all oasis systems in Al Jabal al Akhdar except for Masayrat ar Ruwajah has diminished between 1978 and 2005.

## Acknowledgments

We are indebted to Uta Dickhoefer, who provided demographic information on Omani oases and conducted spring flow measurements, to Dr. Wolfgang Schäper for developing and using the equipment for taking aerial photographs from a remotely controlled airplane and to Dr. Jens Gebauer for helping with vegetation mapping. We further acknowledge the cooperation of Dr. Andreas Bachmann, who made his version of the NUATMOS wind model available, the Waterworks of Al Jabal al Akhdar of the Ministry of Housing, Electricity and Water for providing water use statistics, the Agricultural Extension Center at Sayh Qatanah for general information about the oases and maintenance of the weather station and Sultan Qaboos University at Muscat for infrastructural support. We also wish to express our gratitude towards the German Research Foundation (DFG) for generous funding (BU 1308).

## References

- Abdel-Rahman HA and Omezzine A (1996). Aflaj water resources management: Tradable water rights to improve irrigation productivity in Oman. *Water International* 21(2), 70-75.
- Abercrombie T (1981). Oman: Guardian of the Gulf. *National Geographic* 160(3), 344-377.
- Allen RG, Pereira LS, Raes D and Smith M (1998). Crop evapotranspiration - Guidelines for computing crop water requirements. FAO Irrigation and drainage paper 56, Food and Agriculture Organization of the United Nations, Rome, Italy.
- ASCE (2005). The ASCE Standardized Reference Evapotranspiration Equation. Task Committee on Standardization of Reference Evapotranspiration, American Society of Civil Engineers, Reston, VA, USA.
- Bachmann A (1998). Coupling NUATMOS with the GIS ARC/INFO - Final Report for MINERVE 2. Accessed on 24 August 2007 at <http://www.geo.unizh.ch/gis/research/edmg/fire/papers/minerve/nuatmos.pdf>.
- Bowling LC and Lettenmaier DP (1997). Evaluation of the effects of forest roads on streamflow in Hard and Ware Creeks, Washington. Technical Report No. 155, Department of Civil Engineering, University of Washington, Seattle, WA, USA.
- Buerkert A, Mahler F and Marschner H (1996). Soil productivity management and plant growth in the Sahel: Potential of an aerial monitoring technique. *Plant and Soil* 180(1), 29-38.
- Costa PM (1983). Notes on traditional hydraulics and agriculture in Oman. *World Archaeology* 14(3), 273-295.
- Dorvlo ASS and Ampratwum DB (1998). Summary climatic data for solar technology development in Oman. *Renewable Energy* 14(1-4), 255-262.
- FAO (2007). AQUASTAT Database. Food and Agriculture Organization of the United Nations. Accessed on 10 Sep 2007 at <http://www.fao.org/nr/water/aquastat/dbase/index.stm>.
- Fisher M (1994). Another look at the variability of desert climates, using examples from Oman. *Global Ecology and Biogeography Letters* 4(3), 79-87.

- Garnier M, Zreik L and Bove JM (1991). Witches-Broom, a Lethal Mycoplasmal Disease of Lime Trees in the Sultanate-of-Oman and the United-Arab-Emirates. *Plant Disease* 75(6), 546-551.
- Gebauer J, Luedeling E, Hammer K, Nagieb M and Buerkert A (2007). Mountain oases in northern Oman: An environment for crop evolution and in situ conservation of plant genetic resources. *Genetic Resources and Crop Evolution* 54, 465-481.
- Glennie K, Boeuf M, Hughes Clarke M, Moody-Stuart M, Pilaar W and Reinhardt B (1974). Geology of the Oman Mountains. *Verhandelingen Koninklijk Nederlands geologisch mijnbouwkundig Genootschap* 31, 1-423.
- Khan IA and Grosser JW (2004). Regeneration and characterization of somatic hybrid plants of *Citrus sinensis* (sweet orange) and *Citrus micrantha*, a progenitor species of lime. *Euphytica* 137(2), 271-278.
- Korn L, Häser J, Schreiber J, Gangler A, Nagieb A, Siebert S and Buerkert A (2004). Tiwi and Wadi Tiwi: the development of an oasis on the north-eastern coast of Oman. *Journal of Oman Studies* 13, 57-90.
- Luedeling E and Buerkert A (2008). Typology of mountain oases in Oman based on Landsat and SRTM imagery and geological survey data. *Remote Sensing of Environment* in press.
- Luedeling E, El-Gamal H, Aeschbach-Hertig W, Kipfer R, Nagieb M and Buerkert A (2008a). Hydrological sustainability of mountain oases in northern Oman. *Journal of Hydrology*, submitted.
- Luedeling E, Gebauer J and Buerkert A (2008b). Climate change affects traditional high-altitude fruit production systems in Oman. *Field Crops Research*, submitted.
- Luedeling E, Nagieb M, Wichern F, Brandt M, Deurer M and Buerkert A (2005). Drainage, salt leaching and physico-chemical properties of irrigated man-made terrace soils in a mountain oasis of northern Oman. *Geoderma* 125(3-4), 273-285.
- Luedeling E, Siebert S and Buerkert A (2007). Filling the voids in the SRTM Elevation Model - A TIN-based delta surface approach. *ISPRS Journal of Photogrammetry and Remote Sensing* 62(4), 283-294.
- Melamid A (1992). The Jebel-Al-Akhdar (Oman). *Geographical Review* 82(4), 470-472.
- Nagieb M, Siebert S, Luedeling E, Buerkert A and Häser J (2004). Settlement history of a mountain oasis in northern Oman - evidence from land-use and archaeological studies. *Die Erde* 135(1), 81-106.
- Norman WR, Shayya WH, Al-Ghafri AS and McCann IR (1998). Aflaj irrigation and on-farm water management in northern Oman. *Irrigation and Drainage Systems* 12(1), 35-48.
- Ross DG, Smith IN, Manins PC and Fox DG (1988). Diagnostic Wind-Field Modeling for Complex Terrain - Model Development and Testing. *Journal of Applied Meteorology* 27(7), 785-796.
- Schäper W (2006). Fernrohrbrille und Modellflugzeuge. *Innovation* 17, 52-57.
- Scholz F (1984). Höhengiedlungen am Jabal Akhdar - Tendenz und Probleme der Entwicklung einer peripheren Region im Oman-Gebirge. *Zeitschrift für Wirtschaftsgeographie* 28(1), 16-30.
- Siebert S, Häser J, Nagieb M, Korn L and Buerkert A (2005). Agricultural, architectural and archaeological evidence for the role and ecological adaptation of a scattered mountain oasis in Oman. *Journal of Arid Environments* 62(1), 177-197.
- Siebert S, Nagieb M and Buerkert A (2007). Climate and irrigation water use of a mountain oasis in northern Oman. *Agricultural Water Management* 89(1-2), 1-14.

## Chapter 7

# Conclusions

### Methodology

Filling the gaps in the SRTM elevation model using the proposed methodology was possible and yielded results that substantially improved all previous versions of this model (chapter 2). The combination of digital and physical datasets proved fruitful for producing a high-quality dataset. The resulting elevation model was a useful input for the oasis detection and classification, which could be accomplished reliably using Landsat imagery and geological survey data (chapter 3).

Evaluating the hydrological sustainability of mountain oases was difficult due to the unsaturated conditions that apparently prevail in many aquifers of Oman (chapter 4). This and the likely presence of a natural source of SF<sub>6</sub> complicated water dating. Nevertheless, in combination with spring flow measurements, the determined water ages could still be used to evaluate the stability of the irrigation water supply.

Analysis of climatic records from an official weather station proved useful for estimating agroclimatic conditions in the past (chapter 5). In Oman's fairly uniform climate, correlating these measurements with data recorded in the field yielded very good fits and allowed extrapolating measured temperatures into periods, for which only official weather data were available. This method appears to have potential for similar studies elsewhere, which might provide interesting insights into the effects of past and future climatic changes on the distribution of niche environments, which are determined by biological threshold temperatures.

Finally, using information about water consumption under current land use allowed drawing conclusions about water use in the past, based on land use information from historic aerial photographs (chapter 6). Modeling of water requirements based on modeled wind and radiation and measured temperatures yielded water use estimates, which were in a similar range as the water supply derived from spring flow measurements. Using spatial grid datasets for computing evapotranspiration allowed better spatial resolution than traditional purely numeric calculations.

## **Sustainability of mountain oases in Oman**

While the current number of oases in northern Oman is large, only 75 were classified as mountain oases, with only 16 lying at elevations higher than 1500 m above sea level (chapter 3). While all these oases lie in geologically favorable settings and derive their irrigation water from springs, most other oases obtain their water from sedimentary aquifers. Traditional oases often collect wadi groundwaters and convey it to the fields through aflaj, while modern farms obtain their water from wells dug into the sediments of the coastal plain.

Based on estimates of water ages and spring flow rates, it appears as if most oases in Oman are capable of enduring dry spells of up to about five years, without complete cessation of the water supply (chapter 4). Nevertheless, interannual variation of water availability is a defining characteristic of most oases, which requires agricultural adaptation. This is generally accomplished by dedicating a sizeable proportion of agricultural land to the production of annual crops, and leaving these parcels bare during years of drought. Recent land use changes in several oases of Al Jabal al Akhdar have increased the area under orchards at the expense of annual crops (chapter 6). The distribution of water requirements over the year is less favorable under current land use than under past land use, with a pronounced water consumption peak during the summer, when water is scarcest. Such changes threaten the sustainability of oasis agriculture, elevating the risk of crop failure or tree deaths during dry years. Demographic changes, such as an ageing farm population, emigration of potential farm labor and increasing off-farm employment opportunities further threaten traditional oasis agriculture. Urban environments also increasingly compete with agriculture for water.

Finally, even global processes affect traditional crop production systems. While oasis farmers are increasingly subject to the international dynamics of supply and demand and thus influenced by the economics of globalization, climate change also seems to affect oasis agriculture (chapter 5). The dramatic decrease in chilling hours observed in the high-mountain oases of Al Jabal al Akhdar threatens the productivity of the traditional orchards, which are composed of temperate and subtropical crops. The geographic and climatic niche environment for such crops in Oman is already small and seems to be vanishing rapidly.

Even though Omanis still value their agricultural heritage, oasis agriculture is currently undergoing a transformation process with many causes, some of which might be unavoidable. More than anything else, traditional oasis agriculture faces the challenge of having to adapt quickly to the changes in demographic and economic conditions. Additional political efforts by the government might be necessary to support oasis farmers in this transition and prevent traditional oasis agriculture from disappearing.



## Curriculum vitae

Name: Rolf Eike Luedeling

Born: 01 November 1977 in Hannover, Germany

Nationality: German

### **Education:**

1984-1988 Primary school (Grundschule) at Steinwedel, Lehrte, Germany

1988-1990 Middle school (Orientierungsstufe) at Lehrte, Germany

1990-1997 Secondary school (Gymnasium) at Lehrte, Germany

1997-1998 Civil Service Gut Adolphshof, Lehrte, Germany

1998-1999 Studies of Physics and Mathematics, University of Hannover, Germany

1999-2003 Diplom I program “Organic Agriculture”, University of Kassel, Germany

2003-2004 MSc program “International Ecological Agriculture, University of Kassel, Germany

2004 Exchange semester, University of Western Australia, Perth, Australia

2004-2005 MSc program “International Agricultural Development”, University of California, Davis, CA, USA

2005-2007 Associate Researcher and PhD candidate, Department of Organic Plant Production and Agroecosystems Research in the Tropics and Subtropics, University of Kassel, Germany

### **Degrees:**

1997 Abitur, Gymnasium Lehrte, Germany

2003 Diplom I in Organic Agriculture, University of Kassel, Germany

2004 Master of Science in International Ecological Agriculture, University of Kassel, Germany

2005 Master of Science in International Agricultural Development, University of California, Davis, CA, USA

**Awards:**

2003 Gustav Hacker-Preis 2003

2004 LEAFSE Scholarship (Learning Through Exchange: Agriculture, Food Systems and Environment)

2004/05 Fulbright Scholarship

## List of publications

### Theses

- Luedeling E (2003). Water use and water resources of mountain oases in Oman. Diplom I Thesis, University of Kassel, Germany
- Luedeling E (2004). Geological and topographic determinants of oasis locations in the Oman Mountains - a remote sensing approach. Master Thesis, University of Kassel, Germany

### Articles in peer-reviewed journals

- Buerkert A, Nagieb M, Siebert S, Luedeling E, Quintern M & Al Khanjari S (2005). Plant genetic diversity, irrigation and nutrient cycling in traditional mountain oases of northern Oman. In: Li CJ et al. (Eds.): Plant Nutrition for food security, human health and environmental protection, 1072-1073. Tsinghua University Press, Beijing, China.
- Gebauer J, Luedeling E, Hammer K, Nagieb M & Buerkert A (2007). Mountain oases in northern Oman: an environment for evolution and in situ conservation of plant genetic resources. *Genetic Resources and Crop Evolution* 54, 465-481.
- Luedeling E & Buerkert A. Typology of oases in northern Oman based on Landsat and SRTM imagery and geological survey data. *Remote Sensing of Environment* (in press).
- Luedeling E, Nagieb M, Wichern F, Brandt M, Deurer M & Buerkert A (2005). Drainage, salt-leaching and physico-chemical properties of irrigated man-made terrace soils in a mountain oasis of northern Oman. *Geoderma* 125, 273-285.
- Luedeling E, Siebert S & Buerkert A (2007). Filling the voids in the SRTM elevation model – A TIN-based delta surface approach. *ISPRS Journal of Photogrammetry and Remote Sensing* 62(4), 283-294.
- Luedeling E & Wichern F (2007). The need for site-specific adaptation of organic standards: The example of dryland salinity in Australia. *Journal of Agriculture and Rural Development in the Tropics and Subtropics Supplement* 89, 121-142.
- Nagieb M, Häser J, Siebert S, Luedeling E & Buerkert A (2004). Agriculture, hydro-infrastructural conditions and settlement history of a mountain oasis in northern Oman. *Die Erde* 135, 81-106.
- Wichern F, Luedeling E, Müller T, Joergensen RG & Buerkert A (2004). Field measurements of the CO<sub>2</sub> evolution rate under different crops during

an irrigation cycle in a mountain oasis of Oman. *Applied Soil Ecology* 25, 85-91.

*Currently under review:*

Luedeling E & Buerkert A. Effects of land use changes on the hydrological sustainability of mountain oases in northern Oman. *Plant and Soil* (submitted)

Luedeling E, El-Gamal H, Aeschbach-Hertig W, Kipfer R, Nagieb M & Buerkert A. Hydrological sustainability of mountain oases in Oman. *Journal of Hydrology* (submitted).

Luedeling E, Gebauer J & Buerkert A. Climate change affects traditional high-altitude fruit production systems in Oman. *Field Crops Research* (submitted).

### **Other publications**

Luedeling E, Siebert S, Wichern F, Aeschbach-Hertig W, Nagieb M, Müller T & Buerkert A (2002). The hydrology of mountain oases in Oman. Oral presentation. Tropentag 2002, Witzenhausen.

Luedeling E (2004). The potential of the organic approach to fight salinity. 5<sup>th</sup> Annual Organic Symposium, University of Western Australia, Perth, Australia.

Luedeling E & Zhang M (2005). Spatial assessment of dormant OP and alternatives in almond orchards. 4<sup>th</sup> PUR Workgroup, University of California, Davis, CA, USA.

Luedeling E, Gebauer J & Buerkert A (2006). Climatic requirements of temperate perennials in Oman. Poster presentation. Tropentag 2006, Bonn.

Luedeling E, Gebauer J & Buerkert A (2007). Climate change affects traditional high-altitude fruit production systems in Oman. Oral presentation. Tropentag 2007, Witzenhausen.

Luedeling E, Schumacher J, Gebauer J, El-Siddig K & Buerkert A (2007). Spatial expansion of urban agriculture in Khartoum, Sudan. Poster presentation. Tropentag 2007, Witzenhausen.